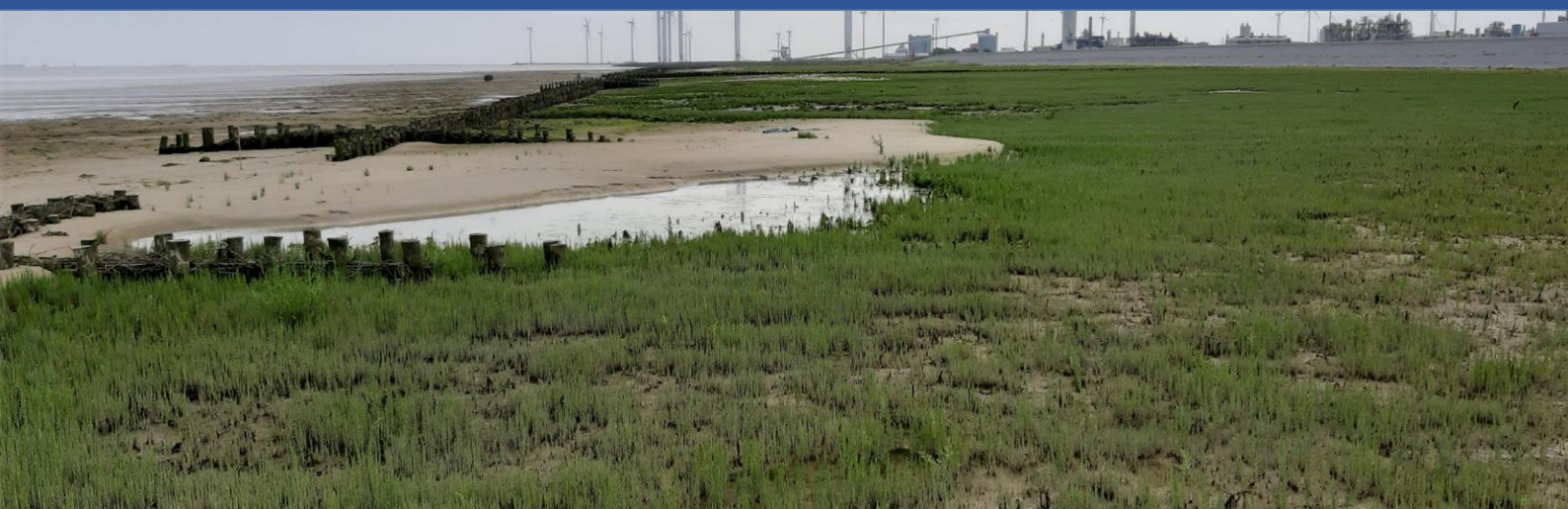




# Seasonal variation in salt marsh vegetation

Impact of physical stressors on the development, decay and seed  
retention of *Salicornia Europaea*

L.H. Eekman, 2021





University of Twente.  
Civil Engineering & Management

---

# Seasonal variation in salt marsh vegetation

Impact of physical stressors on the development, decay and  
seed retention of *Salicornia Europaea*

---

By  
Ing. L.H. (Bert) Eekman  
Master Thesis

November 2021  
Enschede

Contact: [bert.eekman@hotmail.com](mailto:bert.eekman@hotmail.com)

Graduation committee: Prof. dr. K.M. Wijnberg  
dr. ir. E.M. Horstman  
dr. ir. P.W.J.M. Willemsen



## Preface

De thesis die hier voor u ligt vormt het slotstuk van mijn master in Water Engineering and Management aan de Universiteit Twente. Voorafgaand en gedurende mijn afstudeerperiode heb ik veldwerk uitgevoerd op de kunstmatig aangelegde kwelder Marconi in Delfzijl.

Dit onderzoek had niet mogelijk kunnen zijn zonder de hulp van een aantal mensen. Als eerst mijn afstudeercommissie. Ik wil graag de voorzitter van mijn commissie, Kathelijne Wijnberg, bedanken voor de altijd leuke inbreng en statistische kennis. Ook was elke online meeting geheel in stijl, aangezien Kathelijne hier iedere keer een kwelder of duin als achtergrond had. Daarnaast wil ik mijn dagelijkse begeleider, Erik Horstman, bedanken voor de vele input, gedachtewisselingen en positieve feedback gedurende onze wekelijkse meetings. Deze positieve inbreng hielp zeer erg en is erg gewaardeerd, vooral gedurende de momenten dat de motivatie door verschillende redenen wat wegzakte. Tot slot, wilde ik mijn veldwerkbegeleider, Pim Willemsen, bedanken voor het helpen bedenken en uitvoeren van de verschillende veldmetingen. Ook wil ik je bedanken voor de vele input gedurende mijn thesis en uiteraard voor het beschikbaar stellen van jouw laptop als mijn laptop niet over de juiste processor-capaciteiten bleek te beschikken.

Daarnaast wil ik natuurlijk mijn mede-velddwerkers, Emre Ozturk, Tynke Siegersma en Michiel van den Berg bedanken. De laatste veldwerkdagen waren erg prettig met goede temperaturen en een zonnetje, maar dat heeft er wel een aantal keer minder uit gezien. Vooral de veldwerkdag vlak voor kerst kon niet worden beschreven als prettig, gelukkig was de warme auto dan wel weer extra fijn.

Verder ik mijn vrienden en familie bedanken voor de nodige afleiding van mijn onderzoek, maar ook voor de gesprekken die weer nieuwe ideeën en mogelijkheden brachten.

Dan wil ik tot slot mijn vriendin, Lydia Heida, heel erg bedanken voor de continue steun, liefde en motivatie gedurende deze 8 maanden. Als het even tegen zat of ik de motivatie niet meer kon opbrengen, zorgde jij er altijd voor dat ik weer op het goede pad terecht kwam. Nu zijn wij beiden bijna klaar met onze master en heb ik ontzettend veel zin in onze volgende uitdagingen, waar deze dan ook mogen liggen. In elk geval gaan we goed beginnen met een aantal welverdiende vakanties!

Bert Eekman,  
Enschede, 4 november 2021



## Summary

Salt marshes are increasingly being used as (part of) nature based flood defences. A salt marsh is an intertidal area at the coastline with salt-tolerant vegetation species such as *Salicornia Europaea*. These intertidal areas are flooded during high tide during which the aboveground part of the vegetation might reduce the waves and increase sedimentation rates at the marsh, while the belowground part of the vegetation (roots) prevent the bed from eroding. As *Salicornia Europaea* is seasonal vegetation, the decay of the aboveground vegetation and the development of the seedbank are important parameters to predict changes in the vegetation cover over the years. To optimise the design and management of salt marshes, it is important to understand the aspects that play a role in the development and decay of the vegetation cover, including the development of the seedbank. Generally, numerical models are used to simulate the development or decay of the vegetation cover to optimise the design and management of salt marshes. Within these numerical models the sudden decay of *Salicornia* vegetation is simulated going from a fully grown vegetation cover at the end of summer, abruptly to zero vegetation at the start of winter. Whilst the seed availability is simulated using a random constant each year during spring. These assumptions may lead to incorrect predictions as in reality the decay of vegetation might depend on the present vegetation and the different hydro- and morphodynamics. Therefore, the aim of this research is to parameterise the vegetation decay and the seed retention with local hydro- and morphodynamics, like flow velocities, wave height, surface elevation changes and inundation frequency. These parameterisations can be used to predict the development of the seedbank, and with this the development of the vegetation cover in summer, and subsequently the vegetation decay in winter. This leads to the main research question:

*How do the Salicornia development and decay as well as the seedbank correlate with flow velocities, wave height, surface elevation changes, inundation frequency and sediment composition on a salt marsh throughout the winter period and how do the vegetation characteristics correlate with the Salicornia decay and seedbank?*

This study is based on field data collected at an artificially created salt marsh near Delfzijl in the northeast of the Netherlands. Waves, tides, flow velocities and bed level changes have been monitored from November 2020 to April 2021. Moreover, vegetation density, length, strength, root length, number of side roots, length of the longest side root and the number of seeds of the dominant *Salicornia Europaea* have been measured throughout the winter season. The different dynamics and vegetation properties have been correlated by a multiple linear regression analysis to find the driving factors for the development and decay of the vegetation as well as for seed retention.

Firstly, the results show that the density of the fully grown *Salicornia* vegetation at the end of summer is affected negatively by the maximum significant wave height. This means that during the growing season, waves limit the increase of vegetation density. Secondly, during the winter season the decay of the vegetation density is also affected negatively by the maximum significant wave height, meaning that higher waves cause a faster vegetation decay. Thirdly, the results show that the retention of seeds is positively affected by the density of the vegetation that is still present and negatively affected by the flow velocities. The obtained parameterisations quantifying the vegetation decay and the seed availability throughout the winter period are:

$$\text{Vegetation density decay} = -5.02 + 1.9 * H_{s,max} \quad [\%]$$

$$\text{Number of seeds in seedbank} = 1.54 + 2.03 * \rho_{veg} \quad [\text{per } 100 \text{ cm}^2]$$

$$\text{Number of seeds in seedbank} = 224.25 - 439.68 * u_{max} \quad [\text{per } 100 \text{ cm}^2]$$

Wherein  $H_{s,max}$  the maximum significant wave height in centimetres,  $\rho_{veg}$  is the vegetation density in percentage and  $u_{max}$  is the maximum flow velocity in meters per second. The values of the maxima ( $H_{s,max}$  and  $u_{max}$ ) can be chosen over an undefined fieldwork period (period in between fieldwork days). These results are schematised in [Figure 0.1](#).

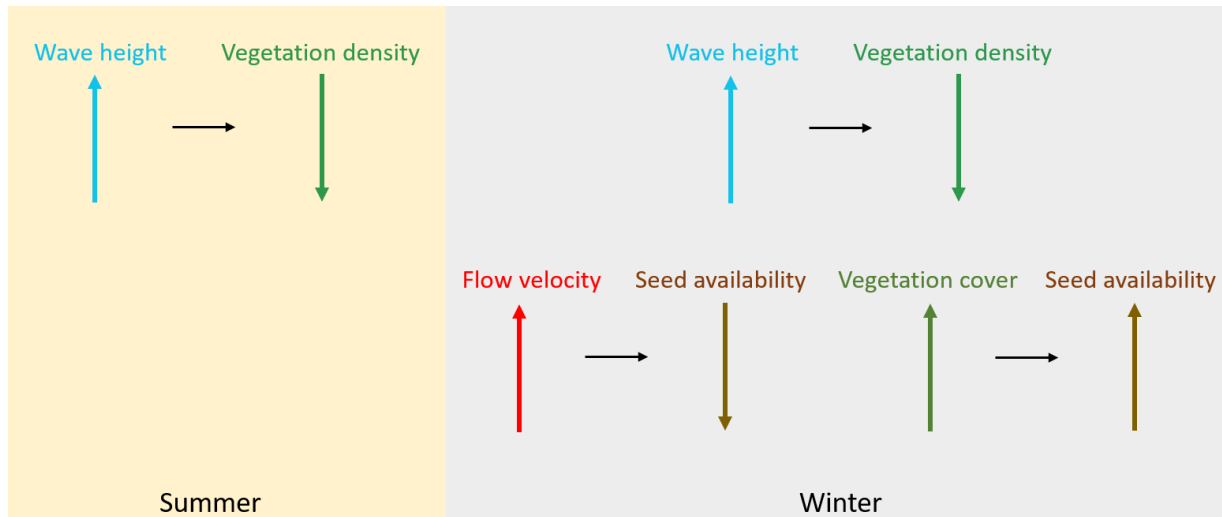


[Figure 0.1](#): Schematisation of the results of this study. An increasing wave height leads to a decreasing vegetation density and decreasing flow velocities and a denser vegetation cover will result in more seed availability throughout the winter period.

The presented parameterisations can be used in modelling studies to predict the vegetation density (decay) based on the wave height and the number of seeds in the seedbank based on the vegetation density and the flow velocities at the marsh. When these parameterisations are implemented into numerical models, it is possible to simulate the impact of physical stressors on the short-term and long-term vegetation development. This will help to develop effective management and restoration strategies for salt-marshes.

# Contents

- Preface..... i
- Summary .....iii
- Abbreviations .....vii
- 1. Introduction..... 1
  - 1.1. Salt marsh dynamics..... 2
    - 1.1.1. Vegetation dynamics ..... 3
    - 1.1.2. Hydrodynamics..... 5
    - 1.1.3. Morphodynamics..... 6
  - 1.2. Study area..... 7
    - 1.2.1. Location and background ..... 7
    - 1.2.2. The Marconi project ..... 8
  - 1.3. Problem definition..... 9
  - 1.4. Research objectives, questions and methods ..... 10
    - 1.4.1. Research objective ..... 10
    - 1.4.2. Research questions..... 10
    - 1.4.3. Research method ..... 10
  - 1.5. Outline thesis..... 11
- 2. Data collection and processing..... 13
  - 2.1. Data collection..... 13
    - 2.1.1. Overview measuring locations and methods ..... 13
    - 2.1.2. Hydrodynamic measurements ..... 15
    - 2.1.3. Surface elevation changes..... 16
    - 2.1.4. Vegetation measurements..... 18
    - 2.1.5. Soil samples ..... 19
  - 2.2. Data processing ..... 19
    - 2.2.1. Hydrodynamic measurements ..... 19
    - 2.2.2. Surface elevation changes..... 22
    - 2.2.3. Vegetation measurements ..... 22
    - 2.2.4. Soil samples ..... 23
    - 2.2.5. Multiple linear regression analysis..... 23
- 3. Results observed parameters..... 25
  - 3.1. Salt marsh profile ..... 25
  - 3.2. Surface elevation changes..... 25
  - 3.3. Hydrodynamics..... 28
    - 3.3.1. Inundation frequency ..... 28

3.3.2.	Flow velocities .....	29
3.3.3.	Significant wave height.....	30
3.4.	Vegetation and seedbank.....	32
3.4.1.	Vegetation characteristics .....	32
3.4.2.	Seed availability.....	35
4.	Explaining vegetation changes .....	37
4.1.	Input parameters.....	37
4.2.	Drivers for vegetation development .....	38
4.3.	Drivers for vegetation decay .....	40
4.4.	Relations between vegetation properties.....	42
4.5.	Drivers for seed retention .....	44
5.	Discussion .....	47
5.1.	Relevance of this research .....	47
5.2.	Implications and applicability.....	49
5.3.	Limitations .....	50
6.	Conclusion .....	53
6.1.	Drivers for vegetation development .....	53
6.2.	Relations between vegetation properties.....	53
6.3.	Drivers for vegetation decay .....	54
6.4.	Drivers for seed retention .....	54
6.5.	Impact of hydro- and morphodynamics on the vegetation decay and the seedbank.....	55
7.	Recommendations.....	57
	Bibliography.....	59
	Appendices .....	63
	Appendix A – Continuous surface accretion and erosion .....	63
	Appendix B – Input parameters regression analysis .....	64

# Abbreviations

ASED	Acoustic sediment elevation dynamics
CED	Critical erosion depth
Dev	Deviation
DGPS	Differential global positioning system
Fitlm	Fit linear regression model
MHWL	Mean high water level
PQ	Vegetation plot
RTK-GPS	Real time kinetic global positioning system
RWS	Rijkswaterstaat
SEB	Surface elevation bar
Std	Standard deviation
TCM	Tilt current meter
WL	Water level
cm	Centimetre
m	Meter
Min	Minutes
Mm <sup>3</sup>	Million cubic meters



# 1. Introduction

The sea level will rise in the upcoming decades due to climate change, which means that lower lying coastal areas have to protect themselves against the rising seawater. As climate change also causes an increasing number of storms with higher intensity, the salt marshes are under a lot of pressure (Duggan - Edwards et al., 2020). Salt marshes are very vulnerable to the changing climate, more specifically vulnerable to more frequent storms with higher intensity and a fast increasing sea level. Already about half of the global habitat of salt marshes is lost (Silliman et al., 2015; Van Loon-Steensma, 2015; Duggan-Edwards et al., 2020; Li et al., 2020). For a long time, the only solution to protect low-lying areas against flooding by rising water was heightening the dikes (Jonkman et al., 2013). Since the last two decades there is more and more interest in the use of coastal ecosystems to help defending against the rising water. The combination of bringing ecological value to the area, while protecting against flooding, and the ability to grow with sea level rise may be more effective and cost-efficient than the traditional solutions (Poppema et al., 2019; Finotello et al., 2020).

A salt marsh is an intertidal area at the coastline with salt-tolerant vegetation species. These intertidal areas are flooded during high tide and the aboveground part of the vegetation might reduce the waves and increase sedimentation rates at the marsh, while the roots prevent the bed from eroding. The specific vegetation partly depends on where the salt marsh is situated. Some species are naturally present in areas, for example in Europe salt marshes include the habitat of three different vegetation types. According to Esselink et al. (2019) the different variants of *Salicornia*, *Spartina* and Atlantic salt meadows are most common in Europe. The focus of this study is on *Salicornia Europaea* vegetation, which is one of the naturally common species in the northwest of Europe (Davy et al., 2011).

*Salicornia Europaea* is seasonal vegetation, meaning that plants die during autumn/winter and the vegetation cover density in summer is completely dependent on the number of seedlings and thus the number of seeds available in the seedbank. As the seeds of *Salicornia* are contained in the branches, the decay of the aboveground vegetation is an important parameter for the vegetation density in the consecutive year (Davy et al., 2011). For this reason, the development of the seedbank is an important parameter as well. To optimise the design and management of salt marshes, it is important to understand the aspects that play a role in the development and decay of the vegetation cover, including the development of the seedbank. To predict the development of salt marshes under certain hydro- and morphodynamics, numerical models are used. Simulations in numerical models can be used to predict the behaviour of salt marsh vegetation. To use these models for restoring and reclaiming salt marshes, a better understanding of the dynamics and development of salt marshes is needed.

## 1.1. Salt marsh dynamics

A salt marsh is an intertidal area at the coastline with salt-tolerant vegetation species, for example *Salicornia* or *Spartina* species, that will be (partially) flooded during high tide. Since the elevation in most salt marshes gradually increases landwards, the salt marsh can be divided in different zones. The pioneer zone at the front of the salt marsh is most frequently flooded and the high marsh zone is the least inundated area as can be seen in Figure 1.1. Due to the differences in inundation frequency, the dominant vegetation species differ. The vegetation in the pioneer zone are called pioneer species and can withstand more stresses than the species in the upper marsh. The *Salicornia* species is intertidal pioneer vegetation, meaning that they mostly grow in the pioneer zone, but can grow in other marsh zones as well.

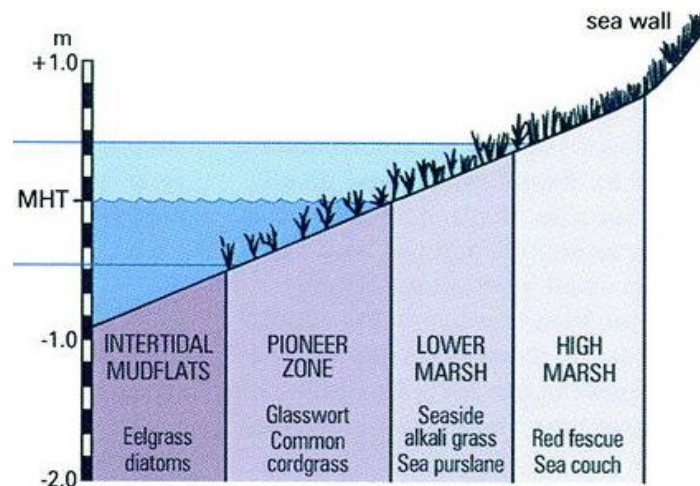


Figure 1.1: Zonation of salt marshes (Bakker et al., 2016).

The number of seedlings and therefore the amount of vegetation may be influenced by the hydrodynamics, however, in reverse, the vegetation might affect the hydrodynamics as well. This is called the biogeomorphological feedback loop visualised in Figure 1.2. Mature salt marsh vegetation, like *Salicornia*, obstructs the flow and currents, which may decrease the flow velocities and bed shear stresses (Temmerman et al., 2007; Hu et al., 2015). This encourages sediment accumulation resulting in an increasing bed level, increasing the accommodation space for intertidal vegetation.

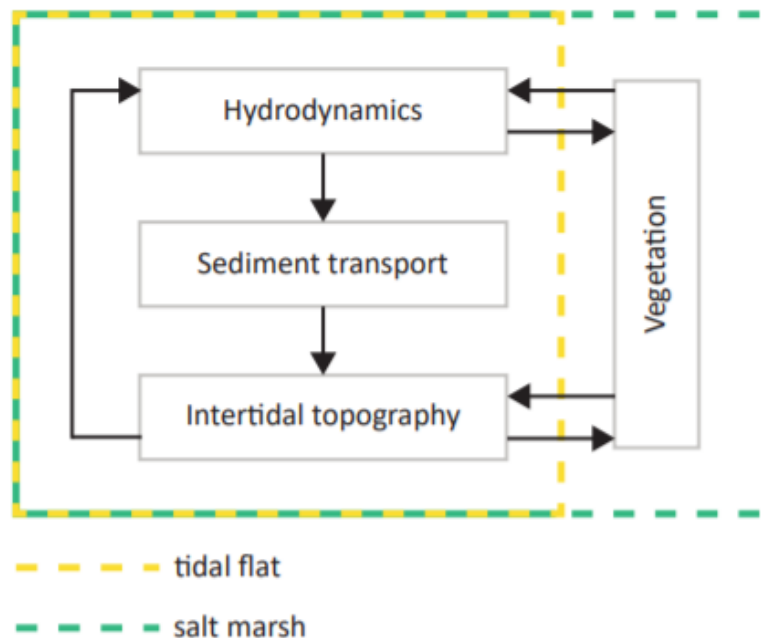


Figure 1.2: The biogeomorphological feedback loop explaining feedback (arrows) between hydrodynamics, morphodynamics (sediment transport and intertidal topography) and vegetation. Primary processes are highlighted with arrows. Biogeomorphological processes at the salt marsh comprise the full biogeomorphological feedback loop (green dashed box) (Willemsen, 2021).

### 1.1.1. Vegetation dynamics

The specific vegetation partly depends on where the salt marsh is situated. Some species are naturally present in areas, for example in Europe salt marshes include the habitat of three different vegetation types. According to Esselink et al. (2019) the different variants of *Salicornia*, *Spartina* and Atlantic salt meadows are most common in Europe. The focus of this study is on *Salicornia Europaea* vegetation, which is one of the naturally common species in the northwest of Europe (Davy et al., 2011).

The *Salicornia Europaea* species, presented in Figure 1.3, is a seasonal halophyte pioneer species. *Salicornia* (common glasswort) is one of the most salt tolerant plants, grows up to 35 cm and is fairly richly branched (Davy et al., 2001). The lowest branches may be nearly as long as the main stem. The colour changes over the seasons; from dark green becoming yellow-green and ultimately flushed pink or red (Davy et al., 2001; Hulisz et al., 2010). The *Salicornia* species is intertidal pioneer vegetation, meaning that they grow in partially flooded areas like the pioneer zone. These areas should have a minimum elevation of 0.5 m to 0.6 m below local MHWL (mean high water level) (Hu et al., 2015). Since the *Salicornia* is a seasonal vegetation species, the whole life cycle occurs in one year, meaning that the vegetation has to re-establish every year.



Figure 1.3: *Salicornia Europaea*, (left) whole bunch by Succulents (2015) and, (right) a close-up by (Hulisz et al., 2010).

In early spring a new population starts to develop with the germination of the seeds. The vegetation is very vulnerable during the first part of the germination, but once they are rooted in the ground, in late spring, the growth rate increases, because the plant becomes less vulnerable and is anchored in the ground. The plant reaches maturity in the end of summer where the flowering season ends (Balke et al., 2011). The growing stages of *Salicornia* are schematised in Figure 1.4. After maturity has been reached, the vegetation will start to decay during autumn and winter. The seeds are contained in the branches and the seeds are therefore less susceptible to being carried away by the waves and currents. When the branches break, the seeds may be transported to other locations, but they may also result in new germinations at the salt marsh. This growth cycle repeats itself each year.

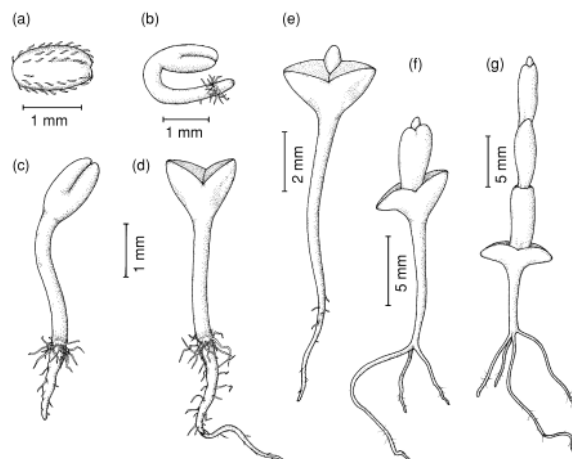


Figure 1.4: Germination and seedling development in *Salicornia Europaea* aggregation (a) seed, (b) germination, and (c-g) developing seedling (Davy et al., 2001).

The frequency of inundation has an effect on the germination of the *Salicornia* seeds and therefore on the density of the vegetation. If the area would be inundated continuously, the seeds do not have the time to germinate. Long inundation-free periods are most likely to occur when the high tide is declining, for example from spring to neap tide. These inundation-free periods may enable seedling establishment (Hu et al., 2015). As said before, the *Salicornia* seeds are very vulnerable, especially before rooting. Currents could carry the seeds away from the salt marsh into the sea. Therefore the establishment of seedlings needs a sufficiently long inundation-free period; the window of opportunity (WoO) (Hu et al., 2015). This window of opportunity is needed to give the seeds enough time to settle and germinate (Figure 1.5). Hydrodynamic forces may cause seedling failure due to erosion or sedimentation as seeds can get carried away by the currents (Hu et al., 2015). The water depth should be zero in WoO1, so the plants can develop roots to withstand stress of flooding. For *Salicornia* this first window of opportunity should be about 2.5 days (Hu et al., 2015). The stress a seedling can withstand increases slowly during the second window, while during the third window the limit remains the same. The second and third windows are defined in terms of bed level dynamics. If the long-term sedimentation rate is higher than the growth rate of the plant, the plant will be buried and thereby fail. While, conversely, if the long-term erosion rate is larger than the growth rate of the roots, the roots will be uncovered, also leading to failure (Temmerman et al., 2007; Hu et al., 2015; Poppema, 2017; Schwarz et al., 2018).

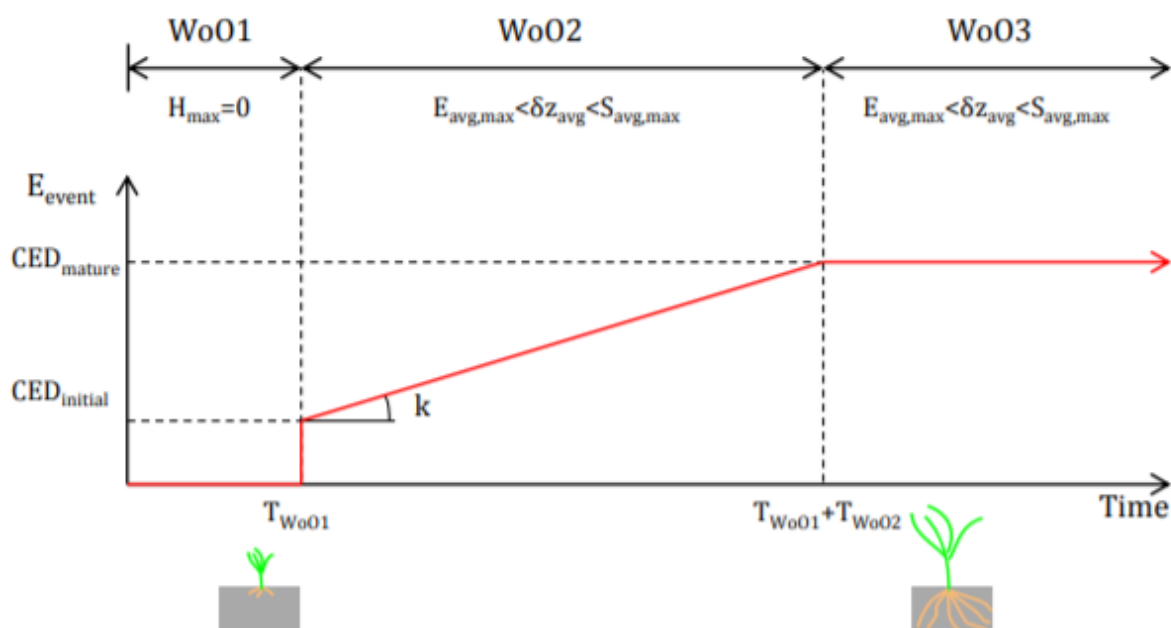


Figure 1.5: Schematisation of the Window of Opportunity (horizontal axis not on scale). In WoO1, the inundation depth should be zero. In WoO2 and WoO3, the average bed level change during a plants life should be between the erosion limit and sedimentation limit. Furthermore, the short-term erosion should be less than the CED. This CED depends on plant age for WoO2 and is constant for WoO3 (Poppema, 2017).

### 1.1.2. Hydrodynamics

The tidal currents may impact the vegetation on the salt marsh. The tidal cycle takes about 12:25 hours, indicating that high tide and low tide happen about two times a day. Therefore, the lower parts of a salt marsh are on average inundated twice a day, whereby high tide also delivers sediments into the marsh. When the tide is increasing, the currents will be towards the salt marsh. If the tide is receding (ebb) the currents might follow the creeks, if present, towards the sea.

Besides the inundation, it is also important to gain knowledge of the other hydrodynamic forces to understand and predict vegetation establishment and decay processes. Hydrodynamic forces may cause seedling failure due to erosion or sedimentation or by carrying the seeds away before the seeds are rooted (Hu et al., 2015). Flow velocities and wave height are, for example, hydrodynamic forces that might affect the marsh and/or vegetation growth. High flow velocities may be caused by either high tidal differences or by waves due to a storm or a steep slope at the seaside of the salt marsh (Temmerman et al., 2013). A steep slope causes higher waves since the energy of the waves coming in remains almost the same, there is only a small decrease caused by friction. Since the water depth is decreasing rapidly and the amount of energy remains the same, the wave height will increase (Bartholdy, 2012). This increase in wave height, called wave run-up, causes an increase of the near-bed velocities, which then increases the shear stresses near the bed.

Artificial structures in the nearshore can influence the flow, currents and the impact of waves. To protect a salt marsh against larger waves and/or storms sometimes a small permeable structure (e.g. a brushwood fence) may be built around the salt marsh. These permeable structures reduce the energy of waves for large parts of the salt marsh, but the flow velocities will increase at parts where the openings are placed. The openings or gaps in the permeable structure are created to retain the salt marsh as an intertidal area, that may be (partially) flooded during high tide. The structures are placed to protect the vegetation from incoming waves and currents by decreasing the flow velocities, which decreases the near-bed stresses as well (Li et al., 2020). Since the flow velocities on the salt marsh will decrease, this will also increase the deposition, which might positively affect the vegetation growth and establishment. These wave damping measures decrease the number of waves affecting the vegetation growth as well as the amount of erosion, increasing the amount of seed establishment as Poppema et al. (2019) stated.

### 1.1.3. Morphodynamics

Tidal currents may influence the bed dynamics as it increases the near-bed velocities, which increases the bed shear stresses (Duggan-Edwards et al., 2020). Depending on the height of the tidal fluctuations and the local water depths, these currents can have stronger or less strong impacts on the deposition/erosion on the salt marsh (Hu et al., 2015). When tidal fluctuations are low, the assessment of the hydrodynamics indicates that the flow field has a limited influence on the seeds and vegetation cover. Likewise, if the shear stress of the tidal current exceeds the critical bed shear stress, this would cause erosion. Therefore it is more likely that water depth and flow velocity have more influence when tidal amplitudes increase (Li et al., 2020).

The waves play an important role in marsh dynamics in terms of bed shear stress (Hu et al., 2011; Duvall et al., 2018). Vegetation may reduce this effect since it reduces the near-bed forces created by the waves and may increase the cohesiveness of the sediment by the increasing strength of the roots (Duggan-Edwards et al., 2020). In the summer, the weather is mostly calmer resulting in lower hydrodynamic forces and thus settling of sediment. If the vegetation is large enough, the settled sediment may remain in the salt marsh during winter depending on the present hydrodynamic forces (Callaghan et al., 2010).

Additionally if the height of the bed level increases, the slope on the seaside of the salt marsh may steepen, which also results in an increasing wave height. This may eventually lead to a shrinking salt marsh. A resilient salt marsh has the ability to at least expand, mostly during summer, as much as it shrinks, mostly during winter (Temmerman et al., 2013; Duvall et al., 2018). An increasing bed level means that the salt marsh is more protected and resilient against sea level rise.

The vegetation may trap the sediment either directly, by trapping the sediment around the stem or at the plant, or indirectly, due to the reduced flow velocities (Best et al., 2018; Poppema et al., 2019). This results in reduced near-bed velocities and currents, which makes it possible for the sediment to settle. This results in a growing and expanding salt marsh and vegetation cover. However, when there are higher waves, causing an increase in orbital flow velocity, less sediment will settle since the sediment remains in suspension. The sediment remains in suspension because the bed shear stress exceeds the critical bed shear stress for deposition and might be transported away when the tide recedes (Bartholdy, 2012).

Flow velocities can differ a lot when the vegetation is fully grown around summer. When low or high tide is approaching, the vegetation obstructs the retracting or rising water. However, the water puts a certain load on the vegetation due to the forces of the tidal current (Temmerman et al., 2007). When high tide is approaching, the tidal current will be towards shore causing the vegetation to slightly bend towards shore as well. On the other hand when low tide is approaching, the tidal current will be offshore causing the vegetation to slightly bend seawards as well. These tidal currents move the vegetation above the bottom influencing the sediment around the trunk. Local erosion or scour holes around the trunk may occur, see [Figure 1.6](#), which indicates the obstruction of flow by the vegetation (Temmerman et al., 2007).

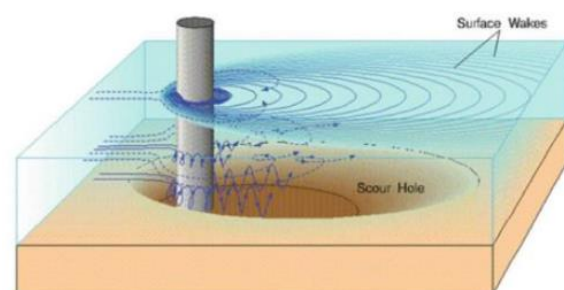


**Figure 1.6:** This schematisation shows the formation of a local scour hole around a pile. This works the same way for vegetation (Abd El Samee & Elsamny, 2019).

## 1.2. Study area

### 1.2.1. Location and background

This study focusses on the Marconi salt marsh, located in the northeast of the Netherlands next to the village of Delfzijl as can be seen in [Figure 1.7](#). This artificially created salt marsh is researched to create a better understanding of the impact of different dynamics impacting the behaviour of salt marshes, especially in areas where salt marshes do not occur naturally. This knowledge could be used for future construction of salt marshes that reduces the necessary dike height for protecting the hinterland, while adding a lot of ecological value to the environment.

The Marconi salt marsh is located in the Ems-Dollard estuary which has a surface area of 467 km<sup>2</sup> (Dankers et al., 2012). Almost the whole estuary is surrounded by dikes, only the part where the Ems enters the estuary and the connection with the Wadden Sea are open. In the area, different dams and dikes are built to conduct the flows, among which the dike (the Schermdam) that created the Zeehavenkanaal in 1971-1972. Since 1975, 3-5 Mm<sup>3</sup> silt is dredged each year to retain the water depth for shipping from the three harbours; Eemshaven, Emden and Delfzijl (Dankers et al., 2012). There is a gradual gradient in salinity, salt water at the Wadden Sea gradually mixing over the area with the fresh water entering from the river the Ems. The average annual discharge of the river Ems is about 110 m<sup>3</sup>/s, but strongly varies per year and during the seasons in a year (Dankers et al., 2012).



**Figure 1.7:** Location of the study area, where the orange square marks the location of the artificial salt marsh. In the right-upper corner the location of the main picture is visualised (Maps, 2021).

The tidal range in the area differs a lot, from 2.4 m near Borkum to 3.2 m near Emden. These locations are shown in [Figure 1.8](#). The amount of water that flows in and out of the area per half tide is about 1000 Mm<sup>3</sup> (Dankers et al., 2012). The Ems-Dollard estuary is dissected by a few navigation channels for shipping, so that ships can enter the ports. The tidal fluctuations have become larger over the years due to the deepening of the navigation channels, sea level rise and subsidence caused by natural gas extraction near Slochteren.

Along the southside of the Dollard, indicated with the small dots in [Figure 1.8](#), wide fringes of salt marshes are found counting for almost 8% of the Dollard area (Dankers et al., 2012). There is only natural occurrence of salt marshes upstream in the Dollard part of the estuary. Since salt marshes are very vulnerable for storms, they will only naturally occur at sheltered places. As can be seen in [Figure 1.8](#), the naturally occurring salt marsh in the Ems-Dollard estuary lies very sheltered for storm waves entering from the Wadden Sea. This area is therefore less exposed to high waves, increasing the survivability of the vegetation and decreasing the amount of erosion.

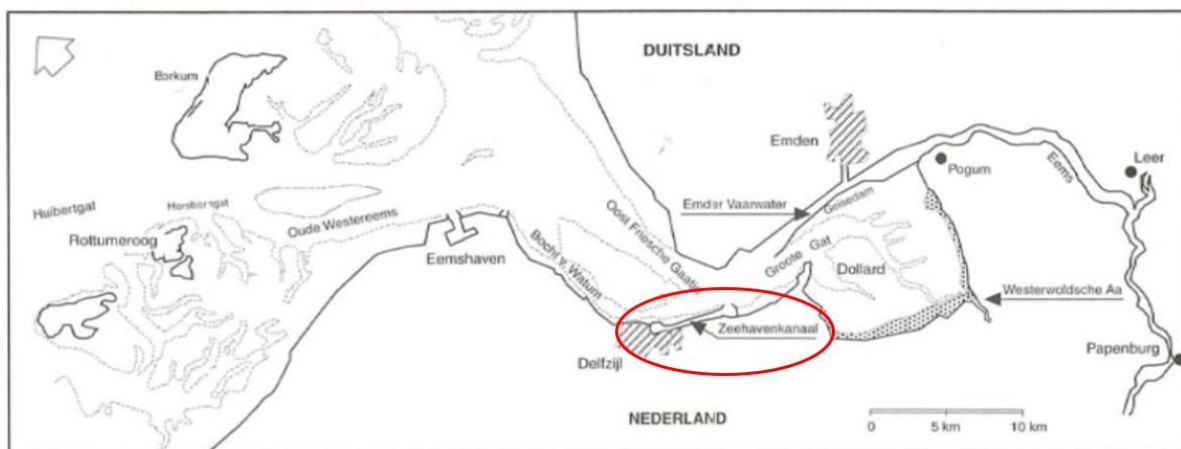


[Figure 1.8](#): Map of the Ems-Dollard estuary. Wherein the red circle shows the location of the Schermdam and the Zeehavenkanaal at the southside of the Schermdam (Dankers et al., 2012).

### 1.2.2. The Marconi project

At the northern side of the manmade dike ‘the schermdam’, that created the Zeehavenkanaal at Delfzijl, a pilot project of an artificially created salt marsh has been finalised in November 2018: the Marconi salt marsh. The Marconi salt marsh has been used as study site in this study to develop a greater understanding of the development of salt marshes and use this understanding in future salt marsh creation (Baptist et al., 2018). Measurements are continuously taking place and data is analysed to understand the behaviour of the salt marsh and the *Salicornia* vegetation species (Baptist et al., 2018).

To create the Marconi salt marsh different silt concentrations were mixed through the upper meter of the sediment, creating areas with different soil characteristics. [Figure 1.9](#) shows the different areas with different percentages of silt. This study will focus on the test areas E and G, which are about the same size (216 m x 85 m). The bed in area E consists of 50% silt and the bed in area G of 5% silt. Furthermore, every area is divided in two same sized areas, a sown and a not sown part. This has been done to see whether sowing contributes to a quicker vegetation establishment at the marsh.

The Marconi salt marsh is way more exposed to waves entering from the Wadden Sea than the natural occurring salt marshes in the south of the Dollard estuary. To protect the salt marsh against larger waves, small permeable brushwood fences, marked as brown lines in [Figure 1.9](#), were built around the salt marsh. These permeable structures reduce the energy of waves and the influences of the currents

for large parts of the salt marsh. The permeable brushwood structure is only interrupted at the openings, which function as a funnel for the tidal in- and outflow.

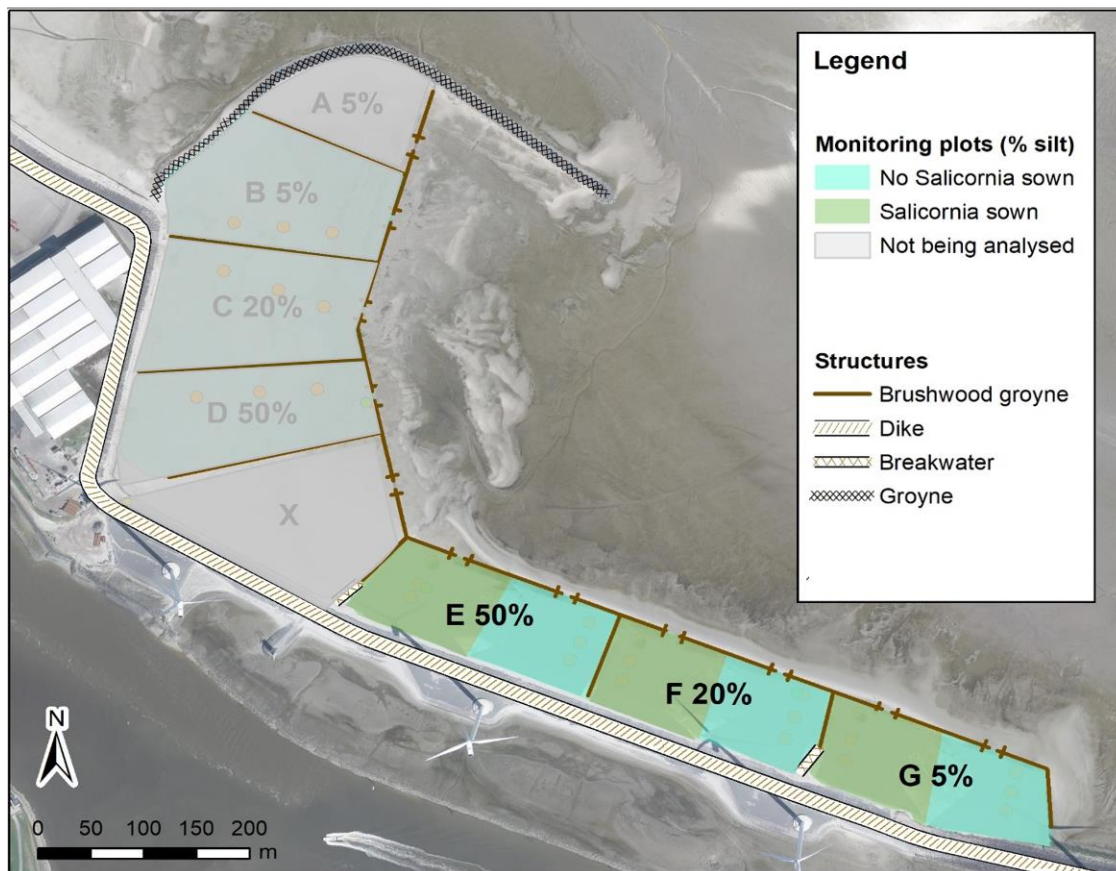


Figure 1.9: Top view of the pilot project of the artificially made salt marsh Marconi with the different areas and silt concentrations. The figure is modified from Willemsen (2020).

### 1.3. Problem definition

Salt marshes are very vulnerable to the changing climate, more specifically vulnerable to more frequent storms with higher intensity and a fast increasing sea level. Also a decrease of the sedimentation rate could affect existing salt marshes, which might be caused by increasing waves and currents (Callaghan et al., 2010). A sustainable or self-organising salt marsh has the ability to grow with the rising sea level and withstand the storms that affect the salt marsh.

A lot of research studies have been done to understand the behaviour of the hydrodynamics and morphodynamics on a salt marsh and their influences on different vegetation species and vice versa. Most studies focus on the growing and flowering seasons, but lack insight in the degradation and seedbank processes (Schwarz et al., 2018; Van Regteren et al., 2019). As *Salicornia Europaea* is seasonal vegetation, the degradation of the vegetation cover and the development of seedbank are important parameters for the vegetation cover in the subsequent summer period. Currently, numerical models apply a sudden decay of *Salicornia* vegetation, from a fully grown vegetation cover at the end of summer to zero vegetation at the start of winter, while the seed availability is simulated as a constant random number each year during spring. These assumptions may lead to incorrect predictions as they do depend on the presence of vegetation and the different hydro- and morphodynamics, rather than that they are the same every year at all marshes. According to Schwarz et al. (2018) and Van Regteren et al. (2019) there is an increasing trend in seed availability once vegetation has been established in former years and the decaying process of the *Salicornia* vegetation

happens much smoother. Therefore, the main aims of this research are to parameterise the vegetation decay as well as the seed retention with the local hydro- and morphodynamics, like flow velocities, wave height, surface elevation changes and inundation frequency. These parameterisations can be used to predict the development of the seedbank, and with this the development of the vegetation cover in summer, and subsequently the vegetation decay in winter.

## 1.4. Research objectives, questions and methods

In this section the research objectives of this study, the research questions and the research methods are described.

### 1.4.1. Research objective

This research aims to provide an understanding on the development of *Salicornia* vegetation at salt marshes. The main objectives of this study are to parameterise the vegetation decay as well as the seed retention with the local hydro- and morphodynamics, like flow velocities, wave height, surface elevation changes and inundation frequency. These objectives function as the base for the main research question, which is:

*How do the Salicornia development and decay as well as the seedbank correlate with flow velocities, wave height, surface elevation changes, inundation frequency and sediment composition on a salt marsh throughout the winter period and how do the vegetation characteristics correlate with the Salicornia decay and seedbank?*

### 1.4.2. Research questions

Four research questions have been compiled, to help answering the main research question.

1. How do wave height, surface elevation changes, inundation frequency and sediment compositions affect the *Salicornia* vegetation cover on the Marconi salt marsh at the end of summer?
2. How does the vegetation density decay correlate with the vegetation properties, like strength, length, root length, number of side roots and length of the longest side root throughout the winter period (November to April)?
3. How does the vegetation density decay correlate with the hydrodynamic exposure and morphodynamic activity throughout the winter period (November to April)?
4. How does the seed availability change throughout the winter period (November to April) and does the seedbank relate to vegetation density, hydrodynamic exposure, morphodynamic activity and sediment composition?

### 1.4.3. Research method

During the winter period (November 2020 till April 2021) hydro- and morphodynamic and vegetation data has been collected at the artificially created Marconi salt marsh. The data from the physical processes that has been collected are: the flow velocities, wave height, water depth and bed level changes. The vegetation characteristics that have been measured are: vegetation density, strength, length, root length, number of side roots and length of the longest side root. The water level has been measured by a monitoring station from Rijkswaterstaat. The vegetation density and the physical processes of the summer period (April 2020 till September 2020) have been collected from earlier research at Marconi and from Rijkswaterstaat.

The flow chart of the research method used in this study is presented in [Figure 1.10](#). At first, all of the needed data has been collected from either other sources or in the field with measurement devices.

Secondly, the data from these devices needs to be processed to create usable data for this research. Once all the data was processed the data is used for further analysis. The first step of this analysis is to describe the properties of the study area with respect to the hydrodynamics, morphodynamics and vegetation dynamics. This is done by either measuring or calculating, at multiple locations at the salt marsh, the following variables: inundation frequency, flow velocities, wave height, bed level changes, seed availability, vegetation density and other vegetation characteristics (Figure 1.10). The second step of this analysis, is to explain the development and decay of *Salicornia* and the seed availability with the different physical processes. This has been done with a multiple linear regression analysis (MLR), which will be explained in section 2.2.5. The third and last step of this analysis, is to create parameterisations that show significant explanations of the observed variability of the vegetation cover. These parameterisations could be used to predict the vegetation density decay and the establishment of seedlings more accurately based on the local hydro- and morphodynamic forces.

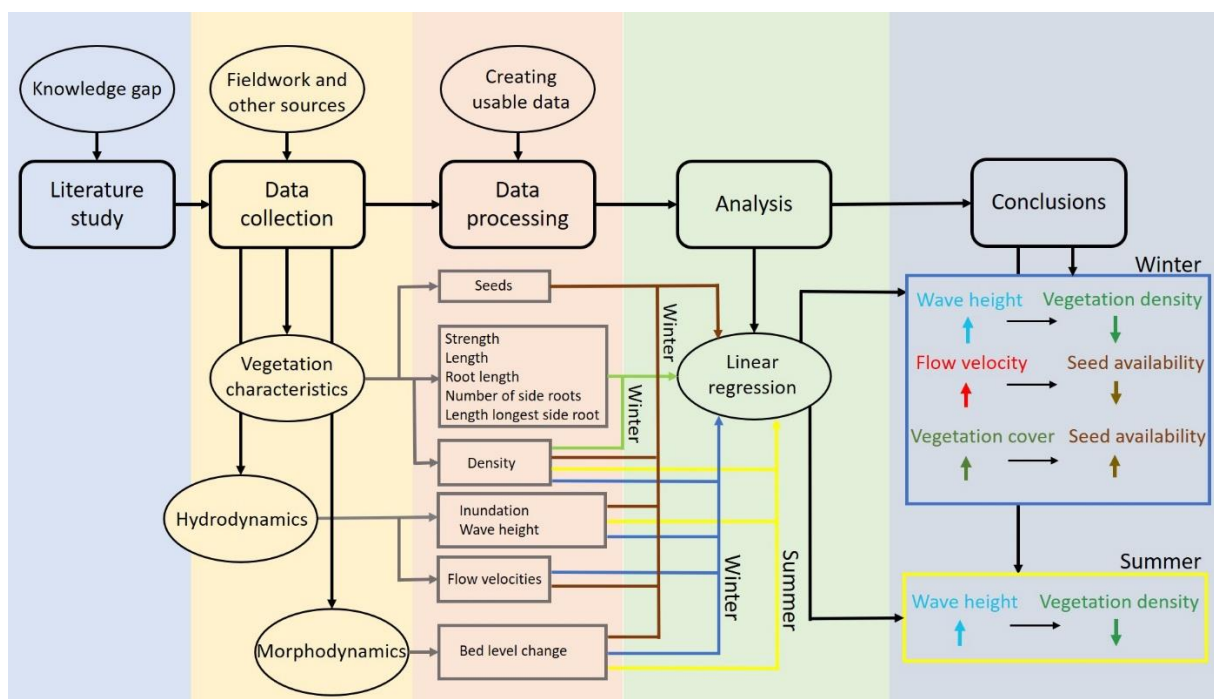


Figure 1.10: Flow chart of the research method in this study, including the parameters that have been researched. Coloured lines represent different multiple linear regression analysis. The multiple linear regression results of (1) the braun line are the relations of seed availability with the flow velocity and the vegetation cover, (2) the blue line is the relation of the wave height on the vegetation density in winter and (3) the yellow line is the relation of the wave height on the vegetation density in summer. The green line says something about the relation in vegetation properties with the vegetation density.

## 1.5. Outline thesis

In chapter 2 the data collection and data processing used in this study will be explained. In this chapter, the functioning of the measurement devices and a short description about the steps taken to transform the measured data into aggregate statistics that can be used for further analysis are explained. Chapter 3 presents the results of the measured hydro-, morpho- and vegetation dynamics in the field. These results are combined into different regression analysis in chapter 4. Whereafter in chapter 5 the relevance, implications and applicability and the limitations of this study will be discussed. The report finishes with a conclusion in chapter 6 and some recommendations in chapter 7.



## 2. Data collection and processing

To be able to study the seasonal variation in salt marsh vegetation a field campaign has been set up to collect and enhance the current datasets. The data were collected at a 4- to 5-week interval during the winter months of November 2020 to April 2021. This chapter consists of two sections: data collection and data processing. At first an overview of all field measurements has been given, whereafter a short description of their functioning is described in section 2.1. Thereafter, in section 2.2., the data analysis and processing steps are given per measured or calculated parameter.

### 2.1. Data collection

To understand the physical properties of the salt marsh, different measurement devices were used for the collection of data. These devices have been setup differently and are explained in the following sections. An overview of the measuring methods is presented in [Figure 2.1](#) and in section 2.1.1.

#### 2.1.1. Overview measuring locations and methods

An overview of the field measurement locations is presented in [Figure 2.1](#) and the field measurements are presented in [Table 2.1](#). An overview of the continuously measured data by Rijkswaterstaat and the already measured parameters of the summer of 2020 can be found in [Table 2.2](#). The used data from Rijkswaterstaat has been collected at monitoring station 'Delfzijl'. The data is freely accessible through the website of Rijkswaterstaat (<https://waterinfo.rws.nl/>).

The hydrodynamic forces that may affect the decay of the vegetation at the salt marsh are presented in [Figure 2.1](#) and listed in section 2.1.2. with the method of how this data has been retrieved. The devices that measure the hydrodynamic forces are placed close to the seaside vegetation plot of the marsh areas, as these devices have to be submerged to measure the hydrodynamics. This does not happen frequently enough at the middle part or landside of the marsh (De Vries et al., 2021). Moreover, the ASEDs measuring at the entrance and in front of the marsh are placed in area F. This is in between the seeded parts of area E and G and serves as an indication of the forces at the entrances and in front of the marsh of area E and G as well.

Measuring the elevation of the salt marsh has been done to create a clear overview of the surface elevation changes at the salt marsh, which are presented in [Figure 2.1](#) listed in section 2.1.3. The surface elevation changes may influence the location where the vegetation might grow or may explain the degradation of the vegetation at certain areas. Therefore, the surface elevation will be measured at the previously installed locations with the SEB, so it can be compared with former research at Marconi. Secondly, the surface elevation is measured close to the seaside vegetation plot of the marsh areas with the ASEDs as the measuring head of the ASED needs to be submerged before it starts measuring.

The vegetation decay at the marsh has been measured to create an understanding of the decaying process of *Salicornia*, which might affect the development of the marsh. The way of measuring is described in section 2.1.4. In [Figure 2.1](#) it can be seen that there are 18 vegetation plots created, nine in area E and nine in area G. The vegetation plots at the SEBs were already used in former Marconi research. The other 2 vegetation plots, at the same alongshore transect as the SEB vegetation plot, serve as replicates, to minimise the effects of local deviations as much as possible. The locations of these replicate vegetation plots have been chosen parallelly to the already existing vegetation plots at the SEBs. The exact location of the replicates may vary a bit from this parallel line, since there is also visually assessed whether the vegetation in the replicate is representative for that part of the area.

The seeds have been collected to create an overview of the amount of seeds in the seedbank throughout the winter period. The collection method has been described in sections 2.1.5. and the same vegetation plot locations have been used, presented in [Figure 2.1](#).

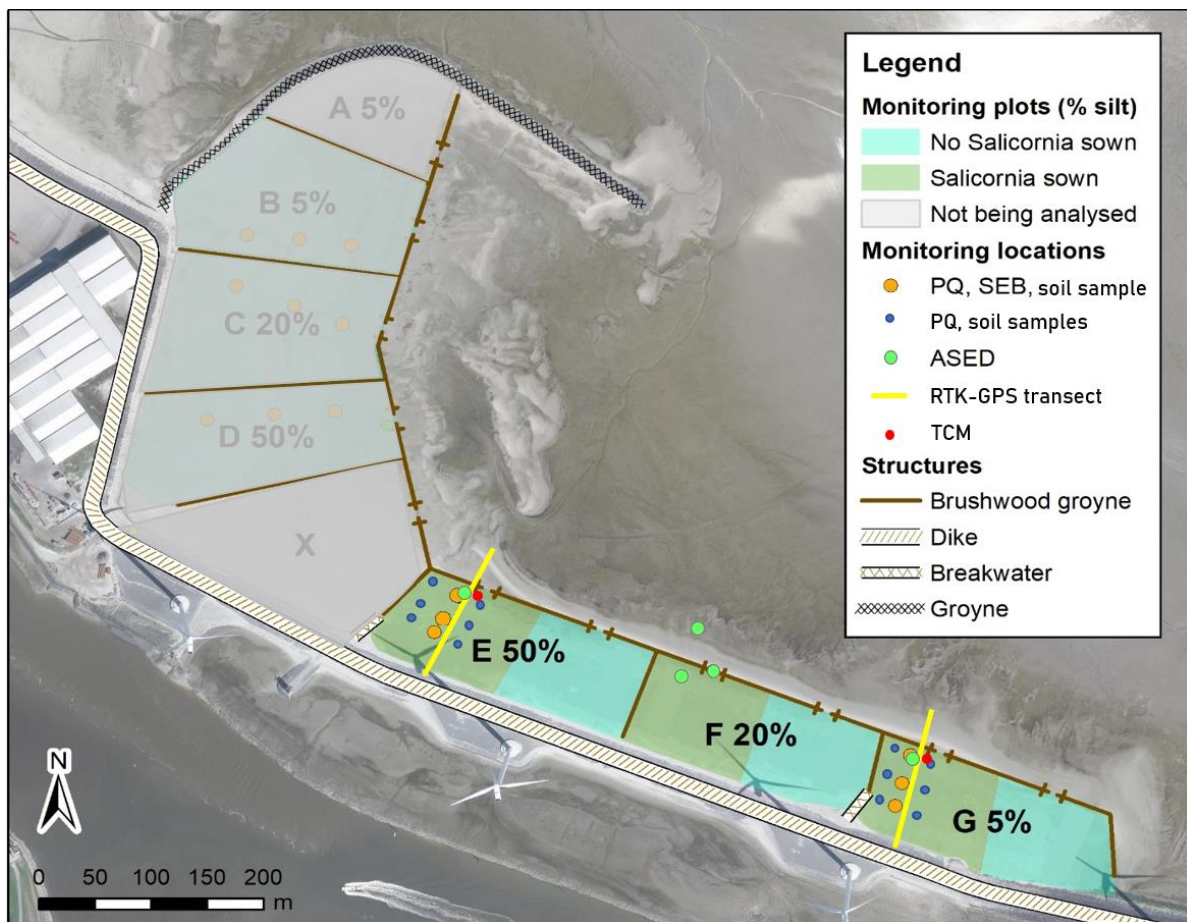


**Figure 2.1:** Top view of the pilot project of the artificially made salt marsh Marconi with the different areas, silt concentrations and measurement locations. The figure is modified from Willemssen (2020).

**Table 2.1:** Overview of the field measurements.

Device	Variable	Frequency	Period	Number of locations
ASED	Bed level change Wave height Water depth	15 min	22 December 2020 – 23 April 2021	5 (in area E, F and G, at the entrance of F and in front of the marsh)
TCM	Flow velocity	15 min	22 November 2020 – 23 April 2021	2 (at the entrance of area E and G)
SEB	Local bed level change	Once a month	22 November 2020 – 23 April 2021	6 (3 per area)
RTK-GPS	Bed level profile	Once per 2 months	22 December 2020 – 23 April 2021	2 transects (along the SEBs in area E and G)
Spring balance/ tapeline	Vegetation characteristics	Once a month	22 November 2020 – 23 April 2021	18 (9 plots per area)

Table 2.2: Overview of used data from other sources.

Source	Variable	Frequency	Period or day(s)	Number of locations
Rijkswaterstaat (station Delfzijl)	Water level	10 min	1 April 2020 – 23 September 2020	1 (station close to Delfzijl)
Former Marconi research (De Vries et al., 2021)	Bed level change Wave height Water depth	15 min	1 April 2020 – 23 September 2020	5 (in area E, F and G, at the entrance of F and in front of the marsh)
Former Marconi research (De Vries et al., 2021)	Local bed level change	Once per 2 months	1 April 2020 – 23 September 2020	6 (3 per area)
Former Marconi research (De Vries et al., 2021)	Density	Once	23 September 2020	6 (3 per area)

## 2.1.2. Hydrodynamic measurements

### 2.1.2.1. Acoustic sediment elevation dynamics pressure sensors

The acoustic sediment elevation dynamics (ASED) sensors are used at the marsh to measure the wave heights during the measurement period from 22<sup>th</sup> of December 2020 till the 23<sup>th</sup> of April 2021. The ASEDS are set at a burst interval of 15 minutes and have therefore a temporal resolution of half an hour. Three ASEDS were placed at the seaside of the marsh of area E, F and G, one ASED is placed in the entrance of area F and one is placed in front of the marsh at area F, as can be seen in [Figure 2.1](#).

The acoustic sediment elevation dynamics sensor is mostly used to observe bed level changes, however, it can also be used to measure the height of the waves. The ASEDS were installed downward looking, with the measuring head aimed vertically at the bottom, as can be seen in [Figure 2.2](#). ASED sensors only collect measurements once the measuring head is fully inundated (De Vries et al., 2021). The ASED measures the pressure in a burst of eight measurements during every 15 minutes. Since the water pressure has a linear increase it can calculate the amount of water above, if the air pressure has been subtracted from this pressure.

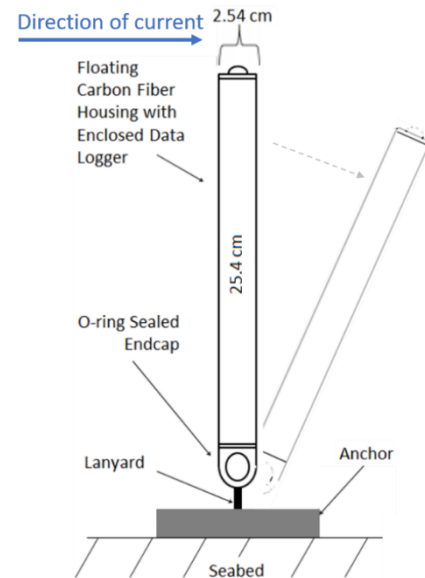


Figure 2.2: Setup example of ASEDS in the field by Mus (2019).

### 2.1.2.2. Tilt current meter

Tilt current meters (TCMs) are used at the salt marsh to measure flow velocities in the x- and y-direction during the measurement period from the 24<sup>th</sup> of November 2020 till the 23<sup>th</sup> of April 2021. The TCMS are set at a burst interval of 15 minutes and have therefore a temporal resolution of half an hour. Two TCMS have been placed at the entrance of area E and area G, as can be seen in [Figure 2.1](#), close to the ASED sensors. Since these stations are positioned close to each other, the flow velocities should be similar to those at the ASEDS.

The TCMs are anchored with a pavement tile to prevent the TCM from moving while the marsh is inundated. The TCM-4 has a length of 25 cm and is able to operate in 30 cm of water, in [Figure 2.3](#) a schematic view of the TCM-4 can be seen. The tilt current meter is buoyant and moves with direction of the flow, with higher flow velocities the TCM will be pushed more skew and measures higher flow velocities. The TCM registers the bearing and tilt, which is used to extract the flow velocities and flow directions. The device measures all the time and since the device is buoyant it lies horizontal on the ground while the marsh is not inundated and therefore measures extremely high flow velocities when not submerged. The tilt current meter measures the flow velocity at the bottom till 25 cm above the bottom, therefore this could be interesting for the sediment transport, but could also indicate why vegetation might be lost or not be lost at certain areas.



[Figure 2.3](#): Schematic principle of the working of the TCM-4 device. Figure is adjusted from LLC (2019).

### 2.1.3. Surface elevation changes

#### 2.1.3.1. Acoustic sediment elevation dynamics sensor

The acoustic sediment elevation dynamics (ASED) sensors are used at the marsh to measure the elevation changes during the measurement period from 22<sup>th</sup> of December 2020 till the 23<sup>th</sup> of April 2021. The ASEDS are set at a burst interval of 15 minutes and have therefore a temporal resolution of half an hour. Three ASEDS were placed at the seaside of the marsh of area E, F and G, one ASED is placed in the entrance of area F and one is placed in front of the marsh at area F, as can be seen in [Figure 2.1](#).

The acoustic sediment elevation dynamics sensor measures the propagation time of an acoustic signal reflected by the bed. The reflection of the signal by the bed is detected by a sudden increase in amplitude (Mus, 2019). The setup of the ASEDS are explained in the section “Acoustic sediment elevation dynamics pressure sensor”. ASED sensors, visualised in [Figure 2.2](#), only collect measurements once the measuring head is fully inundated (De Vries et al., 2021). In this way the changes in bed level can be obtained since the measuring head stays at the same height, but the distance towards the bottom might change. These changes are the changes in sediment elevation; an increase in distance to the bottom shows erosion, while a decrease in distance shows sedimentation.

#### 2.1.3.2. Surface elevation bar

The surface elevation bar (SEB) is used at the marsh to manually measure the elevation changes during the measurement period from 24<sup>th</sup> of November 2020 till the 23<sup>th</sup> of April 2021. The SEBs are used once a month on the fieldwork days and have therefore a resolution of 2 months. The SEBs were already installed when the marsh was constructed and are located at the areas between the brushwood dams. For this study the six SEBs in the seeded areas have been used, three SEBs in area E and three in area G, these are visualised in [Figure 2.1](#).

The sedimentation erosion bar is a simple device consisting of a two meter long bar with 17 holes and two fixed poles where the bar can be placed on, as can be seen in [Figure 2.4](#). With a measuring stick, through each hole, the height will be measured of that specific location. This makes sure that the exact same location is measured every time and gives a good indication of the amount of sedimentation/erosion during the former month in that area. The 17 locations are used for averaging of spatially variable sedimentation/erosion patterns. Moreover, it gives insight in the unevenness of the bed.

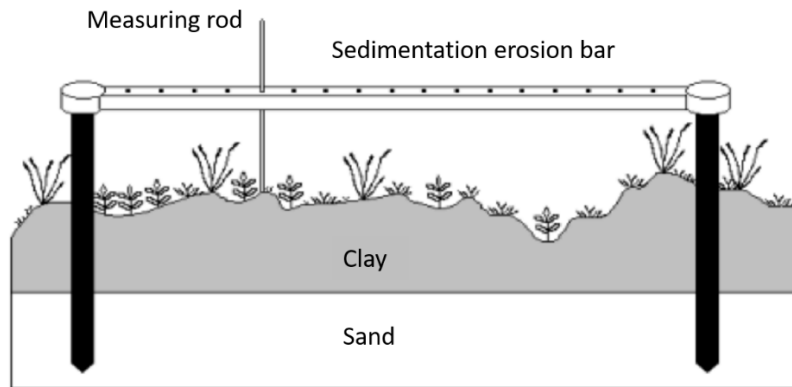


Figure 2.4: Sedimentation Erosion Bar (SEB) (Baptist et al., 2018)

### 2.1.3.3. Real time kinematic global positioning system

The real time kinematic global positioning system (RTK-GPS) is used at the marsh to measure the elevation changes during the measurement period from 22<sup>th</sup> of December 2020 till the 23<sup>th</sup> of April 2021. The RTK-GPS is used at three fieldwork days during this field campaign: the 22<sup>th</sup> of December 2020, the 22<sup>th</sup> of February 2021 and the 23<sup>th</sup> of April 2021. At every fieldwork day, two transects have been measured; one in area E and one in area G. These transects are visualised in [Figure 2.1](#).

The real time kinematic global positioning system is a satellite navigation technique used to enhance precision of the position derived from satellite-based positioning systems. The RTK-GPS is connected to at least three satellites and the portable GPS is called a rover GPS. The rover GPS also calls in on a local levelling network which is connected to a base receiver that corrects the distance errors from the satellites. In [Figure 2.5](#) this system is visualised. These distances combined with the correction of the base station gives an exact location and elevation of the point that is measured. Compared to the standard differential global positioning system (DGPS) this gives a resolution of a factor 10 to 100 higher. In numbers this increases the accuracy from 2-4 m with DGPS to centimetres with RTK-GPS.

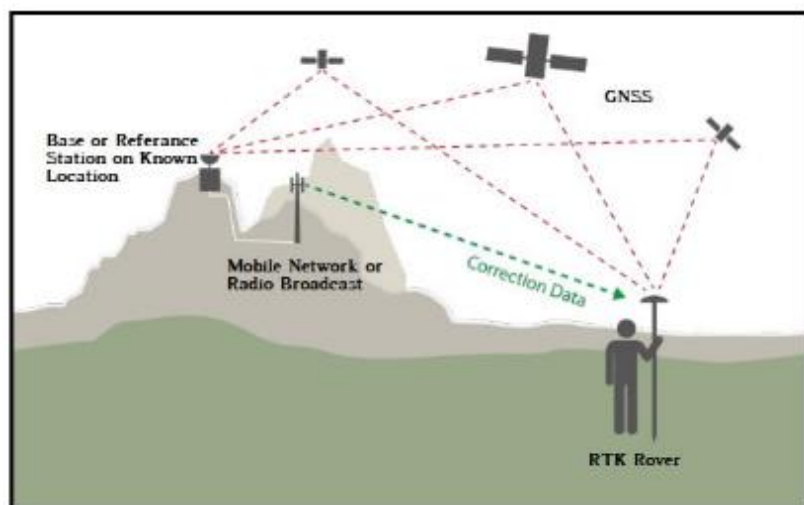
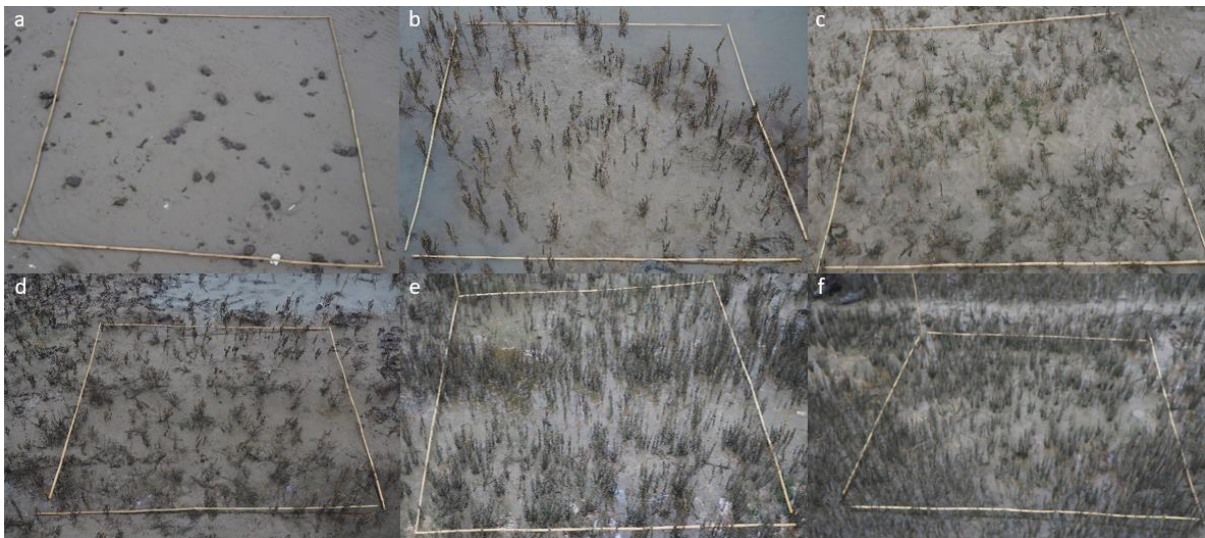


Figure 2.5: Explanation of the RTK-GPS system (DATGNSS, 2021).

### 2.1.4. Vegetation measurements

Characteristics of the vegetation have been measured or estimated during the measurement period from 22<sup>th</sup> of November 2020 till the 23<sup>th</sup> of April 2021 to create a better understanding about the decaying process of *Salicornia*. The percentage ground cover of the vegetation has been estimated. Moreover, the anchoring strength, above- and belowground length, the number of roots and the length of the longest side root of the vegetation have been measured. The vegetation characteristics are measured once a month on the fieldwork days in vegetation plots of 2 m by 2 m. For this study 18 vegetation plots (PQs) are created, nine in area E and nine in area G, locations are visualised in [Figure 2.1](#).

The amount of vegetation cover has been estimated visually in the 2 by 2 meter plots, examples and the estimated vegetation density can be found in (the caption of) [Figure 2.6](#). Markers were placed in the field at the start of the monitoring period and were revisited during each consecutive measurement to make sure the same vegetation plots were monitored through time. These visual estimations have been taken according to the decimal scale (Londo, 1976). To make sure that there is consistency between the estimations, the same researcher has estimated the cover at all fieldwork days. Furthermore, the estimations were always done after walking around the plot to get a complete impression of the vegetation cover from all sides.



**Figure 2.6:** 6 examples of vegetation plots used for estimating the vegetation cover. The estimated vegetation density is (a) 0%, (b) 5%, (c) 10%, (d) 15%, (e) 30% and (f) 40%.

The other characteristics have been measured from plants close by the vegetation plots, to make sure that these plants are similar to the plants inside the vegetation plot. The anchoring strength of the vegetation was measured with help of a spring balance, which is presented in [Figure 2.7](#). This device measures the force required to pull out the vegetation in Newton and has a resolution of 0.25 N. This anchoring strength can be used as a proxy for the hydraulic forces a single plant can withstand. This was done by hand with 5 representative plants per vegetation plot, so 45 plants per area per field visit. These plants were also used to measure the length above- and belowground, the number of side roots longer than 2 cm and the length of the longest side root. These characteristics might explain or give more information about the decaying process of *Salicornia* and have a resolution of a few millimetres to 1 cm, since they are measured with a tapeline. These measurements were collected from the same 5 plants per vegetation plot that were pulled out with the spring balance.

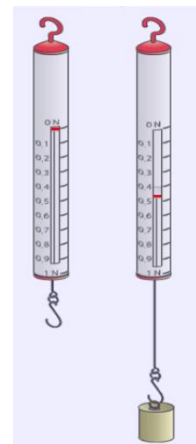


**Figure 2.7:** Principle of a spring balance.

### 2.1.5. Soil samples

Soil samples were taken to analyse the number of seeds in the ground. Close to every vegetation plot a soil sample, of 10 cm in diameter and 4 cm deep, was taken. This means that 9 soil samples per area were taken. Thereafter, the clay was washed out using a 0.45 mm diameter sieve leaving the seeds on the sieve. The seeds were grown in a warm environment and the number of successful seedlings were counted to give an indication of the number of seeds per plot in the seedbank.

Note: These samples have been taken till a depth of 4 cm. This is therefore a good indication about the number of seeds present in the top 4 cm of the seedbank, but does not give an indication about the seeds emerging during spring. Buried seeds of *Salicornia* might not emerge till this depth.

## 2.2. Data processing

The processing of the collected data, as described in section 2.1, will be explained in this section. The processing steps have been explained per parameter. The data has to be processed, which is done in Matlab, before the analyses can be performed. Moreover, the processing of the data gotten from Rijkswaterstaat or previous research will be explained as well in this section. The processing steps are explained per parameter; the hydrodynamic measurements, the surface elevation measurements, the vegetation characteristics by vegetation measurements and the seedbank by the soil samples.

### 2.2.1. Hydrodynamic measurements

The processing steps of the hydrodynamic data are explained in this section per parameter. The data of the hydrodynamic parameters that have been processed are: water level, inundation frequencies, flow velocities and wave heights.

#### 2.2.1.1. Water level

The water level is used for multiple parameters like, the inundation frequencies, the water depth and the wave heights. The monitoring station from Rijkswaterstaat that, among other things, measures the water level is located in the harbour of Delfzijl as can be seen in [Figure 1.7](#). The monitoring station is located close to the Marconi project, but might still differ since Marconi is more influenced by weather conditions or the Zeehavenkanaal might function as a funnel which could increase the water level locally. Therefore, it has been compared to the water level calculated with the bed level height (measured by the GPS) and the water depth (measured by the ASEDs). Moreover, the ASEDs only have measured the water depth when the measuring head of the ASED is submerged, while the monitoring station from Rijkswaterstaat has measured the water level in Delfzijl continuously at an interval of 10 minutes. The water level measured by Rijkswaterstaat has been shifted to get a more accurate water level representation ([Figure 2.8](#)).

The linear fits, created to adjust the water level measured by Rijkswaterstaat to more location dependent water levels, are presented in [Figure 2.8](#). Since this linear fit differs per location, the formula has been applied to correct the water levels from Rijkswaterstaat for the locations separately. These formulas have been applied per location, wherein 'x' is the water level measured by Rijkswaterstaat and 'y' is the resulting water level for that location.

Some outliers had to be corrected in the water level data from Rijkswaterstaat with linear interpolation. The outliers were at the 4<sup>th</sup> of march 2021 at 10:40, 10:50, 11:00 and 11:10. Moreover, the data had to be transformed from data with a 10min interval to data with a 15 min interval to make it comparable with the other continuous data.

A remark about the derived water depth by the ASEDs needs to be made, as in the script written by Grandjean (2021) the air pressure is assumed to be constant, but in reality might fluctuate. Therefore, the calculated water level might differ from the real water level. The calculated water level might be 2 cm higher or 4 cm lower, since the air pressure fluctuates between 9800 Pa and 10400 Pa in the Netherlands.

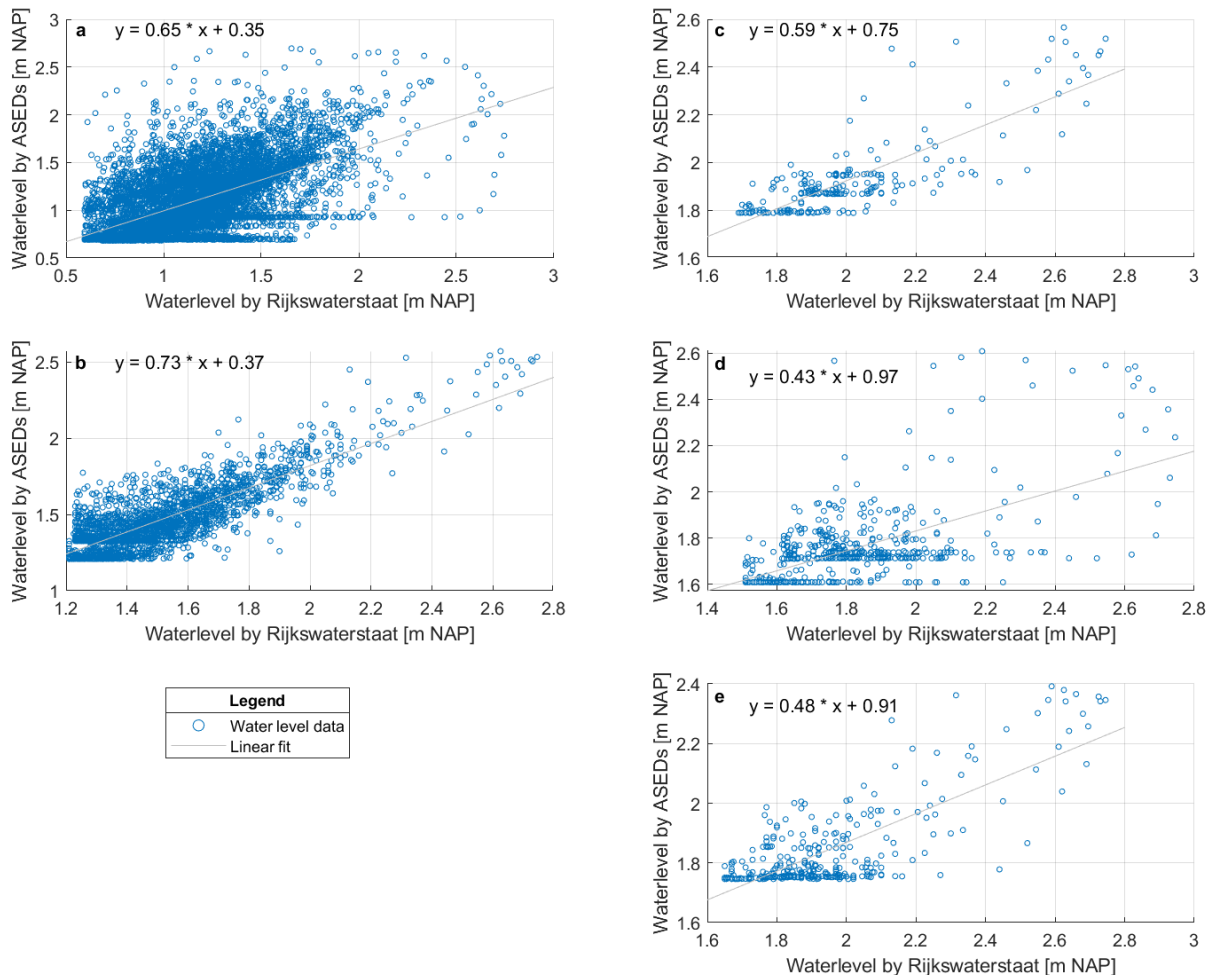


Figure 2.8: Scatterplot of the water level measured by the ASED and by Rijkswaterstaat with (a) front, (b) entrance, (c) E, (d) F and (e) G location of the salt marsh. The formula of the linear fit (gray line) is based on the water level data and is presented in the plots.

### 2.2.1.2. Inundation frequency

The inundation frequency represents the amount of times that the marsh is (partly) inundated. The inundation frequency has been calculated by subtracting the surface elevation profile from the adjusted water level. The surface elevation that was taken is the average of the measured bed level height by RTK-GPS system between the fieldwork days, meaning that the same bed level height has been used for November, December and January and the same bed level height has been used for the months February, March and April. The water level that has been used are the adjusted water levels, as explained in section 2.2.1.1. When the outcome results in positive values it means that the marsh is inundated, while negative results mean that the marsh is not inundated. From these inundation moments, the average inundation frequency per day can be calculated. This average inundation frequency per day has been calculated per measurement period to make it comparable with the other measured data, like the vegetation data.

### 2.2.1.3. Tilt current meter

The tilt current meter measures the flow velocities every 15 minutes. Since the TCM device measures the whole time and not only when the marsh is inundated, the measured data needs to be filtered. This is done with the adjusted water level, as explained in section 2.2.1.1., and the average bed level height measured by the RTK-GPS device. The data that needs to be filtered out is when the water level is below the surface elevation level from where the TCM is located plus the height needed for the TCM to be operable (30cm of water depth). Next to that, all of the fieldwork days have been deleted to be sure of deleting all the incorrect data and to be sure that both of the TCMs have the exact same measuring periods. This results in two measurement series of equal length with a frequency of 15 minutes. As the flow velocity has only been measured at the seaside vegetation plot, but should represent the flow velocities at the more landward vegetation plots as well, the maximum flow velocity has been taken. To make this data compatible with for example the vegetation data, this data has been averaged per fieldwork period (period in between the fieldwork days). This results in a maximum flow velocity for every fieldwork period.

### 2.2.1.4. ASED-pressure sensors

The acoustic sedimentation erosion dynamics pressure sensors are used to measure the wave height. The exact same device is also used to measure the surface elevation changes, but the collected data has been transformed. The wave height has been retrieved from the data of the ASED with a script written by Grandjean (2021). The ASED pressure sensors measures the total pressure at a 15 minute interval. This means the air pressure and, if the measuring head is submerged, the water pressure.

For this research the air pressure is assumed to be equal to the standard atmospheric pressure: 10000 Pascal. When the measuring head is submerged, the pressure will increase linearly with the water column. Since the ASED measures in a burst of eight it measures the whole wave amplitude and, if present, a significant wave height can be calculated.

Since there were five ASEDs operable in the field, some stations had missing periods for different reasons. To create data of equal length some periods have been deleted, as can be seen in [Table 2.3](#). From the remaining data a mean, maximum and standard deviation of the significant wave height can be calculated per fieldwork period. The significant wave height has been obtained according to the script written by Grandjean (2021). The maximum significant wave height per fieldwork period has been used in this research, as the wave height has only been measured at the seaside vegetation plot, but should represent the wave height at the more landward vegetation plots as well.

[Table 2.3](#): Deleted periods to create data of equal length for all ASEDs.

From - Till [Date and time]		From - Till [Date and time]	
24-06-2020 11:44	02-07-2020 14:10	15-03-2021 23:53	16-03-2021 11:53
21-07-2020 23:52	21-08-2020 14:03	27-03-2021 12:07	30-03-2021 11:53
22-11-2020 11:44	22-12-2020 12:00	08-04-2021 12:07	10-04-2021 11:53
08-02-2021 11:53	28-02-2021 23:53	23-04-2021 12:07	05-03-2021 08:00

## 2.2.2. Surface elevation changes

The processing steps of the surface elevation data are explained in this section per measuring device. The measuring devices that have measured the surface elevation are the acoustic sediment elevation dynamics sensor, the surface elevation bar and the real time kinematic global positioning system.

### 2.2.2.1. *Acoustic sediment elevation dynamics sensor*

The ASEDs were used to continuously measure the surface elevation changes on 5 locations. The ASED measures, when submerged, with a frequency of 15 minutes. The height between the measuring head and the bed has been measured when the device was installed and functions as the null measurement. The differences in heights in the measurements are subtracted or added to this null measurement to represent the surface elevation change. A pre-existing script written by Grandjean (2021) has been used to convert this data.

The ASED data has been used to quantify variabilities of the bed level within a fieldwork period, since with the SEB only the surface elevation at the fieldwork day can be measured. This data can therefore indicate more clearly what happens in the time between the fieldwork days.

### 2.2.2.2. *Surface elevation bar*

The surface elevation bar is used to manually measure elevation changes at the fieldwork days, resulting in 17 heights per SEB plot. These 17 points have been averaged to get one height per SEB per fieldwork day. Next to the average height, a standard deviation has been calculated to show the spatial variability. The surface elevation change is the difference over time since the first measurement.

### 2.2.2.3. *Real time kinematic global positioning system*

The surface elevation profile, measured with the RTK-GPS, is measured to map the profile of area E and G from the landside towards the seaside of the marsh. This profile has been measured at 3 fieldwork days in December, February and April.

Ideally the surface elevation will be measured in a straight line from the dike towards the seaside of the marsh. In practice this is not done in a straight line and therefore the measurements have to be adjusted in such a way that they are at a straight line. This has been done by a linear regression through the datapoints and moving the datapoints perpendicular towards the linear fit. Once this practical error has been adjusted it might be the case that the brushwood dam is not always at the right spot. Since the brushwood dam does not move, all of the transects have been adjusted to get the brushwood dam at the same place.

## 2.2.3. Vegetation measurements

There are 9 vegetation plots per area where three of them are replicates of each other. The vegetation properties for the most seaward three plots are replicates and are averaged to account for spatial variability. The same goes for the middle three plots and the three plots at the landside. Three replicates are created per plot to get more reliable data that is more representative for that plot. The data from these vegetation plots will result in an average and a standard deviation per plot.

The density has been estimated per vegetation plot and has been averaged for the three replicates at that vegetation plot. The vegetation characteristics might differ strongly per mature plant, which is the reason for the collection of five plants per vegetation plot. Therefore the vegetation characteristics like, the length above- and below ground, the number of side roots longer than 2 cm, the length of the longest side root and the strength are measured for five plants per vegetation plot. This means that in total there are 15 plants averaged per plot. Therefore, the results of this data are an average and a standard deviation per plot.

### 2.2.4. Soil samples

Soil samples were taken to count the number of seeds in the ground which can represent the seedbank. The soil sample has been taken close to all vegetation plots, resulting in nine soil samples per area. The number of seeds within the soil samples of every plot (seaside, middle part and landside) have been averaged to account for spatial variability in the seedbank, like what has been done with the vegetation measurements. This data results in an average number of seeds per plot and a standard deviation per plot.

### 2.2.5. Multiple linear regression analysis

In [Table 2.1](#) and [Table 2.2](#) it can be seen that the parameters have not been of equal length. For executing a multiple linear regression analysis, the different datasets should be of equal length. Therefore, all parameters have been transformed into one value for each fieldwork period (period in between fieldwork days) by either taking the average or the maximum value in these periods. A multiple linear regression analysis has been executed to correlate the different parameters. The linear regression model is used, as it is easy in use and provides adequate fits for the data used in this research. By executing a multiple linear regression analysis the effect of a single-variable and combinations of these parameters can be determined. For this analysis the Matlab function `fitlm` (fit linear model) is used. This function is defined as a model and returns a linear regression model for the different variables. The `fitlm` function gives the coefficient of determination ( $R^2$ ), the probability value for testing statistical significance ( $p$ ) and coefficient estimates for the corresponding terms in the model ( $\beta_n$ ) as output. The coefficient of determination lies between 0 and 1, where a value closer to 1 represents a stronger relationship or fit between the dependent and independent factors. Moreover, to test the statistical significance, the  $p$ -value has been calculated. The  $p$ -value should be below 0.05 to have a confidence interval of at least 95%. The regression model provides a fit through the data that can be written as:

$$y = \beta_0 + \beta_1x_1 + \beta_2x_2 + \beta_3x_3 + \varepsilon \quad (2.1)$$

Wherein:

$y$  = the dependent variable

$\beta_0$  = the intercept

$\beta_n$  = the coefficients corresponding to the observations  $x_n$

$x_n$  = the independent variable

$\varepsilon$  = a random error term

In the explanation it can be seen that  $\beta_0$  represents the intercept. The definition of the intercept is: “the mean of Y, when all predictors (X) are zero”. Therefore the intercept is only useful if every X in the model actually has some values of zero. As zero settings for all of the predictor variables can be outside the data range, it cannot be said that the intercept has to be statistical significant. The intercept, however, is needed for a good working linear regression model. If the intercept is not used, the linear line is forced to go through the origin, meaning that the x and y variables both equal zero at that point. If the fitted line does not naturally go through the origin, the regression coefficients and predictions will be biased if the constant is not included (Sweet & Grace-Martin, 2008).



### 3. Results observed parameters

In this chapter the salt marsh profile and the results of the hydrodynamics, surface elevation changes and vegetation characteristics are visualised. This consists of results of the measured data in the field.

#### 3.1. Salt marsh profile

The Marconi salt marsh profile is visualised in [Figure 3.1](#). These transects have been measured per area with the RTK-GPS device in December, February and April. The locations of the landside, middle and seaside vegetation plots are presented with the dashed red line. The location and width of the dam is presented with the dashed black line.

The top plot visualises the bed level in area E and the bottom plot visualises the bed level in area G. The sandbank is clearly visible in both areas between the middle and seaside plots. Moreover, it can be seen that the seaside plot in area G has a lower elevation than the seaside plot of area E, while the other plots have a higher elevation in area G.

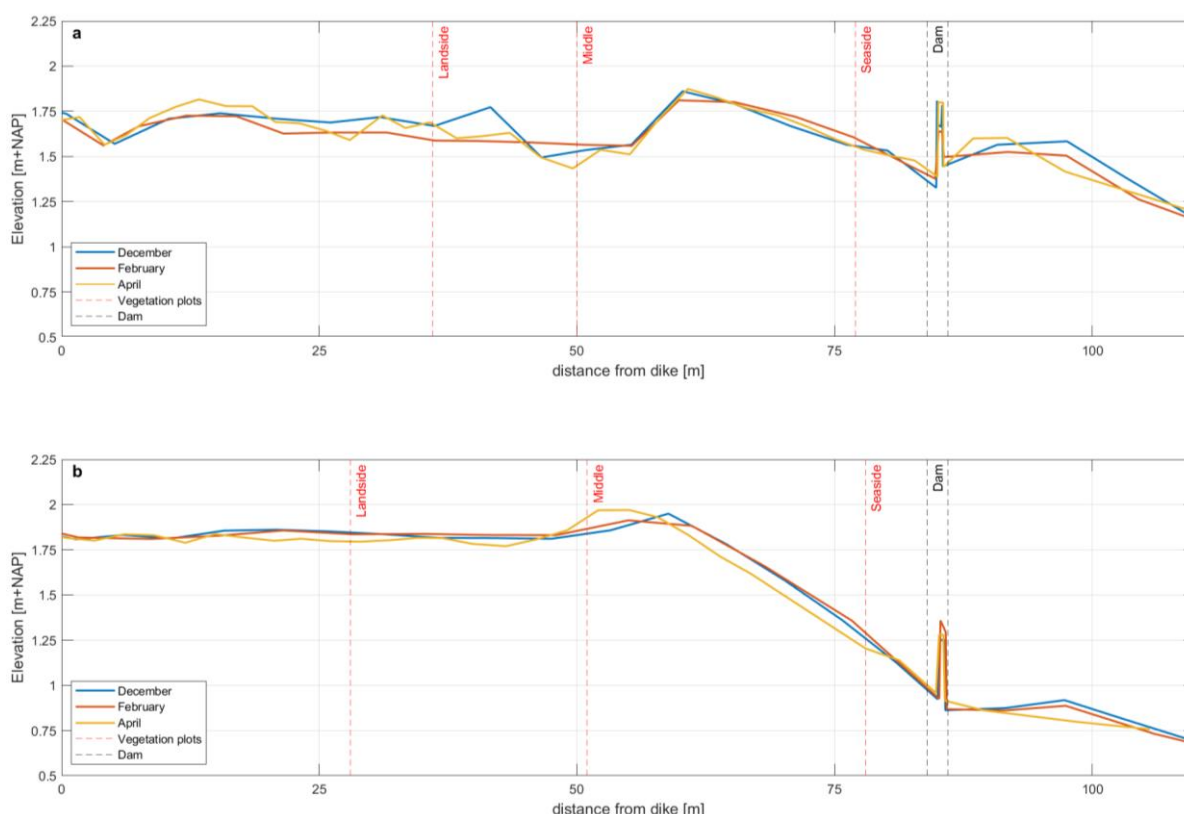


**Figure 3.1:** Height of the bed level during the winter period (December 2020-April 2021) measured by the RTK-GPS device. Cross-shore transect has been measured in (a) area E and (b) area G.

#### 3.2. Surface elevation changes

The surface elevation changes have been measured on different locations and different time scales. The continuous measurements of the ASEs are presented in Appendix A. The monthly measurements of the SEBs are presented in this section.

The surface elevation level over time has been plotted in [Figure 3.2](#). The surface elevation level is referred to the first observation in April 2020. The standard deviations per plot during the winter period (November 2020-April 2021) are presented in [Table 3.1](#). This data was not available for the summer period (April 2020-November 2020).

In the figures it can be seen that in the beginning the surface elevation level increases for all plots in both areas. However, at the end of the winter period (April 2021) the surface elevation level has been declined for the seaside plots in both areas when compared to the first measurement in April 2020. The elevation level has been increased most at the middle plot of area E and at the landside plot of area G. By comparing both areas it can be seen that area G is more dynamic, since there are more and higher fluctuations for the plots.

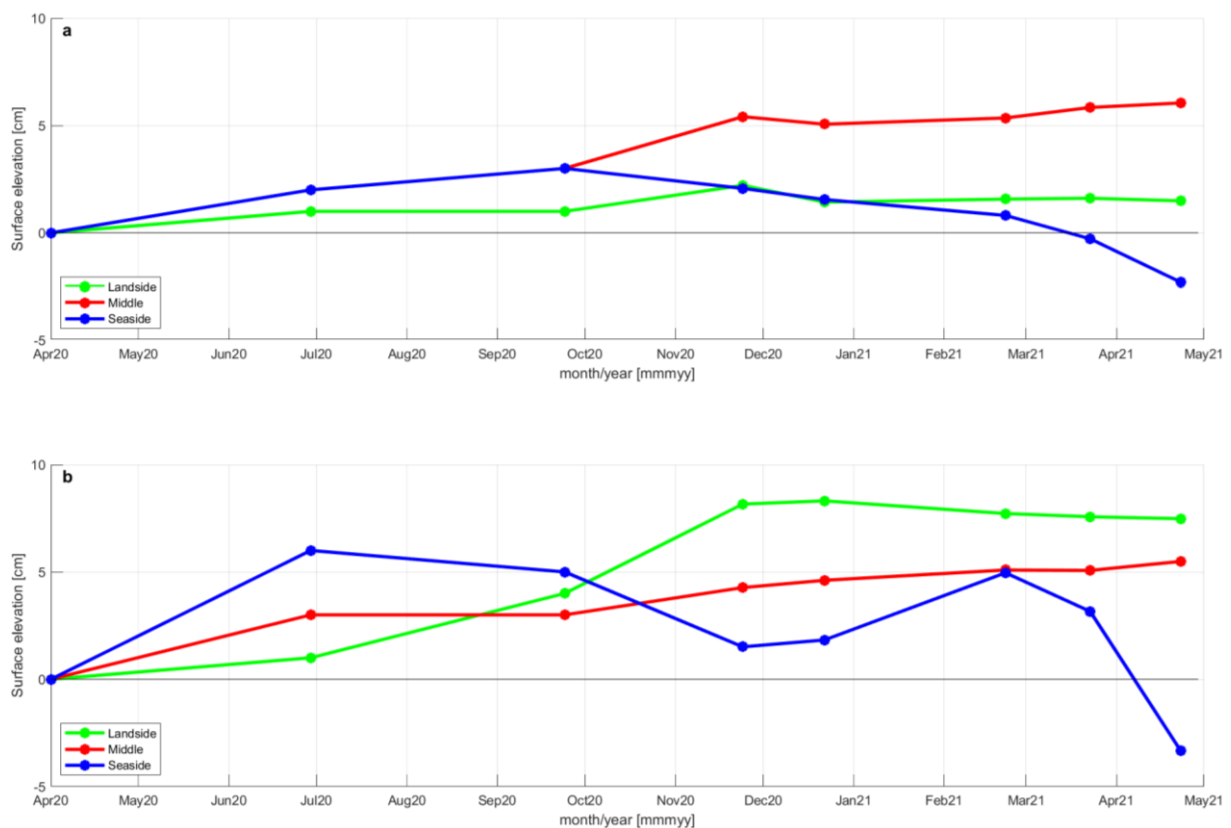


[Figure 3.2](#): Temporal surface elevation level measured by the SEBs for the period April 2020 till April 2021 in (a) area E and (b) area G.

The monthly surface elevation changes have been calculated from the surface elevation level measured by the sedimentation erosion bars (SEBs). In [Figure 3.3](#) the surface elevation change has been plotted from April 2020 till April 2021. The standard deviation has only been measured in the winter period (from November-April) and is given in [Table 3.1](#).

When comparing both plots it can be seen that the bed is much more dynamic in the lower lying area G than in area E. More precisely the bed level change is most dynamic at the seaside plot of area G. The trends in both graphs look very similar, but the fluctuations are a few times higher in area G. At the start of the winter period (end of November) sedimentation took place in both areas at the landside and middle plots. However, at both seaside plots erosion took place. This is also most visible in area G, where it looks like a sandbank has been created between the end of November and the end of February. In this period the surface level has been increased with about 4 cm. After this, from March to May, a lot of erosion took place, especially in area G.

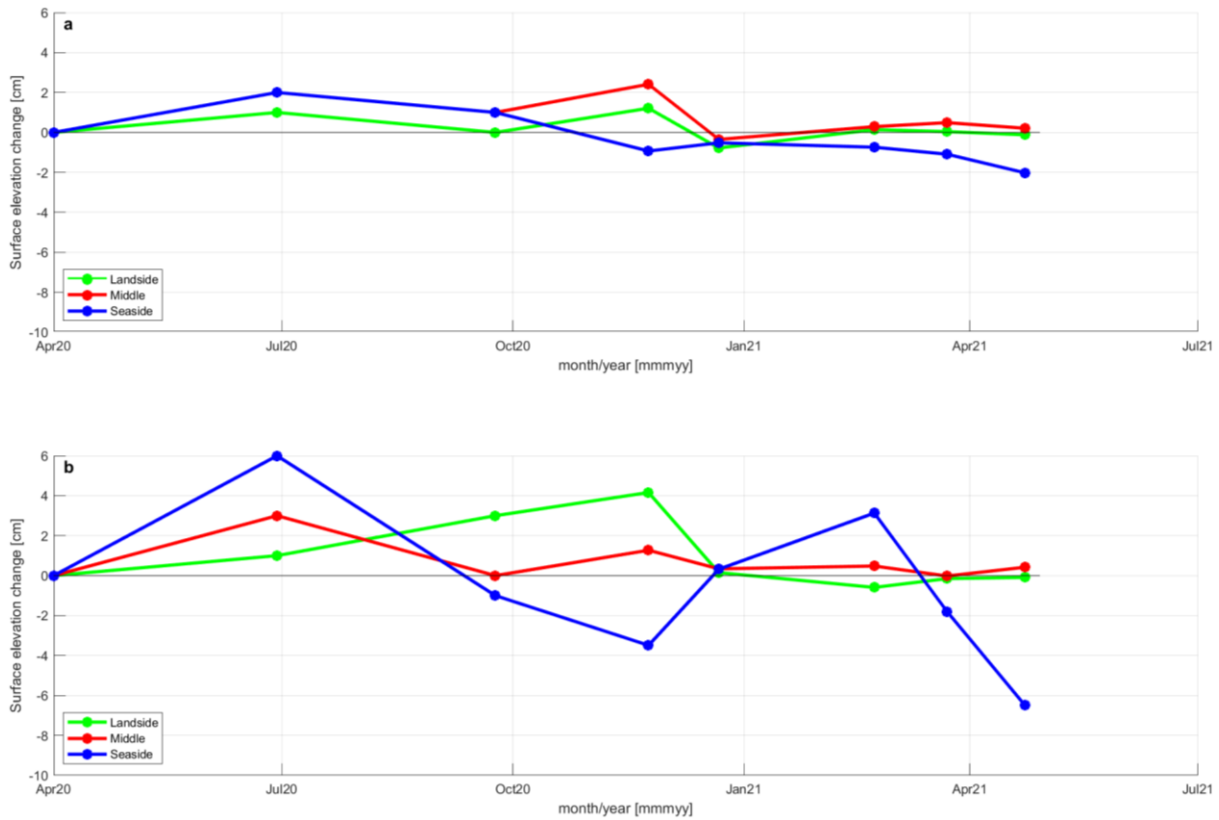


Figure 3.3: Temporal surface elevation changes measured by the SEBs for the period April 2020 till April 2021 in (a) area E and (b) area G.

Table 3.1: Overview of the mean and standard deviations of the surface elevation level and changes per vegetation plot and per fieldwork period. First column of the surface elevation level is the mean, second column is the standard deviation from the mean and the third is the percentage deviation of the standard deviation.

Area	Date	Area E			Area E			Area	Date	Area G			Area G		
		Mean [cm]	Std [cm]	Dev [%]	Mean [cm]	Std [cm]	Dev [%]			Mean [cm]	Std [cm]	Dev [%]	Mean [cm]	Std [cm]	Dev [%]
E-Land	04_2020	0,0	-	-	0,0	-	-	G-Land	04_2020	0,0	-	-	0,0	-	-
E-Land	06_2020	1,0	-	-	1,0	-	-	G-Land	06_2020	1,0	-	-	1,0	-	-
E-Land	09_2020	1,0	-	-	0,0	-	-	G-Land	09_2020	4,0	-	-	3,0	-	-
E-Land	11_2020	2,2	2,0	90	1,2	-	-	G-Land	11_2020	8,2	0,8	10	4,2	-	-
E-Land	12_2020	1,4	2,1	147	-0,8	0,7	95	G-Land	12_2020	8,3	0,9	10	0,2	0,5	322
E-Land	02_2021	1,6	2,2	142	0,1	0,5	351	G-Land	02_2021	7,7	0,7	9	-0,6	0,4	71
E-Land	03_2021	1,6	2,2	135	0,0	0,5	1314	G-Land	03_2021	7,6	0,4	6	-0,2	0,6	408
E-Land	04_2021	1,5	2,1	142	-0,1	0,4	325	G-Land	04_2021	7,5	0,6	9	-0,1	0,4	487
E-Mid	04_2020	0,0	-	-	0,0	-	-	G-Mid	04_2020	0,0	-	-	0,0	-	-
E-Mid	06_2020	2,0	-	-	2,0	-	-	G-Mid	06_2020	3,0	-	-	3,0	-	-
E-Mid	09_2020	3,0	-	-	1,0	-	-	G-Mid	09_2020	3,0	-	-	0,0	-	-
E-Mid	11_2020	5,4	2,0	37	2,4	-	-	G-Mid	11_2020	4,3	0,8	19	1,3	-	-
E-Mid	12_2020	5,1	2,1	41	-0,4	0,5	129	G-Mid	12_2020	4,6	0,8	17	0,3	0,3	101
E-Mid	02_2021	5,4	1,9	36	0,3	0,4	139	G-Mid	02_2021	5,1	0,5	9	0,5	0,8	168
E-Mid	03_2021	5,8	1,5	26	0,5	0,6	120	G-Mid	03_2021	5,1	0,8	15	0,0	0,6	2770
E-Mid	04_2021	6,1	1,5	25	0,2	0,6	293	G-Mid	04_2021	5,5	0,7	12	0,4	0,4	88
E-Sea	04_2020	0,0	-	-	0,0	-	-	G-Sea	04_2020	0,0	-	-	0,0	-	-
E-Sea	06_2020	2,0	-	-	2,0	-	-	G-Sea	06_2020	6,0	-	-	6,0	-	-
E-Sea	09_2020	3,0	-	-	1,0	-	-	G-Sea	09_2020	5,0	-	-	-1,0	-	-
E-Sea	11_2020	2,1	0,9	42	-0,9	-	-	G-Sea	11_2020	1,5	1,5	101	-3,5	-	-
E-Sea	12_2020	1,6	1,1	71	-0,5	0,4	77	G-Sea	12_2020	1,8	1,7	95	0,3	1,1	340
E-Sea	02_2021	0,8	1,1	134	-0,7	0,5	72	G-Sea	02_2021	5,0	1,8	35	3,1	0,6	21
E-Sea	03_2021	-0,3	1,2	434	-1,1	0,6	56	G-Sea	03_2021	3,2	1,2	38	-1,8	0,4	23
E-Sea	04_2021	-2,3	1,9	83	-2,0	1,3	65	G-Sea	04_2021	-3,3	1,3	38	-6,5	0,4	7

Color meaning:   ≥ 100 %        ≥ 100 %        ≥ 100 %        ≥ 100 %

### 3.3. Hydrodynamics

The hydrodynamics that have been measured in the field are the flow velocity and significant wave height. Moreover, the inundation frequency has been calculated with the elevation level, as presented in [Figure 3.1](#), and the water level, as presented in [Figure 2.8](#).

#### 3.3.1. Inundation frequency

In [Figure 3.4](#) the inundation frequency over the whole summer period (April-September) and winter period (October-April) are presented. It can be seen that the inundation frequency is only higher for the seaside plots during the winter period. The inundation frequency during the summer period is either higher or equal compared to the winter period. Due to an increased chance of storms during the winter period, the water might be higher more frequently and the marsh could therefore be inundated more frequently. However, this is not the case, the water level is only slightly higher during the winter period. The increase in surface elevation level at the landside and middle plots and the decrease in surface elevation level at the seaside plots (see [Figure 3.2](#)) are therefore the main drivers in the changing inundation frequency.

It would be expected that the inundation frequency increases for the seaside plots. However, during the winter and summer period the inundation frequency in area E is higher at the middle plot than at the seaside plot. This is due to the difference in surface elevation level. A sandbank is located at the seaside plot, which increases the bed level at the seaside plot. This causes the lower inundation frequency at the seaside vegetation plot.

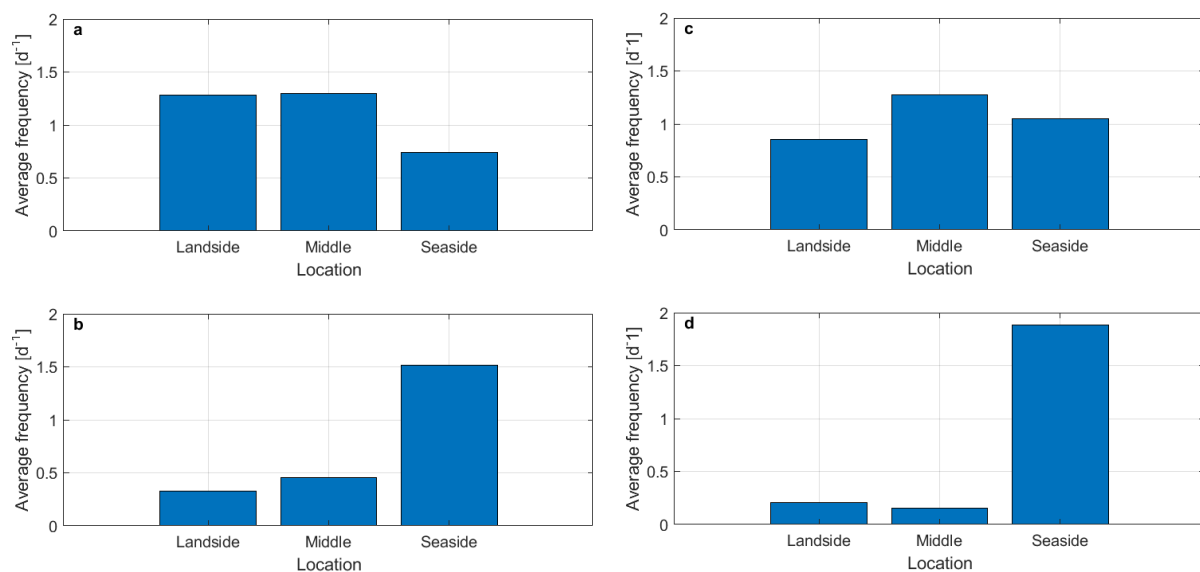


**Figure 3.4:** Inundation frequency per plot per area for the summer period (April 2020-September 2020) in (a) area E and (b) area G and for the winter period (October 2020-April 2021) in (c) area E and (d) area G.

### 3.3.2. Flow velocities

The flow velocities have been measured during the winter period (November-April) by the TCMs and are presented in [Figure 3.5](#). In this figure the water levels and flow velocities in both of the areas are presented. As can be seen halfway February there is a period missing, which is caused by a period of frost where all of the measuring devices had to be removed from the field.

What stands out in [Figure 3.5](#) are the more frequently occurring flow velocities in area G. The seaside of area G has a lower surface elevation and is therefore more frequently inundated. According to the many gaps, keeping in mind that the device measured in a burst of 15 minutes, there are a lot of moments where the TCM device has not measured flow velocities. The reason for this is that the TCM device needs a layer of 30 cm water to measure, which only happens during high tides.

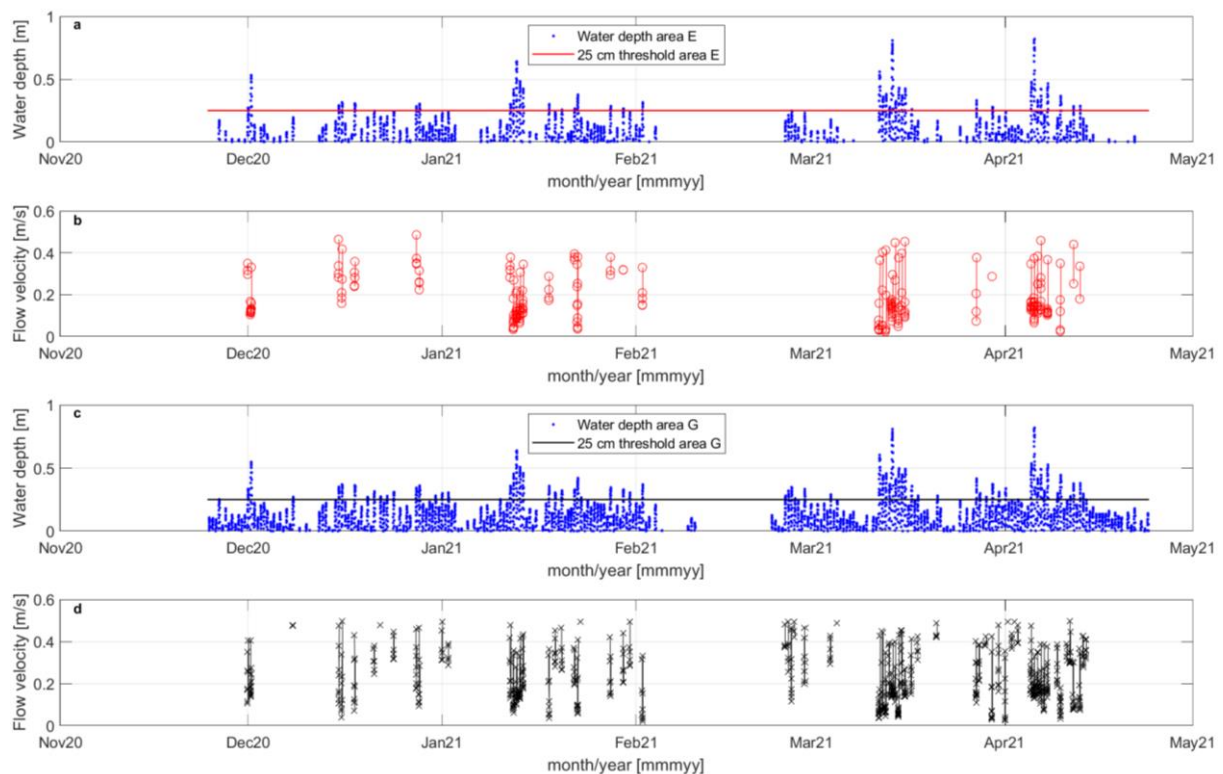


[Figure 3.5](#): Measured water depth and the 25 cm threshold for the TCM in (a) area E and (c) area G and flow velocities in (b) area E and (d) G during the winter period (November-April).

In [Figure 3.6](#) a close up of part of the data is presented in [Figure 3.5](#) to get a better understanding about the development of the flow velocities during a tidal cycle. It can be noted that the flow velocities are highest at the start of the incoming and the end of the outgoing tides and the maximum velocity at the outgoing tide is slightly higher than at the rising tide. Moreover, the flow velocities seem to increase when the tide turns from rising to falling, followed by a drop and another rise of the flow velocity during ebb. In the top figure of [Figure 3.6](#) it can be seen that the TCM in area G starts measuring at a lower water level than the TCM in area E due to the difference in surface elevation.

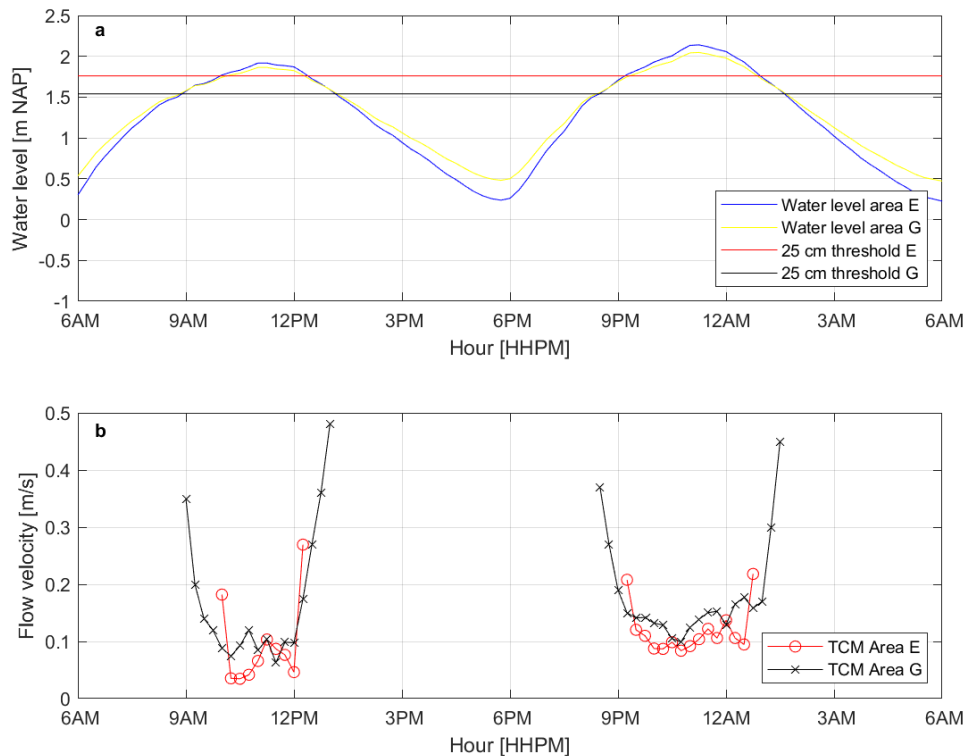


Figure 3.6: Close up of the (a) water level in area E and G including the 25 cm threshold and the (b) flow velocities in area E and G from 12 to 13 January for 24 hours (one tidal cycle).

### 3.3.3. Significant wave height

The significant wave heights have been measured with the ASED-pressure sensors which are located at the seaside plots of area E, F and G, at the entrance of area F and in front of the marsh of area F, as can be seen in Figure 2.1. In Figure 3.7 the measured significant wave heights at the entrance and front of the marsh are presented in the top figure and in the bottom figure the significant wave heights at the seaside plots of the marsh have been plotted. Since the ASEDs were not placed in the field for the period October till the end of December, this is the time between the summer and winter measuring period, a gap can be seen. Note that the scale on the y-axis is logarithmic.

In the top plot of Figure 3.7 it can be noticed that the ASED in front of the marsh is located lowest, since this gives the most measuring points. The highest waves occurred in spring 2020 and spring 2021 with significant wave heights up to 40 cm. What stands out is that the location with the highest occurring wave heights differs over time. For example, the maximum significant wave height at the start of January 2021 is highest at the front, while the next peak is much higher at the entrance of the marsh. Moreover, the only measured wave heights between April 2020 and July 2020 are in area F, while the first wave heights in January 2021 have been measured at area E and G.

In the bottom plot of Figure 3.7 it is noticeable that the ASED rarely measures waves, since there are a lot of gaps in the timeseries. This happened due to the high water depth ( $\pm 30$  cm) needed for the ASED to start measuring.

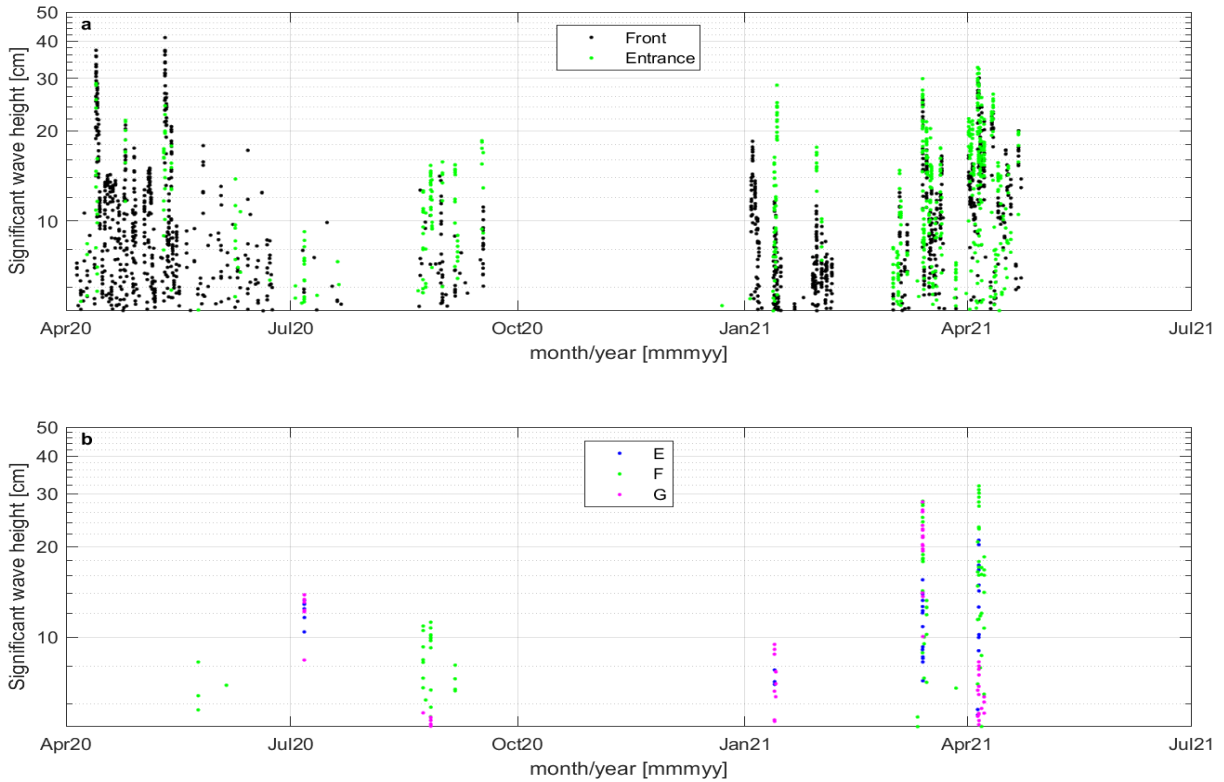


Figure 3.7: The significant wave heights (a) at the entrance of area F (black) and in front of the marsh (green) and in (b) area E (blue), F (green) and G (pink).

In Figure 3.8 the standard deviation, mean and maximum significant wave heights occurring during the summer (6 months; from April 2020 till September 2020) and winter period (5 months; from December 2020 till April 2021) are presented per measuring location. It can be seen that the maximum wave height at the front is highest during the summer period, while the measured maximum wave height is about equal at the other stations during the winter period, except for area E. Moreover, it can be noticed that the mean wave height for most stations is about the same during both periods. For the ASED in area F this trend seems to be different, since the mean wave height is almost doubled. Also the maximum measured wave height has increased most in area F for the winter period compared to the summer period.

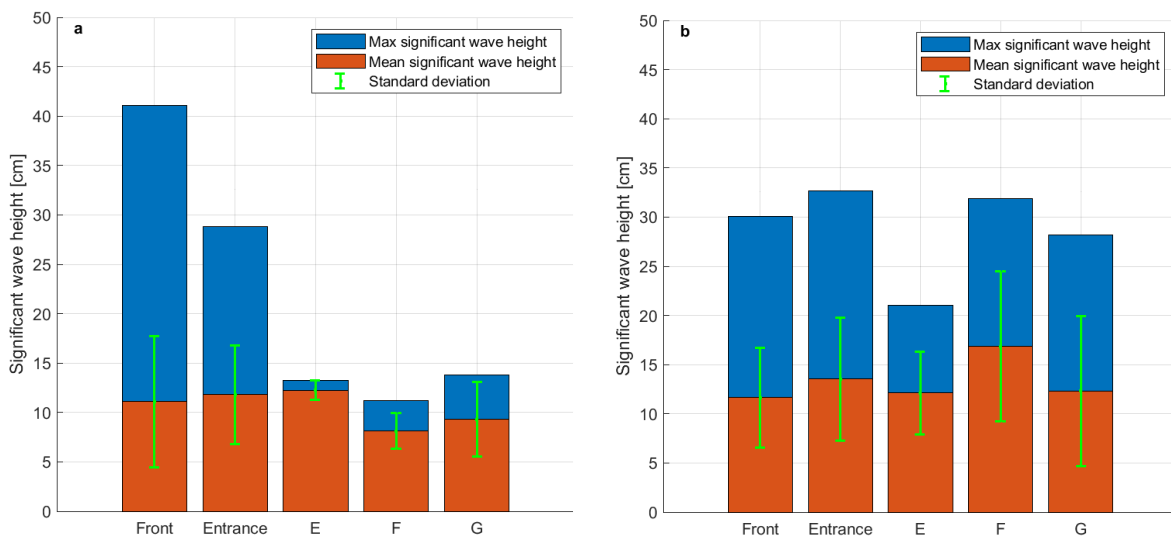


Figure 3.8: The mean, maximum and standard deviation of the significant wave heights during (a) the summer period (April 2020-September 2020) and (b) the winter period (December 2020-April 2021) per measurement location.

### 3.4. Vegetation and seedbank

#### 3.4.1. Vegetation characteristics

The vegetation density per vegetation plot at the of the summer of 2020 has been visualised in [Figure 3.9](#). It can be noted that there is zero vegetation present in the seaside vegetation plot of area G. Moreover, it is clearly visible that the densities in area E are much higher than the densities in area G. It can be seen that the vegetation density in the seaside plot of area E is 20% higher than at the seaside plot in area G and the vegetation density is 22% higher in the middle plot of area E compared to the middle plot of area G. The plots at the landside, however, differ only 5% in vegetation density.

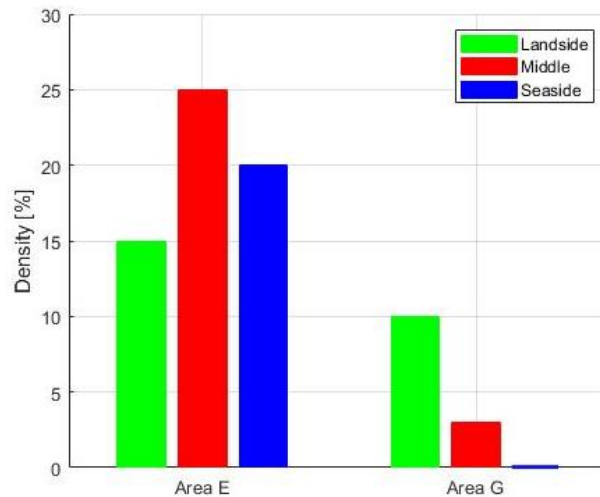


Figure 3.9: Vegetation density per vegetation plot measured in September 2020.

The measured vegetation characteristics during the winter period are presented in [Figure 3.10](#). In the density graph it can be seen that there is no vegetation at the seaside plot of area G. For this reason the seaside plot of area G has not been taken into account for the other parameters, since there is no vegetation present. In the graphs of the number of side roots and the length of the longest side root it can be seen that they have not been measured at the first fieldwork day. The number of side roots and the length of the longest side root have not been measured at the landside plot of area E the first two fieldwork days. These measurements were added through knew insights in potential interesting vegetation characteristics.

In the plot of the vegetation density it can be seen that the density is much higher in area E compared to area G. The density of the vegetation in area E is at the start of winter highest in the seaside plot and is slowly decreasing landwards. However, the density decreases rapidly in December at the seaside plot causing the density to be lowest at the seaside plot of area E. After this sudden decline, the density gradually decreases till the new growing season starts. The landside plot of area E seems to decline very steadily, while the middle plot has a slightly steeper decline, especially in the first and last part of the winter period. The decay in density in area G is almost the same for the middle and landside plots. A sidenote needs to be made as the standard deviations differ quite a lot, as can be seen in [Table 3.2](#). The highest deviations occur in the seaside plot indicating that the choice of location of the measuring plot might be very important (section 2.1.4.).

The aboveground length of the vegetation has been visualised in the b plot of [Figure 3.10](#). The measured length seems to differ up to almost 4 cm in between the fieldwork days. In this graph the same kind of pattern in the vegetation data of area E can be noticed. Noteworthy is the stronger decline of the vegetation length in the seaside plot between January and March, nonetheless the standard deviations are also highest for the seaside plot as could be seen in [Table 3.2](#). The length of

the vegetation is mostly lower in area G, when comparing it to the same plot in area E. However, there does not seem to be a same kind of trend as in area E. The vegetation length at the landside plot seems to decrease steadily, while at the middle plot the length seems to fluctuate more.

The strength of the vegetation that has been measured is presented in the c plot of [Figure 3.10](#). Despite that the data of area E seems to have an opposite shape, the values do not seem to differ strongly. This opposite shape changes over time when comparing the landside, middle and seaside plot of area E. It can be seen that in the beginning of the winter period the shape of the middle plot is the opposite of the landside and seaside plot of area E, while at the end of the winter period the shape of the landside plot is more like the opposite of the middle and seaside plot of area E. Most noticeable in the strengths of area E is that the highest values occur in the seaside plot. Furthermore it stands out that the strength of the vegetation of the middle plot in area G is highest during most of the winter period, but at least always higher than the strength of the middle plot in area E. In [Table 3.2](#) it can be seen that the standard deviations are mostly above 25% in area E and below 25% in area G. It must be noted, that at the end of the winter period, more plants were pulled out before the strength could be measured. More and more plants broke off at the location where the trunk crosses the surface, and leaving the roots behind in the ground. These plants have not been considered in this research, since the data of the roots of the plants needed to be collected as well.

Information about the roots has been presented in the d, e and f plots of [Figure 3.10](#). It can be seen that in all graphs the roots in area G and the seaside plot of area E come up as the longest or the largest amount. The measured root length seems to be steady for all vegetation plots in area E during the whole period, while the plots in area G have a larger decline between January and April. As can be seen in [Table 3.2](#) it should be noted that there is a standard deviation of a few centimetres for most of the vegetation plots. This indicates a strong difference between the replicates. Moreover, the graphs of the number of side roots and the length of the longest side root seem to have the same kind of trend. At the start of the measurements all graphs of the roots are quite divergent, while at the end of the winter period all data has become more closer to each other with less variations.

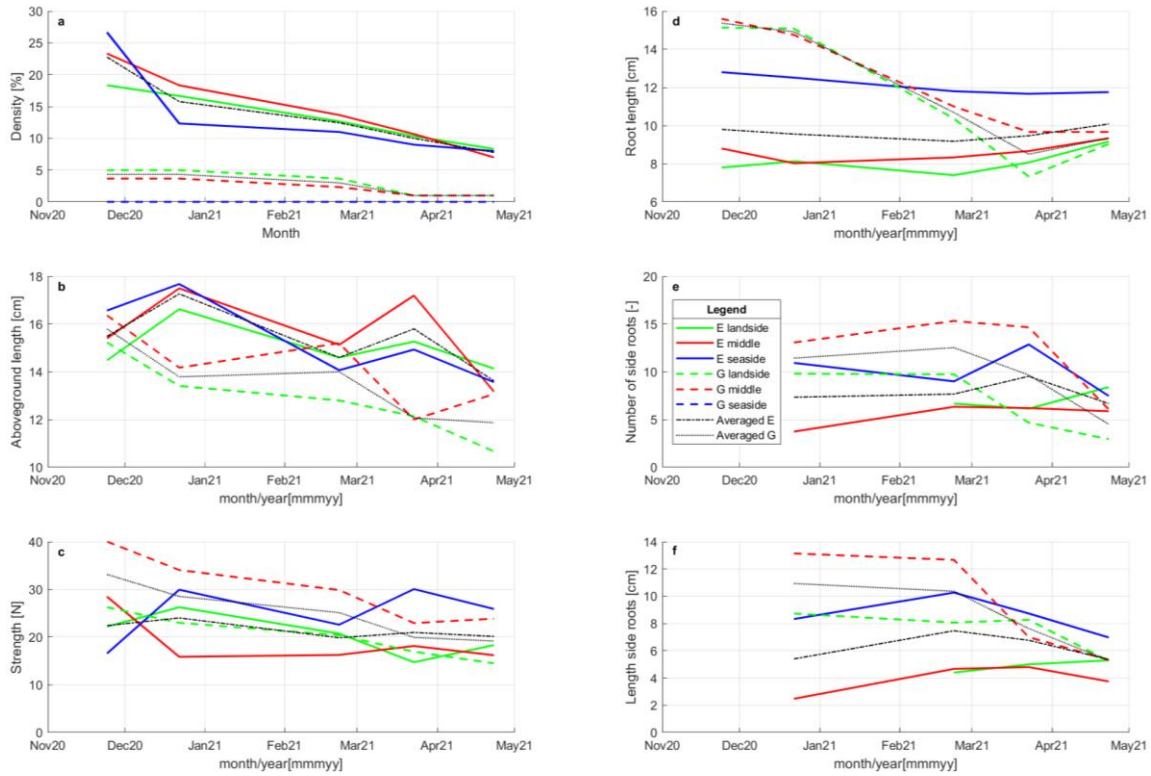


Figure 3.10: The locations are averages over three plots as could be read in the method description. These locations can be found in Figure 2.1. The vegetation characteristics (a) density, (b) aboveground length, (c) strength, (d) rootlength, (e) number of side roots and (f) length of the longest side root per vegetation plot in area E and G during the winter period (November 2020-April 2021), including the averages per area. The legend is applicable to all graphs.

Table 3.2: Overview of the mean and standard deviations of the vegetation characteristics per vegetation plot and per fieldwork day. First column of every vegetation characteristic is the mean, second is the standard deviation from the mean and the third is the percentage deviation of the standard deviation.

Area	Date	Density			Aboveground length			Strength			Root length			Number of side roots			Length of longest side root		
		Mean [%]	Std [% dev]	Dev [%]	Mean [cm]	Std [cm]	Dev [%]	Mean [N]	Std [N]	Dev [%]	Mean [cm]	Std [cm]	Dev [%]	Mean [-]	Std [-]	Dev [%]	Mean [cm]	Std [cm]	Dev [%]
E-Land	11_2020	18	10	57	14	2	14	22	2	10	8	2	24	-	-	-	-	-	-
E-Land	12_2020	17	8	46	17	2	13	26	1	3	8	2	23	-	-	-	-	-	-
E-Land	02_2021	13	5	36	15	3	17	21	11	54	7	1	17	7	3	47	4	2	42
E-Land	03_2021	10	5	48	15	1	5	15	6	40	8	2	24	6	3	46	5	1	21
E-Land	04_2021	8	4	50	14	1	5	18	7	38	9	2	26	8	6	72	5	3	61
E-Mid	11_2020	23	14	62	15	3	17	28	10	35	9	2	19	-	-	-	-	-	-
E-Mid	12_2020	18	6	31	18	2	14	16	5	32	8	1	9	4	3	71	2	1	44
E-Mid	02_2021	14	8	60	15	2	11	16	1	8	8	2	24	6	0	5	5	1	22
E-Mid	03_2021	11	8	76	17	1	8	18	4	23	9	0	1	6	3	52	5	1	22
E-Mid	04_2021	7	5	76	13	4	30	16	5	30	9	2	19	6	4	66	4	1	35
E-Sea	11_2020	27	25	92	17	4	26	17	4	26	13	4	35	-	-	-	-	-	-
E-Sea	12_2020	12	8	61	18	3	18	30	14	48	13	3	21	11	4	37	8	3	36
E-Sea	02_2021	11	11	102	14	3	22	23	9	38	12	2	19	9	1	12	10	6	63
E-Sea	03_2021	9	11	125	15	2	13	30	8	25	12	3	27	13	4	32	9	2	28
E-Sea	04_2021	8	10	130	14	4	33	26	9	35	12	3	22	7	2	26	7	2	24
G-Land	11_2020	5	0	0	15	1	9	26	4	14	15	3	17	-	-	-	-	-	-
G-Land	12_2020	5	0	0	13	2	14	23	8	34	15	1	6	10	3	30	9	1	9
G-Land	02_2021	4	1	16	13	1	7	20	3	15	10	1	7	10	2	24	8	2	20
G-Land	03_2021	1	0	0	12	2	12	17	3	18	7	1	11	5	1	19	8	2	28
G-Land	04_2021	1	0	0	11	1	8	15	6	39	9	2	17	3	1	45	5	1	14
G-Mid	11_2020	4	1	31	16	3	17	40	4	10	16	1	6	-	-	-	-	-	-
G-Mid	12_2020	4	1	31	14	1	9	34	4	11	15	1	9	13	2	14	13	1	9
G-Mid	02_2021	2	1	25	15	1	9	30	2	7	11	1	9	15	4	24	13	2	14
G-Mid	03_2021	1	0	0	12	1	12	23	11	50	10	3	29	15	11	75	7	3	45
G-Mid	04_2021	1	0	0	13	1	7	24	1	4	10	3	31	6	2	38	5	2	36
G-Sea	11_2020	0	0	0	0	0	0	0	0	0	0	0	0	-	-	-	-	-	-
G-Sea	12_2020	0	0	0	0	0	0	0	0	0	0	0	0	0	0	0	0	0	0
G-Sea	02_2021	0	0	0	0	0	0	0	0	0	0	0	0	0	0	0	0	0	0
G-Sea	03_2021	0	0	0	0	0	0	0	0	0	0	0	0	0	0	0	0	0	0
G-Sea	04_2021	0	0	0	0	0	0	0	0	0	0	0	0	0	0	0	0	0	0
<b>Color meaning:</b>		≥ 25 %			≥ 25 %			≥ 25 %			≥ 25 %			≥ 25 %			≥ 25 %		

### 3.4.2. Seed availability

Soil samples have been taken to count the potential number of seedlings available in the seedbank. The *Salicornia* seeds have been grown and the number of seedlings have been presented in Figure 3.11. It can be seen that the seed availability decreases in most vegetation plots in March, the landside vegetation plot in area E is an exception. In April, the seed availability increases significantly at middle vegetation plots, while it stays about equal at the landside and seaside vegetation plots. It is remarkable that, next to the absence of vegetation, there are no seeds available in the seaside plot of area G.

The standard deviations have been listed in Table 3.3. It can be seen that there is a large variation in the number of seeds per replicate. Nevertheless, the number of seeds seem to match the vegetation density as there are more seeds found in the denser vegetation plots.

The data in November has been made grey, as a wrong sowing method was used. Therefore the number of seedlings might be lower than the actual number of seeds in the soil samples. Therefore, the number of seeds measured in November has been left out in further analysis.

Table 3.3: Overview of the mean, standard deviation and the percentage deviation of the standard deviation of the seed availability per vegetation plot.

Area	Date	Seeds		
		Mean [-]	Std [-]	Dev [%]
E-Land	11_2020	2	1	50
E-Land	02_2021	26	13	50
E-Land	03_2021	34	38	112
E-Land	04_2021	35	20	57
E-Mid	11_2020	3	3	96
E-Mid	02_2021	21	7	33
E-Mid	03_2021	14	17	123
E-Mid	04_2021	36	22	62
E-Sea	11_2020	6	4	62
E-Sea	02_2021	27	17	63
E-Sea	03_2021	8	9	112
E-Sea	04_2021	8	10	129
G-Land	11_2020	0	1	173
G-Land	02_2021	8	12	162
G-Land	03_2021	1	1	173
G-Land	04_2021	1	1	100
G-Mid	11_2020	0	1	173
G-Mid	02_2021	7	2	23
G-Mid	03_2021	2	3	138
G-Mid	04_2021	6	6	87
G-Sea	11_2020	0	0	0
G-Sea	02_2021	0	0	0
G-Sea	03_2021	0	0	0
G-Sea	04_2021	0	0	0

Color meaning:   ≥ 50 %

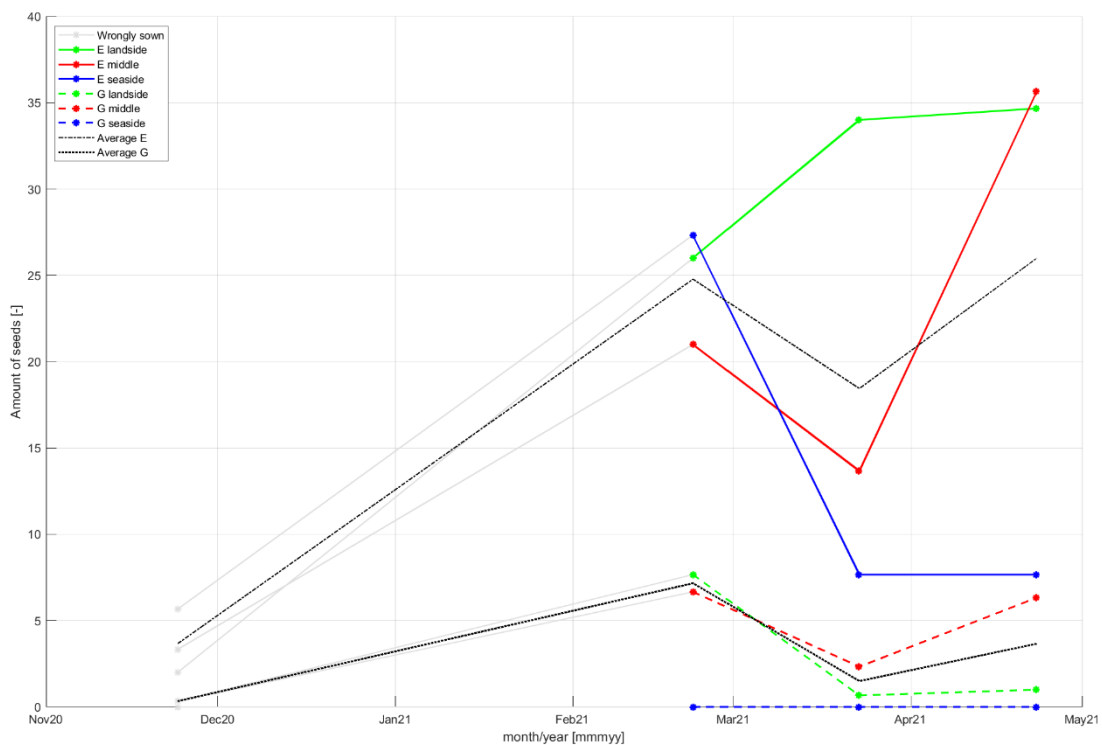


Figure 3.11: Temporal differences in seed availability per vegetation plot.



## 4. Explaining vegetation changes

In this chapter the parameters, as presented in the previous chapter 'Results', are related by a correlation and regression analysis. In this way effects of the different parameters on the vegetation density (decay) are determined. This is done for the summer and winter period separately, since the summer is a growing season and during winter the vegetation disappears or diminishes. At first the input for the correlation and regression analysis will be presented in section 4.1, whereafter in section 4.2 the drivers for vegetation development will be presented. In section 4.3 the drivers for the vegetation decay will be given including a parameterisation of the vegetation decay and in section 4.4 the drivers for vegetation change will be presented. In section 4.5 the drivers for the seed retention will be presented including a parameterisation of the seed retention.

### 4.1. Input parameters

In [Table A.1](#) of appendix B, the parameters for the summer period are given that are used for the correlation analysis. The vegetation density has been measured once at 23 September 2020, at the end of the summer period. Therefore all other variables have been averaged over the whole summer period (1 April 2020 – 23 September) as the events during this period affect the vegetation density at the marsh. The absolute bed level change has been taken, since the movement of the bed is considered more important than whether erosion or sedimentation took place. The maximum significant wave height has been measured only at the seaside of the area of the marsh as can be seen in [Figure 2.1](#), but is assumed to be equal for all plots in area E and for all plots in area G. This might differ slightly from the actual wave height at the vegetation plots, however, since the maximum significant wave height is used it can be assumed to be equal at all vegetation plots of the specific area.

In [Table A.2](#) of appendix B, the average monthly values during the winter period (24 November 2020 – 23 April 2021) are given per parameter. As field data was not collected in January, and to create data of equal length, the data measured in February is considered the same for January. For these months: the maximum significant wave height and maximum flow velocity during the period 24 December – 22 February has been used, the average inundation frequency during this period has been taken and the vegetation density decay and the bed level change during these two months have been divided by two, to simulate a linear change. The absolute bed level change has been taken, since the movement of the bed is considered more important than whether erosion or sedimentation took place.

In [Table A.3](#) of appendix B, the measured vegetation characteristics at the fieldwork days during the winter period (24 November 2020 – 23 April 2021) are given per vegetation characteristic. As field data was not collected in January, and to create data of equal length, the data measured in February is considered the same for January. The vegetation density has been taken instead of the vegetation density decay, since it is more useful to compare the amount of vegetation, the density, that is still present at the vegetation plots with the measured vegetation characteristics. Moreover, the number of *Salicornia* plants grown from the soil samples are presented from February to April, since these are the fieldwork days where the seeds have been successfully grown.

The regression model (presented in Equation 2.1 in section 2.2.5.) gives information about the dependence between the variables that are presented in [Table A.1](#), [Table A.2](#) and [Table A.3](#) of Appendix B.

## 4.2. Drivers for vegetation development

In Table 4.1 the results of the fitted linear regression model are presented for the summer period. The table shows the correlations of all vegetation plots (landside, middle and both of the seaside plots), as vegetation might develop in all vegetation plots. For the single-variables, the maximum significant wave height shows the strongest relation with the vegetation density. Moreover, the  $p$ -values show significant correlations as well (Figure 4.1 and Table 4.1). For the 2-variable linear regression, the combined maximum significant wave height and the inundation frequency as well as the maximum significant wave height with the absolute bed level change show the strongest relation with the vegetation density. However, the  $p$ -values do not show consistent good values as the  $p$ -values of either the inundation frequency or the absolute bed level change are higher than 0.05. The 3-variable linear regression (maximum significant wave height, absolute bed level change and inundation frequency) shows very strong correlations with the vegetation density, however the  $p$ -values are not sufficiently small. For the 2- and 3-variable fits a relatively good significance of the correlation with the maximum significant wave height can be seen, but the additional parameters are not significantly correlated (high  $p$ -values). Therefore a single-variable model of the maximum significant wave height is most effective to describe the vegetation density.

The relation between the maximum significant wave height and the vegetation density has been visualised in Figure 4.1. A linear relation can be seen with a strong correlation coefficient. The vegetation density becomes lower when the waves become higher.

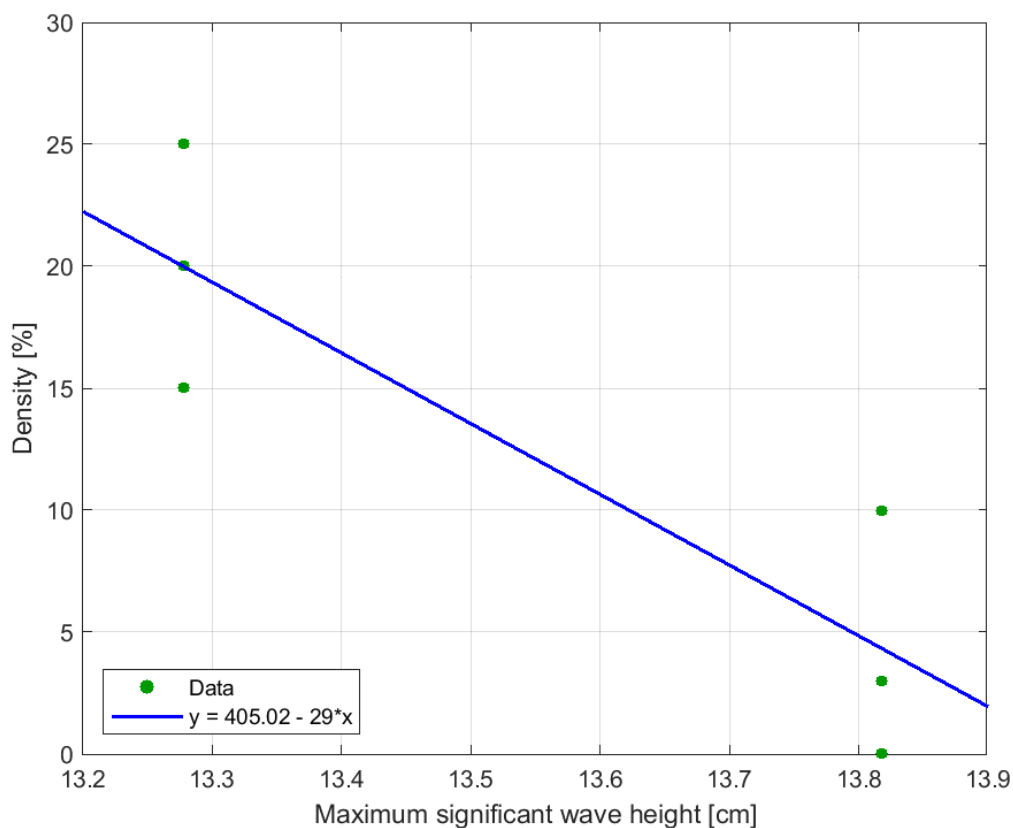


Figure 4.1: Explaining the location of the vegetation density by the maximum significant wave height during the summer period (April 2020 – September 2020). The vegetation density correlates significantly ( $r = -0.88$ ;  $p = 0.02$ ) with the maximum significant wave height.

**Table 4.1:** Results of the fit linear regression model for relating the parameters during the summer period.  $R^2$  is the coefficient of determination,  $p$  is the probability value for testing the statistical significance and  $\beta_n$  are the coefficient estimates for the corresponding terms in the model. The significant correlations have been written in red.

Variables: 1	All vegetation plots		
	$R^2$	$p$	$\beta_n$
Intercept	0.25	0.09	23.70
$\Delta z_b$		0.31	-3.64
Intercept	0.01	0.38	10.08
Inundation		0.83	2.23
Intercept	0.78	0.02	405.02
$H_s$ max		0.02	-29.00
Variables: 2	$R^2$	$p$	$\beta_n$
Intercept	0.26	0.26	21.90
$\Delta z_b$		0.39	-3.61
Inundation		0.86	1.83
Intercept	0.84	0.03	452.01
Inundation		0.39	-4.99
$H_s$ max		0.03	-32.12
Intercept	0.80	0.05	462.95
$H_s$ max		0.06	-33.63
$\Delta z_b$		0.60	1.50
Variables: 3	$R^2$	$p$	$\beta_n$
Intercept	0.89	0.07	565.37
$\Delta z_b$		0.41	2.52
Inundation		0.32	-6.70
$H_s$ max		0.07	-40.96

### 4.3. Drivers for vegetation decay

In Table 4.2 the results of the fitted linear regression model are presented for the winter period. The table shows the correlations of all vegetated plots (landside, middle plots and the seaside plot of area E). The seaside plot of area G has been left out, since there is no vegetation at all. For the single variables, the maximum significant wave height shows the strongest relation with the vegetation decay and the  $p$ -value is sufficiently low. It can be seen that the  $p$ -value of the intercept is not sufficiently low, but, as explained in section 2.2.5., the intercept does not have to be statistical significant. For the 2-variable linear regression, the variable with the highest individual correlation (maximum significant wave height) has been combined with the other variables. The 2-variable linear regression shows strong relations when the maximum significant wave height is part of the analysis. However, the  $p$ -values only show significance for the maximum significant wave height and not for the second variable. The exact same results are visible for the 3- and 4-variable linear regression analysis. For the 2-, 3- and 4-variable, the  $R^2$  increases for an increasing number of variables, however, the significance of the additional coefficients is low (high  $p$ -values). Therefore a single-variable model of the maximum significant wave height is most effective to describe the vegetation decay.

The relation between the maximum significant wave height and the vegetation decay has been visualised in Figure 4.2. A positive linear relation can be seen with a strong correlation coefficient. The vegetation decay becomes larger when the waves are higher as well. Based on the results as presented in Table 4.2, the vegetation decay can be best parametrised with the following formula:

$$y = -5.02 + 1.9 * H_{s,max} \quad (4.1)$$

Wherein  $H_{s,max}$  is the maximum significant wave height during the fieldwork period in centimetres.

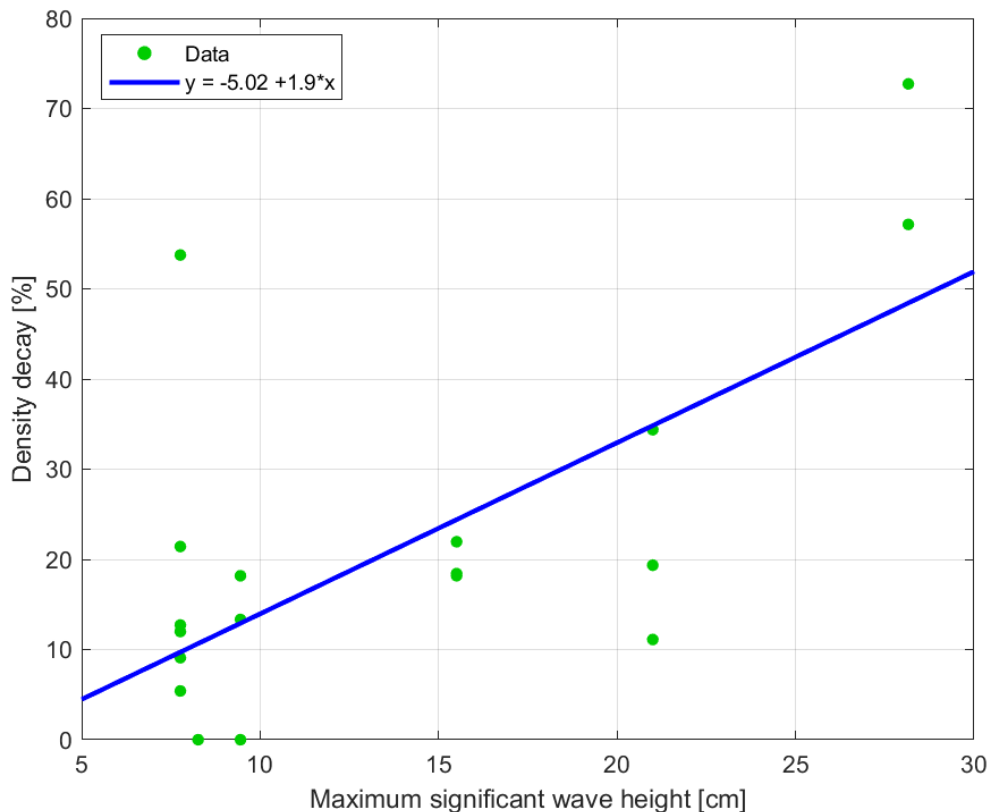


Figure 4.2: Explaining the vegetation decay in the landside, middle plots and in the seaside plot of area E with the maximum significant wave height during the winter period (November 2020 – April 2021). The vegetation decay correlates significantly at all vegetated plots ( $r = 0.68$ ;  $p = 1.86e^{-4}$ ) with the maximum significant wave height.

**Table 4.2:** Results of the fit linear regression model for relating the parameters during the winter period.  $R^2$  is the coefficient of determination,  $p$  is the probability value for testing the statistical significance and  $\beta_n$  are the coefficient estimates for the corresponding terms in the model. The significant correlations have been written in red.

<b>Landside, middle plots and the seaside plot of area E</b>			
<b>Variables: 1</b>	<b><math>R^2</math></b>	<b><math>p</math></b>	<b><math>\beta_n</math></b>
Intercept	0.04	3.86e <sup>-4</sup>	22.42
$\Delta z_b$		0.33	8.81
Intercept	0.03	0.03	14.21
Inundation		0.38	7.58
Intercept	0.46	0.41	-5.02
$H_s$ max		1.86e <sup>-4</sup>	1.90
Intercept	0.02	0.39	94.22
Max velocity		0.49	-157.91
<b>Variables: 2</b>	<b><math>R^2</math></b>	<b><math>p</math></b>	<b><math>\beta_n</math></b>
Intercept	0.47	0.491	-4.42
Inundation		0.75	-2.23
$H_s$ max		3.64e <sup>-4</sup>	1.95
Intercept	0.46	0.80	-22.70
$H_s$ max		3.2e <sup>-4</sup>	1.92
Max velocity		0.84	36.23
Intercept	0.51	0.88	-1.02
$\Delta z_b$		0.18	-8.90
$H_s$ max		1.64e <sup>-4</sup>	1.90
<b>Variables: 3</b>	<b><math>R^2</math></b>	<b><math>p</math></b>	<b><math>\beta_n</math></b>
Intercept	0.51	0.87	-1.10
$\Delta z_b$		0.21	-9.07
Inundation		0.94	0.55
$H_s$ max		4.97e <sup>-4</sup>	1.89
Intercept	0.47	0.85	39.88
Inundation		0.75	-5.34
$H_s$ max		5.06e <sup>-4</sup>	1.96
Max velocity		0.84	-89.05
Intercept	0.51	0.81	21.74
$H_s$ max		4e <sup>-4</sup>	1.87
Max velocity		0.80	-46.10
$\Delta z_b$		0.19	-9.48
<b>Variables: 4</b>	<b><math>R^2</math></b>	<b><math>p</math></b>	<b><math>\beta_n</math></b>
Intercept	0.51	0.70	81.80
$\Delta z_b$		0.20	-9.46
Inundation		0.75	-5.13
$H_s$ max		6.31e <sup>-4</sup>	1.91
Max velocity		0.70	-166.34

#### 4.4. Relations between vegetation properties

In Table 4.3 the results of the fit linear regression model for the vegetation characteristics during the winter period are presented. The table shows the differences between the correlations of the vegetated plots (landside, middle plots and seaside plot of area E) only, as there is no vegetation at the seaside plot of area G. The vegetation characteristics have been compared to the measured density. None of the single-variables show a strong relation with the vegetation density, the aboveground length shows the best relation, as can also be seen in Table 4.3. However, the  $p$ -values are significant for the correlations of the aboveground length, number of side roots and the length of the side roots with the vegetation density. The 2-variable linear regression presents stronger significant relations of the combined vegetation properties with the vegetation density. The strongest relations are obtained when the aboveground length is combined with the number of side roots, the combinations with the root length, length of the side roots and the strength also show significant  $p$ -values. A further improvement of the regression can be obtained by adding one more variable. In Table 4.3 only one combination of 3-variables is presented, since the other combinations do not show significant  $p$ -values. The presented combination considers the aboveground length, strength and the number of side roots and shows a strong relation with the vegetation density. Moreover, this 3-variable combination shows good results for the  $p$ -values as well. These 3-variables can therefore best be used to describe the vegetation density by the presented vegetation characteristics. The strongest single-variable is plotted in Figure 4.3.

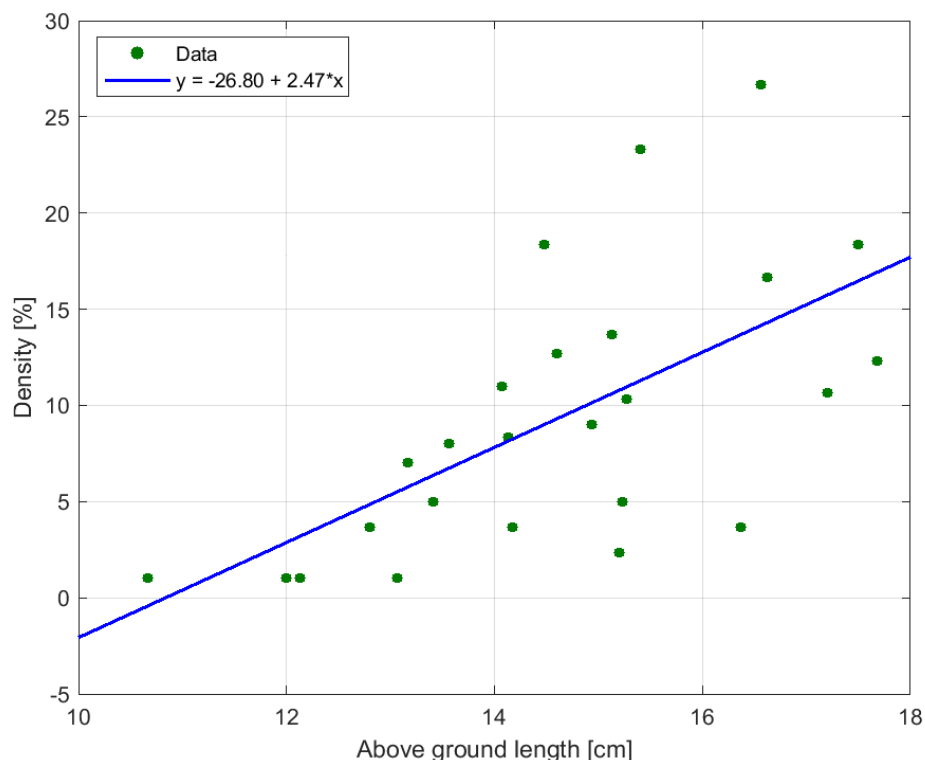


Figure 4.3: Comparing the vegetation density with the aboveground length of the vegetation during the winter period (November 2020 – April 2021). The vegetation density correlates significantly ( $r = 0.61$ ;  $p = 3.53e^{-3}$ ) with the aboveground length.

**Table 4.3:** Results of the fit linear regression model for relating the vegetation characteristics.  $R^2$  is the coefficient of determination,  $p$  is the probability value for testing the statistical significance and  $\beta_n$  are the coefficient estimates for the corresponding terms in the model. The significant correlations have been written in red.

Variables: 1	Landside, middle plots and the seaside plot of area E		
	$R^2$	$p$	$\beta_n$
Intercept	0.37	5.56e-3	-26.80
Aboveground length		3.53e-4	2.47
Intercept	0.07	4.26e-3	16.55
Root length		0.17	-0.71
Intercept	0.27	4.20e-8	14.37
Number of side roots		3.33e-3	-0.75
Intercept	0.32	1.09e-8	14.83
Length side roots		1.11e-3	-0.97
Intercept	0.05	4.77e-3	14.49
Strength		0.26	-0.23
Variables: 2	$R^2$	$p$	$\beta_n$
Intercept	0.47	0.04	-19.55
Aboveground length		9.98e-5	2.60
Root length		0.03	-0.88
Intercept	0.53	0.05	-17.42
Aboveground length		7.69e-4	2.10
Number of side roots		6.83e-3	-0.57
Intercept	0.52	0.11	-14.87
Aboveground length		2.12e-3	1.93
Length side roots		6.58e-3	-0.71
Intercept	0.52	8.33e-3	-23.01
Aboveground length		2.19e-5	2.88
Strength		8.47e-3	-0.43
Intercept	0.30	4.10e-4	19.23
Root length		0.28	-0.50
Number of side roots		5.63e-3	-0.70
Intercept	0.34	4.15e-4	18.50
Root length		0.39	-0.38
Length side roots		2.48e-3	-0.92
Intercept	0.07	5.32e-3	17.10
Root length		0.40	-0.56
Strength		0.73	-0.09
Intercept	0.32	2.69e-8	14.87
Number of side roots		0.91	-0.06
Length side roots		0.16	-0.91
Intercept	0.28	4.78e-4	16.89
Number of side roots		6.14e-3	-0.71
Strength		0.51	-0.12
Intercept	0.33	2.53e-4	17.31
Length side roots		2.10e-3	-0.94
Strength		0.50	-0.12
Variables: 3	$R^2$	$p$	$\beta_n$
Intercept	0.60	0.05	-16.46
Aboveground length		9.89e-5	2.49
Strength		0.03	-0.33
Number of side roots		0.02	-0.45

## 4.5. Drivers for seed retention

In Table 4.4 the results of the fit linear regression model of the available seeds with the different variables are presented. As the seeds have only been collected in February, March and April, only these periods have been taken into account. The table shows the differences between the correlations of all of the vegetation plots in area E and G. The variables density, absolute bed level change, inundation frequency, maximum significant wave height and maximum flow velocity have been correlated with the number of *Salicornia* plants grown from the soil samples that were taken. For the single variables the vegetation density and the maximum flow velocity show the strongest significant relations with the available seeds. The vegetation density and the maximum flow velocity both can therefore be correlated significantly with the number of available seeds. For the 2-variable linear regression the combinations with individually the highest  $R^2$  are presented, since the other variables correlate poorly with the seed availability. These combinations show stronger  $R^2$ , but also higher  $p$ -values and are therefore not statistically significant. Therefore the single variable correlations of the seed availability with either the vegetation density or the maximum flow velocity can be used to determine the number of available seeds. The seed retention can be calculated or predicted with the following equations, which can also be seen in Figure 4.4 and Figure 4.5:

$$a = 1.54 + 2.03 * \rho_{veg} \quad (4.2)$$

$$a = 224.25 - 439.68 * u_{max} \quad (4.3)$$

Wherein  $a$  is the number of available seeds,  $\rho_{veg}$  is the vegetation density in percentage and  $u_{max}$  is the maximum flow velocity during the fieldwork period in meters per second.

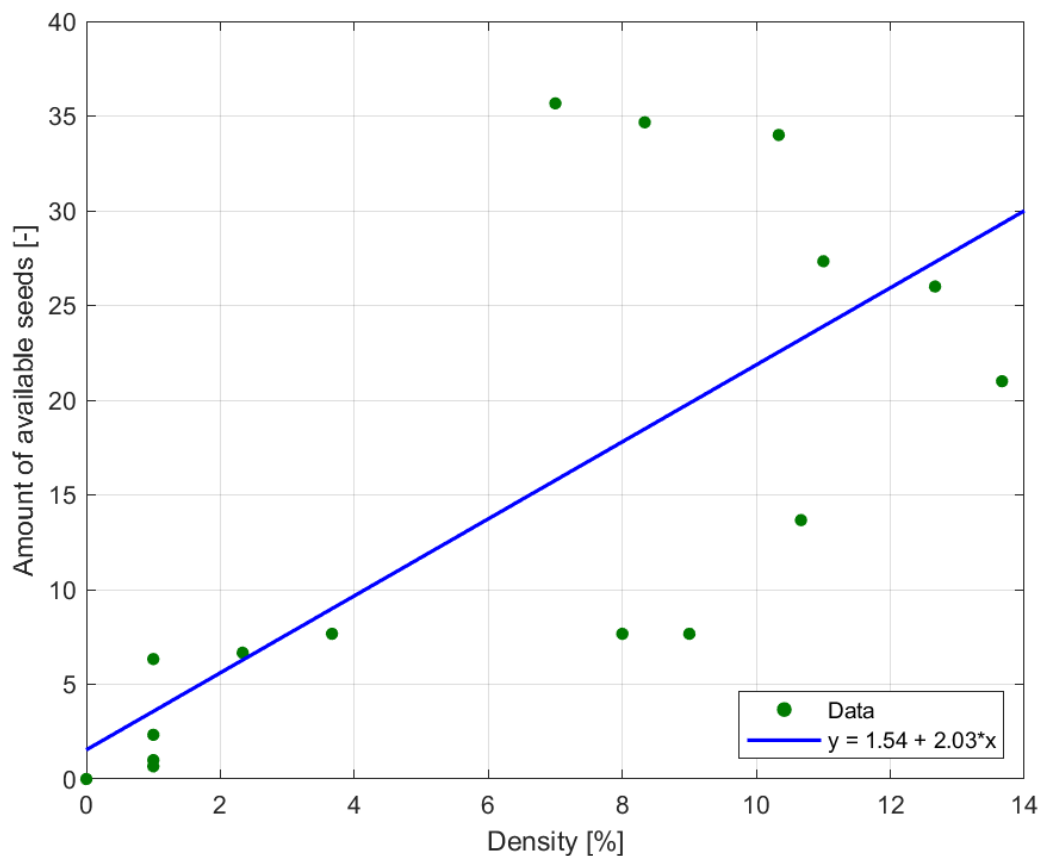


Figure 4.4: Explaining the number of available seeds by the vegetation density during the winter period (November 2020 – April 2021). The seed availability correlates significantly ( $r = 0.76$ ;  $p = 2.54e^{-4}$ ) with the vegetation density.

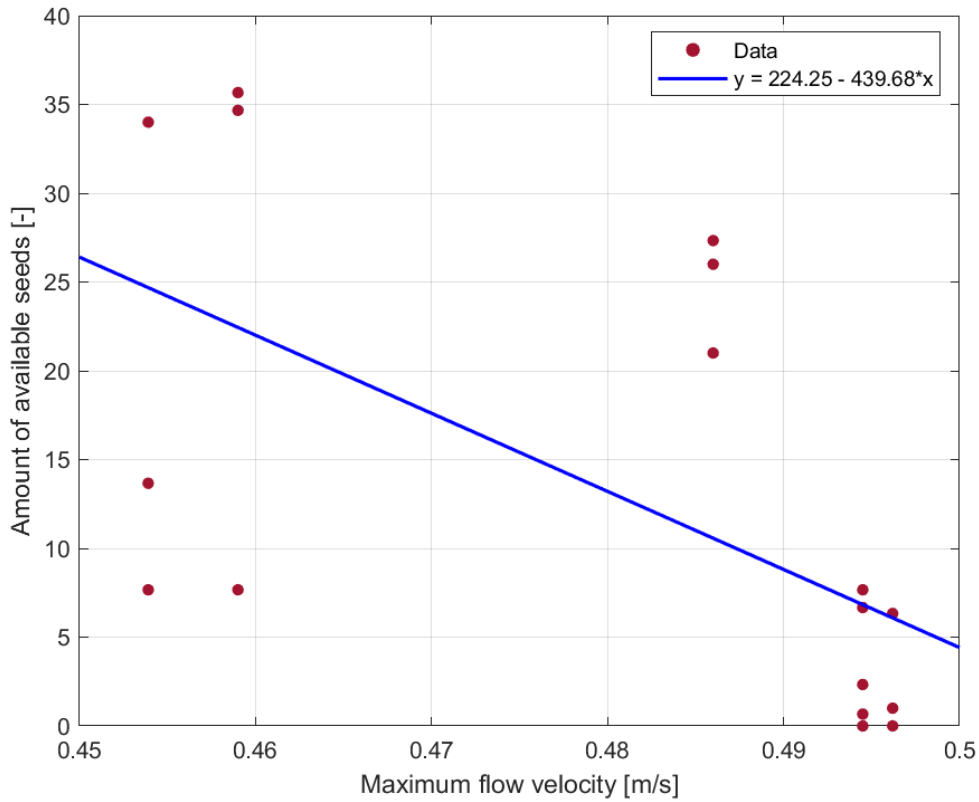


Figure 4.5: Explaining the number of available seeds by the maximum flow velocity during the winter period (November 2020 – April 2021). The seed availability correlates significantly ( $r = -0.60$ ;  $p = 0.02$ ) with the maximum flow velocity.

Table 4.4: Results of the fit linear regression model for relating the available seeds to the different variables.  $R^2$  is the coefficient of determination,  $p$  is the probability value for testing the statistical significance and  $\beta_n$  are the coefficient estimates for the corresponding terms in the model. The significant correlations have been written in red.

Variables: 1	All vegetation plots		
	$R^2$	$p$	$\beta_n$
Intercept	0.18	$2.15e^{-4}$	16.47
$\Delta z_b$		0.08	-3.50
Intercept	$7.73e^{-3}$	0.08	11.14
Inundation		0.73	1.88
Intercept	$6.27e^{-3}$	0.05	14.94
$H_s$ max		0.75	-0.13
Intercept	<b>0.36</b>	<b>0.01</b>	<b>224.25</b>
Max velocity		<b>0.02</b>	<b>-439.68</b>
Intercept	<b>0.58</b>	<b>0.64</b>	<b>1.54</b>
Density		<b><math>2.54e^{-4}</math></b>	<b>2.03</b>
Variables: 2	$R^2$	$p$	$\beta_n$
Intercept	0.45	$9.49e^{-3}$	203.43
Max velocity		0.02	-390.96
$\Delta z_b$		0.13	-2.55
Intercept	0.60	0.37	70.93
Density		$6.36e^{-3}$	1.70
Max velocity		0.38	-140.50
Intercept	0.60	0.36	3.80
Density		$1.25e^{-3}$	1.87
$\Delta z_b$		0.37	-1.33



## 5. Discussion

This study researched the vegetation density decay and the seed availability throughout the winter period and the vegetation density at the end of summer at the Marconi salt marsh in Delfzijl, the Netherlands. The results and findings will be discussed in this chapter. In the first section the results of this study will be compared to other studies, in the second section the implications and applicability of the findings will be presented and the limitations and/or improvements of this study will be discussed in the last section.

### 5.1. Relevance of this research

At salt marshes, the density and location of the vegetation is usually determined by a balance between bed elevation, sedimentation and/or erosion, hydrodynamics and seed availability (Balke et al., 2011; Bouma et al., 2016). In this research the hydrodynamics (inundation frequency, wave height and flow velocity) and bed level changes that might affect the vegetation development, vegetation density decay and seed availability at salt marshes have been studied at the Marconi salt marsh. According to this study, the vegetation density development and the vegetation density decay can be related significantly to the maximum significant wave height. The seed availability is influenced significantly by the vegetation density and the maximum flow velocity individually.

The vegetation density present at the end of the growing season correlates significantly with the maximum significant wave height (Figure 4.1). It was found that higher waves had occurred at the locations where a lower vegetation density was present at the end of summer (Figure 3.9). According to Hu et al. (2015) waves and currents affect the location and density of the vegetation. Moreover, the *Salicornia* vegetation present at the Marconi salt marsh does only attenuate the waves for about 3% (Willemsen, 2021). When there are higher waves, causing an increase in orbital flow velocity, less sediment will settle since the sediment remains in suspension, preventing the bed level to increase (Callaghan et al., 2010). An increasing slope of the bed level may also cause higher waves, which then affects the vegetation density (Duvall et al., 2018). Bed level changes also affect the vegetation density in summer, while in this study the bed level changes do not seem to be related to the vegetation density. This might be partly caused by the different sediment compositions at the study sites. The clayey area E shows locally alternating sedimentation and erosion, since the clay and sand are not mixed equally. Changes in bed level occur locally, which might be caused by a thicker clay layer which will not erode easily (plot c of Figure A.1 shows more changes than plot a of Figure 3.3, while these changes both have been measured in area E). Another reason might be that too long of a period has been considered. The density has been measured only once, at the end of summer, as can be seen in Figure 3.9, and therefore all other variables are averages over the whole summer period (April 2020 - September 2020). This might negatively affect the direct correlation between these variables.

The decay of the vegetation density during the winter period correlates positively with the maximum significant wave height at all vegetated plots (Figure 4.2). It was found that higher waves result in a faster decay of vegetation density. This can also be seen in the figures of the wave height and the vegetation density decay. In Figure 3.7 the significant wave height of the different locations has been plotted and in Figure 3.10 the vegetation density decay throughout the winter can be seen. The waves measured in January can be linked to the vegetation decay in January and February. The wave event happening in March, where especially high waves have been measured in area G, can be linked to the faster decrease in vegetation density in March in area G.

The decreasing vegetation density during the winter period has been correlated with the different vegetation characteristics to find interactions between the vegetation density and other vegetation characteristics. It was found that the vegetation density shows a significantly strong correlation with a combination of factors: aboveground length, strength and number of side roots (Figure 4.3 and Table 4.3). The vegetation density and length are much lower in area G, while the strength and the number of side roots are higher in area G, when comparing these to area E (Figure 3.10). These differences might be caused by the differences in sediment composition and therefore the amount of nutrients in the ground (Chaudhary et al., 2018; Löhmus et al., 2020). Another reason for the greater strength and higher number of roots in area G could be, that area G is located more exposed to waves. This could lead to stronger plants with a higher number of roots. However, this cannot be surely stated by the results from this study. Further research on the ecological and meteorological aspects that affect the vegetation characteristics outside the growing season is therefore necessary.

The seed availability during the winter period (February 2021 – April 2021) correlates significantly with the vegetation density (Figure 4.4) and the maximum flow velocity (Figure 4.5). It was found that more vegetation resulted in a higher number of seeds and that higher flow velocities occurred at the locations where fewer seeds were available. The vegetation density plays the first role in the seed availability, after all, if no vegetation is present, the flow velocities cannot affect the non-existing seeds. If seeds are present, the occurring flow velocities move the seeds around or away from the marsh. In Figure 3.5 and Figure 3.6 it can be seen that the flow velocities are higher in area G and in Figure 3.11 it can be seen that the number of seeds is higher in area E, which confirms this negative correlation. Since the seeds of the *Salicornia* vegetation do not fall of the plant, but stick to the stem (Davy et al., 2001; Hulisz et al., 2010; Balke et al., 2011), more and more plants will break down during the winter period, meaning that more branches with seeds become available. These branches might stick around when velocities are low, adding to the local seedbank, but can be transported away under high flow velocities, resulting in a lower seed availability. A sidenote needs to be made, since the flow velocity has been measured at the lower laying seaside plots only and is assumed to be equal at all vegetation plots of that specific area (similar to the assumed wave heights). This is the best approximation since the flow velocities at the marsh can only occur when the marsh is inundated, indicating that there would also be a high tide at the more landward plots and therefore higher flow velocities. Nevertheless, the flow velocities may differ from the flow velocities measured at the seaside plot. It is most likely that the flow velocities at the more landward vegetation plots will be lower than at the seaside plot. If this was the case than the correlation would probably be even higher, as the maximum flow velocities and the number of available seeds are negatively correlated. This means that the flow velocities would be lower at the more dense vegetated plots, resulting in an even stronger negative correlation.

## 5.2. Implications and applicability

This study contributes to the general knowledge of the biogeomorphological processes at salt marshes. To gain more knowledge about the processes affecting the vegetation density in the growing season of salt marsh vegetation, the processes have been correlated with the vegetation density at the end of summer 2020. Based on our results (Figure 5.1), a parameterisation can be used to predict the vegetation cover within biogeomorphic models more accurately. The *Salicornia* vegetation cover can be modelled and predicted by the locally occurring wave heights. This parameterisation might improve the predictions of the effects of hydro- and sediment dynamics on the vegetation density at the marsh. Since the outcome differs from former research, as the bed level change does not seem to be individually correlated with the vegetation density, the results could also be used for validating existing models. In this way the vegetation density can be predicted more accurately. These models can be used to create optimal conditions for resilient salt marshes that have the ability to expand and increase the density of the vegetation cover. This can be done by decreasing the wave heights by, for example, placing permeable dams that are high enough to reduce the wave energy.

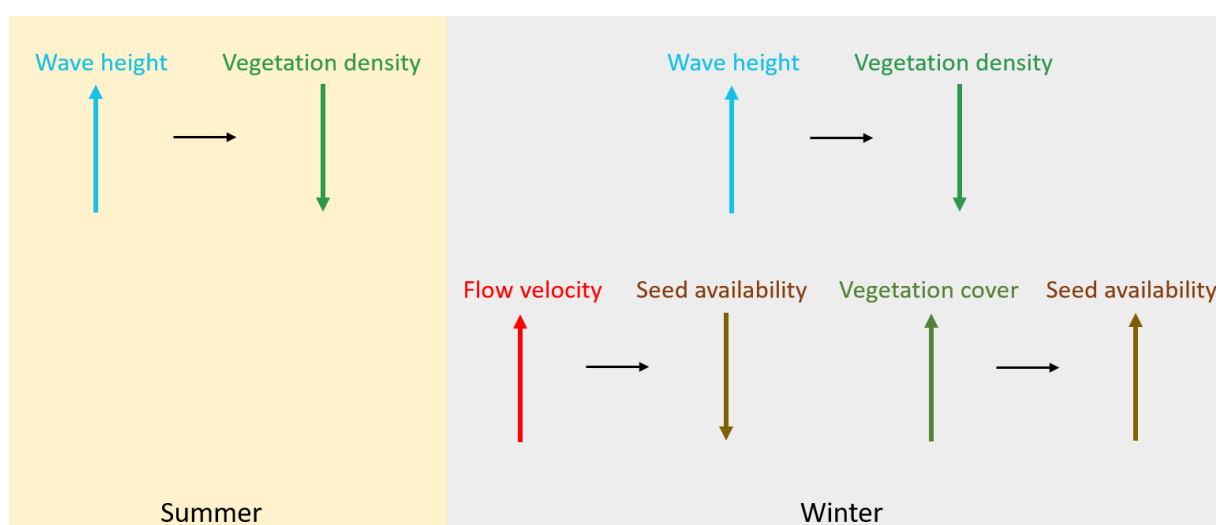


Figure 5.1: Schematisation of the results of this study. An increasing wave height leads to a decreasing vegetation density in summer and winter. Increasing flow velocities lead to less available seeds, while a denser vegetation cover will result in more seed availability throughout the winter period.

Most studies focus on the growing and flowering seasons of salt marsh vegetation, but lack insight in the degradation processes (Schwarz et al., 2018; Van Regteren et al., 2019). As *Salicornia Europaea* is seasonal vegetation, the degradation of the vegetation cover needs to be researched as well, since this degradation may interact with the hydro- and morphodynamics at the salt marsh. The decaying process is currently modelled with a sudden removal of the vegetation cover, from a full vegetation at end of the summer to a salt marsh without any vegetation (Schwarz et al., 2018; Van Regteren et al., 2019), leaving a bare intertidal flat that is directly exposed to the winter hydrodynamics. This sudden vegetation disappearance does not match with reality. Based on our results, a parameterisation can be used to describe the decaying process instead, and this parameterisation can be used to predict the decaying process within such models. Incorporating the decaying process within such models could contribute to a more realistic simulation of the salt marsh. The impact of the hydro- and morphodynamics on the changes of the marsh throughout the winter period might change if the vegetation density decay is modelled more realistically. When the vegetation does disappear more smoothly throughout the winter period, this also affects the number of seeds in the seedbank and the moment of entering the seedbank. In addition, a more realistic vegetation density decay may also impact the dispersion of the seeds, as the seeds are contained in the branches of the vegetation. Moreover, if the seeds are released later in the winter period, there is a larger probability that they

stay at the marsh instead of washing away. This retention of seeds might also affect the vegetation establishment, and with this the vegetation density, in the next season. Altogether, this improves the simulated long-term marsh development in models. These models can be used to create optimal conditions for a sustainable salt marsh that has the abilities to expand and grow with sea level rise. This can be done by decreasing the wave height by, for example, placing permeable dams at the marsh edges that are high enough to reduce the wave energy.

According to this study the seed availability throughout the winter period is related to the vegetation density and the maximum flow velocity at the salt marsh. The parameterisations for the seed availability are therefore based on the vegetation density and the maximum flow velocity, meaning that the seed availability can be predicted by the amount of vegetation cover and the occurring maximum flow velocities. In this way the number of seeds available at the marsh can be predicted, and with this, the expected amount of vegetation cover in the next growing season. Currently the seed availability is modelled as a constant random number each year during spring. The result that the seed availability is dependent on the vegetation density and the occurring flow velocities contributes to a better understanding of the salt marsh development. This result can be used in modelling studies to predict the vegetation cover in the next growing season more accurate rather than the random establishment of seedlings that is currently used (Hu et al., 2015). The seed availability can be calculated more locally depending on the local vegetation cover and flow velocities, by taking account spatial variability in vegetation density and flow velocity. In future salt marsh development this can be used to increase the survivability of salt marshes by, for example, (locally) decreasing the flow velocities at the marsh. The flow velocities can be decreased by, for example, decreasing the slope or limit the number of obstructions.

### 5.3. Limitations

The first part of this study consists of collecting data from the field at a number of similar time intervals. The bed level and vegetation dynamics have been measured locally and at an interval of one month. The measured bed level has been used to calculate the inundation frequency, but has some uncertainties. The height of the bed at the specific vegetation plot has been taken, while it is possible that a sandbank between the vegetation plot and the seaside location, where the water level was measured, already reduces the inundation frequency. The inundation frequency has been calculated by subtracting the bed level height, measured with the GPS device, from the water level, measured at the seaside plots. To know for sure that the correct inundation frequency per vegetation plot has been calculated, a profile of the bed level height of the whole salt marsh could be made, or water levels could be monitored at multiple locations throughout the marsh. In this way the inundation frequency can be presented more precisely. Next to these uncertainties, there might also be issues with the accuracy of the measurement devices. The ASSED, for example, measures the wave height by differences in pressure. The wave sensor does not take into account the water pressure only, but measures the total pressure, wherein the air pressure is included. As the air pressure changes over time, the actual wave height might deviate a few centimetres.

The hydrodynamics, like the significant wave height and flow velocities have been measured at the seaside vegetation plot only and the maximum values have been assumed to be equal at all vegetation plots of that area. This is the best approximation since the maximum wave height at the marsh can only occur when the marsh is inundated, indicating that there would also be higher waves at the more landward plots. Nevertheless, the wave height at the landside plots might differ from the wave height measured at the seaside plots, since the bed friction increases, water depth decreases and the vegetation might cause more friction in the landside direction. In reality, the wave height might decrease towards the dike, as the slope of the marsh is rather gentle and wave energy is lost due to

friction. This could cause the correlation to drop, depending on the decrease in wave height and the difference in wave height between the middle and landside vegetation plots. The same applies to the maximum flow velocity. The assumption that the maximum flow velocity is equal at all vegetation plots is the best approximation, but might differ per vegetation plot. This could be measured more precisely when a measuring device is placed at every vegetation plot. This device should, however, measure more close to the bed to increase the frequency when data is collected. Another way could be to compute or simulate the wave height and flow velocities at the middle and landside vegetation plots in a bio-geophysical model, by taking into account the distance between the vegetation plots, decreasing water depth and friction from the bed and vegetation.

For the number of seeds in the seedbank, we collected soil samples till a depth of 4 cm. This gives a good overview of the number of seeds available in the top 4 cm layer, but does not give an indication about the number of seedlings in the subsequent summer. Only the seeds in the upper 5 mm of the sediment might sprout and grow into seedlings (Davy et al., 2001). From our data, it cannot be determined if the seeds counted were distributed equally over the depth of the soil sample. To predict the number of seedlings that might sprout, and with this the vegetation cover in the next growing season, soil samples from the upper 5 mm of the sediment should be taken.

The seedbank in area E differs strongly from the seedbank in area G. This might be partly caused by the difference in vegetation cover and hence with this the number of available seeds. Another reason could be that the sediment composition of area E is able to retain more seeds. Soils with less than 20% mud, the soil in area G consists of 5% mud, are considered non-cohesive soils and have a lower resistance to wave and current erosion (De Vries et al., 2021). It was found by Van Regteren et al. (2019) that washing away of seeds by waves and currents causes a high mortality rate of the seeds. It is therefore most likely, that the difference of the seedbank is caused by the difference in sediment composition.

The influences of ecological factors on the decaying process of the *Salicornia* vegetation on the salt marsh, like for example rotting, have not been researched in this study. During the fieldwork, plants were pulled out of the ground to measure the strength of the vegetation. The strength does not decrease substantially (Figure 3.10), however, in the data it cannot be seen that at the end of the winter more and more plants broke off at the location where the trunk crosses the surface. For this reason it is most likely that rotting plays a large role in the decaying process of *Salicornia* and is therefore interesting to include in future research in the decay of salt marsh vegetation. The causes of rotting could be researched and these meteorological and ecological processes could be added in the biogeomorphic model, explaining the vegetation density decay more accurate.



## 6. Conclusion

The goal of this study is to determine how the vegetation density of *Salicornia Europaea*, its decay and its seed retention are related to, a combination of, the flow velocity, wave height, surface elevation changes, inundation frequency or the sediment composition. To achieve this goal, data were collected at the artificially created Marconi saltmarsh in order to answer four research questions and one main research question. The conclusions will be given per research question.

### 6.1. Drivers for vegetation development

The first research question is: *“How do wave height, surface elevation changes, inundation frequency and sediment compositions affect the Salicornia vegetation cover on the Marconi salt marsh at the end of summer?”*

The field data from the Marconi salt marsh showed that the vegetation density at the end of summer is strongly related to the maximum significant wave height during the summer period (April 2020 – September 2020). A higher maximum significant wave height is associated with a lower vegetation cover ( $r = -0.88$ ;  $p = 0.02$ ). The inundation frequency and surface elevation changes cannot be related with the vegetation cover, individually nor combined, and do therefore not affect the vegetation cover at the end of summer on the salt marsh. The effect of the different sediment compositions could not be studied due to a lack of observations for the summer period.

### 6.2. Relations between vegetation properties

The second research question is: *“How does the vegetation density decay correlate with the vegetation properties, like strength, length, root length, number of side roots and length of the longest side root throughout the winter period (November to April)?”*

The *Salicornia* vegetation at the Marconi salt marsh decays throughout the winter period (November 2020 – April 2021). The vegetation density throughout the winter period, at all vegetation plots where vegetation is present, can be linked to a combination of the aboveground length, strength and the number of side roots of the vegetation. A higher aboveground length, strength and number of side roots correlates positively with the remaining vegetation density ( $r = 0.77$ ;  $p = 2.04e^{-5}$ ). This indicates that the bigger/stronger plants tend to remain in place longer than the smaller/weaker plants.

### 6.3. Drivers for vegetation decay

The third research question is: *“How does the vegetation density decay correlate with the hydrodynamic exposure and morphodynamic activity throughout the winter period (November to April)?”*

The field data from the Marconi salt marsh showed that the vegetation density decay throughout the winter period (November 2020 – April 2021) is correlated positively with the maximum significant wave height. A higher maximum significant wave height results in a faster decay ( $r = 0.87$ ;  $p = 6.61e^{-7}$ ). The parameterisation belonging to this data is:

$$y = -5.02 + 1.9 * H_{s,max} \quad (6.1)$$

Wherein  $y$  is the vegetation density decay in percentage and  $H_{s,max}$  is the maximum significant wave height during the fieldwork period in centimetres.

The inundation frequency, flow velocity and surface elevation changes cannot be related to the vegetation density decay, individually nor combined, and are therefore concluded to not affect the *Salicornia* density decay throughout the winter period at the salt marsh. There does not seem to be a relation between the vegetation decay and different sediment compositions either.

### 6.4. Drivers for seed retention

The fourth research question is: *“How does the seed availability change throughout the winter period (November to April) and does the seedbank relate to vegetation density, hydrodynamic exposure, morphodynamic activity and sediment composition?”*

The field data showed that the seed retention in the top four centimeters of the soil at the Marconi salt marsh throughout the winter period (November 2020 – April 2021) at all vegetation plots correlated positively with the vegetation density and negatively with the maximum flow velocity. A higher vegetation density resulted in more seeds ( $r = 0.76$ ;  $p = 2.54e^{-4}$ ) and higher flow velocities resulted in less seed retention ( $r = -0.60$ ;  $p = 8.32e^{-3}$ ). The parameterisations belonging to these trends are:

$$a = 1.54 + 2.03 * \rho_{veg} \quad (6.2)$$

$$a = 224.25 - 439.68 * u_{max} \quad (6.3)$$

Wherein  $a$  is the number of available seeds per circa 100 cm<sup>2</sup> as the soil sample has a diameter of 10 cm (see section 2.1.5.),  $\rho_{veg}$  is the vegetation density in percentage and  $u_{max}$  is the maximum flow velocity during the fieldwork period in meters per second.

The vegetation density and the maximum flow velocity are correlated individually (single-variable) with the number of available seeds. There is no 2-variable correlation with the seed retention. The inundation frequency, maximum significant wave height and surface elevation changes cannot be significantly related to the seed retention, individually nor combined, and do therefore not affect the seed retention throughout the winter period at the salt marsh. There does not seem to be a relation between the seed retention and different sediment compositions either.

## 6.5. Impact of hydro- and morphodynamics on the vegetation decay and the seedbank

The main research question is: *“How do the Salicornia development and decay as well as the seedbank correlate with flow velocities, wave height, surface elevation changes, inundation frequency and sediment composition on a salt marsh throughout the winter period and how do the vegetation characteristics correlate with the Salicornia decay and seedbank?”*

The presented parameterisations can be used in modelling studies to predict the vegetation density (decay) based on the wave height and the number of seeds in the seedbank based on the vegetation density and the flow velocities at the marsh. When these parameterisations are implemented into numerical models, it is possible to simulate the impact of physical stressors on the short-term and long-term vegetation development. This will help to develop effective management and restoration strategies for salt-marshes.

Currently, the vegetation density decay is modelled with a sudden decrease at the start of winter, meaning that the vegetation density abruptly changes to zero. The last column of

Table 6.1 presents the remaining vegetation density at the end of the winter period as a percentage of the reference density in percentages. From the table can be noted that, of the vegetation density at the start of the winter period, still 20-45% of the vegetation remains at the end of the winter period. This shows that the zero-vegetation assumption in the numerical models at the start of winter is a large misrepresentation of the actual vegetation density. This difference in approach of the vegetation density (decay) could impact the salt marsh development for long-term simulations, as the remaining vegetation during the winter period may trap sediment and increase the seed availability in the seedbank over time. This emphasises the importance of including parameterisations for the vegetation density decay and the seed availability in numerical models and for further studies of salt marsh vegetation at the Marconi project and in general.

Table 6.1: Amount of vegetation cover of the first measurement still present at the end of the winter period.

Vegetation plot	Density 24-11-'20 [%]	Density 23-04-'21 [%]	$\left(\frac{\rho_{veg,(23/04)}}{\rho_{veg,(24/11)}} * 100\%\right)$
E landside	18	8	45
E middle part	23	7	30
E seaside	27	8	30
G landside	5	1	20
G middle part	4	1	25
G seaside	0	0	-



## 7. Recommendations

Based on the results of this study at the Marconi salt marsh, the vegetation development and vegetation density decay of *Salicornia* in salt marshes can be explained by the maximum significant wave height. The parameterisation obtained in this study for the vegetation decay might be used in models to predict the decaying process at salt marshes. At locations where new salt marshes are created, these processes might be predicted based on the significant wave height. Based on the results it can be concluded whether measures to decrease the maximum significant wave height are necessary at the specific location. The decaying process of vegetation is currently modelled with a sudden removal of the vegetation cover, from a full vegetation cover at the end of summer to zero vegetation cover at the start of winter. By using the parameterisation developed in this study, the 'real-life' process of the decaying vegetation might be predicted more precisely.

A biogeomorphic model, like Schwarz et al. (2018) have used, could be built, based on the presented parameterisations, to validate the general applicability of the empirical relations.

Most of the numerical bio-geophysical models currently work with a random establishment of seeds, while this does not match the field observations. According to the results of this study, the seed retention can best be parameterised by the maximum flow velocity and the vegetation density. This parameterisation can be used to predict the seedbank development, and with this the growth of the marsh, more precisely. If the growth is limited or the marsh is shrinking, a reduction of the flow velocities might give a positive effect.

The results of this study show that the maximum wave height has the highest correlation with the development and decay of the vegetation cover. The maximum wave height has been measured at the lower, more exposed vegetation plots, at the seaside, of the marsh only and has been assumed to be equal at all more landward located vegetation plots. This is currently the best approximation since the maximum wave height at the marsh can only occur when the marsh is inundated, indicating that there would also be high waves at the more landward plots. Nevertheless, it would be recommended to measure the wave height at the more landward plots separately. This could be done by for example a measurement device that can measure in lower water depths or by creating a model that predicts the wave height based on, for example, the change in bed level, the amount of friction caused by vegetation or the bed and the decrease of water depth.

In this study we collected seeds from the 4 cm top layer of the soil, while not all seeds from this layer are germinating in the next growing season. Most seeds that are buried will stay in the seedbank for a longer period or till that much erosion has taken place that they are located at the surface. According to Davy et al. (2001), 95% of the germinated seeds are concentrated in the upper 5 mm of the sediment. It might be best to take a soil sample of this surface layer right before spring, to create a better indication of the number of seedlings in the next growing season.



# Bibliography

- Abd El Samee, W. N., & Elsamny, M. K. (2019). Effect of Scour Depth on Ultimate Capacity and Settlement of Piled Foundation. In *Sustainability Issues for the Deep Foundations* (pp. 258-284).
- Bakker, J. P., Baas, A. C. W., Bartholdy, J., Jones, L., Ruessink, G., Temmerman, S., et al. (2016). Environmental Impacts—Coastal Ecosystems. In *North Sea Region Climate Change Assessment* (pp. 275-314).
- Balke, T., Bouma, T. J., Horstman, E. M., Webb, E. L., Erftemeijer, P. L. A., & Herman, P. M. J. (2011). Windows of opportunity: thresholds to mangrove seedling establishment on tidal flats. *Marine Ecology Progress Series*, 440, 1-9. doi:10.3354/meps09364
- Baptist, M. J., Willemsen, P. W. J. M., Elschot, K., & Cleveringa, J. (2018). Monitoring plan Marconi salt marshes. *Ecoshape*, 12.
- Bartholdy, J. (2012). Salt Marsh Sedimentation. In *Principles of Tidal Sedimentology* (pp. 151-185).
- Best, Ü. S. N., Van der Wegen, M., Dijkstra, J., Willemsen, P. W. J. M., Borsje, B. W., & Roelvink, D. J. A. (2018). Do salt marshes survive sea level rise? Modelling wave action, morphodynamics and vegetation dynamics. *Environmental Modelling & Software*, 109, 152-166. doi:10.1016/j.envsoft.2018.08.004
- Bouma, T. J., van Belzen, J., Balke, T., van Dalen, J., Klaassen, P., Hartog, A. M., et al. (2016). Short-term mudflat dynamics drive long-term cyclic salt marsh dynamics. *Limnology and Oceanography*, 61(6), 2261-2275. doi:10.1002/lno.10374
- Callaghan, D. P., Bouma, T. J., Klaassen, P., van der Wal, D., Stive, M. J. F., & Herman, P. M. J. (2010). Hydrodynamic forcing on salt-marsh development: Distinguishing the relative importance of waves and tidal flows. *Estuarine, Coastal and Shelf Science*, 89(1), 73-88. doi:10.1016/j.ecss.2010.05.013
- Chaudhary, D. R., Rathore, A. P., & Jha, B. (2018). Aboveground, belowground biomass and nutrients pool in *Salicornia brachiata* at coastal area of India: interactive effects of soil characteristics. *Ecological Research*, 33(6), 1207-1218. doi:10.1007/s11284-018-1634-9
- Dankers, P., Verhoogt, H., Grasmeijer, M., De Groot, A., Baptist, M., Smit, C., et al. (2012). Beschrijving huidige situatie. *Ecoshape*, 19.
- DATGNSS. (2021).
- Davy, A. J., Brown, M. J. H., Mossman, H. L., & Grant, A. (2011). Colonization of a newly developing salt marsh: disentangling independent effects of elevation and redox potential on halophytes. *Journal of Ecology*, 99(6), 1350-1357. doi:10.1111/j.1365-2745.2011.01870.x
- Davy, A. J., F., B. G., & Costa, C. S. B. (2001). *Salicornia* L. (*Salicornia pusilla* J. Woods, *S. ramosissima* J. Woods, *S. europaea* L., *S. obscura* P.W. Ball & Tutin, *S. nitens* P.W. Ball & Tutin, *S. fragilis* P.W. Ball & Tutin and *S. dolichostachya* Moss). *Ecology*, 27.

- De Vries, B., Willemsen, P. W. J. M., Van Pruijenbroek, M., Coumou, L., Baptist, M., Cleveringa, J., et al. (2021). Salt marsh pilot Marconi - Monitoring results. *Ecoshape*, 88.
- Duggan-Edwards, M. F., Pagès, J. F., Jenkins, S. R., Bouma, T. J., Skov, M. W., & Moore, J. (2020). External conditions drive optimal planting configurations for salt marsh restoration. *Journal of Applied Ecology*, 57(3), 619-629. doi:10.1111/1365-2664.13550
- Duvall, M. S., Wiberg, P. L., & Kirwan, M. L. (2018). Controls on Sediment Suspension, Flux, and Marsh Deposition near a Bay-Marsh Boundary. *Estuaries and Coasts*, 42(2), 403-424. doi:10.1007/s12237-018-0478-4
- Esselink, P., Van Duin, W. E., Bunje, J., Folmer, E. O., Frikke, J., Glahn, M., et al. (2019). Salt marshes. In: Wadden Sea Quality Status Report *waddensea worldheritage*, 41. Retrieved from [qsr.waddensea-worldheritage.org/reports/salt-marshes](https://qsr.waddensea-worldheritage.org/reports/salt-marshes)
- Finotello, A., Marani, M., Carniello, L., Pivato, M., Roner, M., Tommasini, L., et al. (2020). Control of wind-wave power on morphological shape of salt marsh margins. *Water Science and Engineering*, 13(1), 45-56. doi:10.1016/j.wse.2020.03.006
- Grandjean, T. (2021).
- Hu, Z., Stive, M. J. F., Zitman, T. J., Ye, Q. H., Wang, Z. B., Luijendijk, A., et al. (2011). Interaction between hydrodynamics and salt marsh dynamics - An example from Jiangsu Coast. 8.
- Hu, Z., van Belzen, J., van der Wal, D., Balke, T., Wang, Z. B., Stive, M., et al. (2015). Windows of opportunity for salt marsh vegetation establishment on bare tidal flats: The importance of temporal and spatial variability in hydrodynamic forcing. *Journal of Geophysical Research: Biogeosciences*, 120(7), 1450-1469. doi:10.1002/2014jg002870
- Hulisz, P., Elvisto, T., Karasiewicz, M. T., & Piernik, A. (2010). Abiotic factors influencing the occurrence of *Salicornia europaea* in West Estonia. *Ecological Questions*, 14(1). doi:10.2478/v10090-011-0017-4
- Jonkman, S. N., Hillen, M. M., Nicholls, R. J., Kanning, W., & van Ledden, M. (2013). Costs of Adapting Coastal Defences to Sea-Level Rise— New Estimates and Their Implications. *Journal of Coastal Research*, 290, 1212-1226. doi:10.2112/jcoastres-d-12-00230.1
- Li, X., Lei, G., Li, Y., Wang, Y., & Tan, Z. (2020). Assessing hydrodynamic effects of ecological restoration scenarios for a tidal-dominated wetland in Liaodong Bay (China). *Sci Total Environ*, 752, 142339. doi:10.1016/j.scitotenv.2020.142339
- LLC, L. i. (2019). TCM-4 Tidl Current Meter.
- Löhmus, K., Balke, T., Kleyer, M., & Török, P. (2020). Spatial and temporal patterns of initial plant establishment in salt marsh communities. *Journal of Vegetation Science*, 31(6), 1122-1132. doi:10.1111/jvs.12915
- Londo, G. (1976). The Decimal Scale for Relevés of Permanent Quadrats. *Vegetatio*, 33, 61-64. doi:10.1007/BF00055300
- Maps, G. (2021).

- Mus, A. (2019). The applicability of the ASED-sensor for measuring bed level changes in intertidal areas. 100. Retrieved from <https://www.utwente.nl/en/et/wem/education/msc-thesis/2019/mus.pdf>
- Poppema, D. W. (2017). *Experiment-supported modeling of salt marsh establishment : Applying the Windows of opportunity concept to the Marconi pioneer salt marsh design*.
- Poppema, D. W., Willemsen, P. W. J. M., de Vries, M. B., Zhu, Z., Borsje, B. W., & Hulscher, S. J. M. H. (2019). Experiment-supported modelling of salt marsh establishment. *Ocean & Coastal Management*, 168, 238-250. doi:10.1016/j.ocecoaman.2018.10.039
- Schwarz, C., Gourgue, O., van Belzen, J., Zhu, Z., Bouma, T. J., van de Koppel, J., et al. (2018). Self-organization of a biogeomorphic landscape controlled by plant life-history traits. *Nature Geoscience*, 11(9), 672-677. doi:10.1038/s41561-018-0180-y
- Silliman, B. R., Schrack, E., He, Q., Cope, R., Santoni, A., van der Heide, T., et al. (2015). Facilitation shifts paradigms and can amplify coastal restoration efforts. *Proc Natl Acad Sci U S A*, 112(46), 14295-14300. doi:10.1073/pnas.1515297112
- Succulents, W. o. (2015). *Salicornia Europeana (Common Glasswort)*. *World of Succulents*, 4.
- Sweet, S. A., & Grace-Martin, K. (2008). *Data Analysis with SPSS: A First Course in Applied Statistics*.
- Temmerman, S., Bouma, T. J., Van de Koppel, J., Van der Wal, D., De Vries, M. B., & Herman, P. M. J. (2007). Vegetation causes channel erosion in a tidal landscape. *Geology*, 35(7). doi:10.1130/g23502a.1
- Temmerman, S., Meire, P., Bouma, T. J., Herman, P. M., Ysebaert, T., & De Vriend, H. J. (2013). Ecosystem-based coastal defence in the face of global change. *Nature*, 504(7478), 79-83. doi:10.1038/nature12859
- Van Loon-Steensma, J. M. (2015). Salt marshes to adapt the flood defences along the Dutch Wadden Sea coast. *Mitig Adapt Strateg Glob Chang*, 20(6), 929-948. doi:10.1007/s11027-015-9640-5
- Van Regteren, M., Colosimo, I., De Vries, P., Van Puijenbroek, M. E. B., Freij, V. S., Baptist, M. J., et al. (2019). Limited seed retention during winter inhibits vegetation establishment in spring, affecting lateral marsh expansion capacity. *Ecol Evol*, 9(23), 13294-13308. doi:10.1002/ece3.5781
- Willemsen, P. W. J. M. (2020). ASED measurements and results at Marconi. 8.
- Willemsen, P. W. J. M. (2021). Biogeomorphology of salt marshes understanding the decadal salt marsh dynamics for flood defense. 223. doi:10.3990/1.9789036551120
- Willemsen, P. W. J. M., Horstman, E. M., Bouma, T. J., Baptist, M. J., van Puijenbroek, M. E. B., & Borsje, B. W. Facilitating salt marsh restoration: the importance of event-based bed level dynamics and annual trends in bed level change.



# Appendices

## Appendix A – Continuous surface accretion and erosion

The continuous surface elevation changes have been measured at a burst interval of 15 minutes by the ASEDs. The results of the measurements are presented in [Figure A.1](#). The ASED only measures while the measuring head is submerged, resulting in more measuring points for the lowest locations (at the front and entrance of area F) than the ones situated at the seaside plots of the areas. Moreover, a gap in the measuring points can be seen between October and December. During this period the ASED devices were not installed in the field.

Since the measuring head needs to be submerged before the ASED starts measuring, not a lot of data has been collected for the locations at the seaside plots at the marsh. This can be seen in the three plots on the right of [Figure A.1](#). Even though there are not that many measuring point at the seaside plots of the marsh, it is clearly visible that the bed level changes over time. In area E erosion and sedimentation has occurred, while in area F mostly sedimentation seems to occur. Area G seems to fluctuate most, with sedimentation in April 2020 and February 2021, but erosion in March/April 2021.

The bed level changes measured by the ASEDs are used to create a better understanding of the changes in between the fieldwork days. The bed level has been obtained with a pre-existing script written by Willemssen et al. This gives more information about the existing dynamics at and close to the marsh. Moreover, it shows that the locations, that are not protected by the brushwood dams, are more dynamic than at the ASEDs located at the marsh.

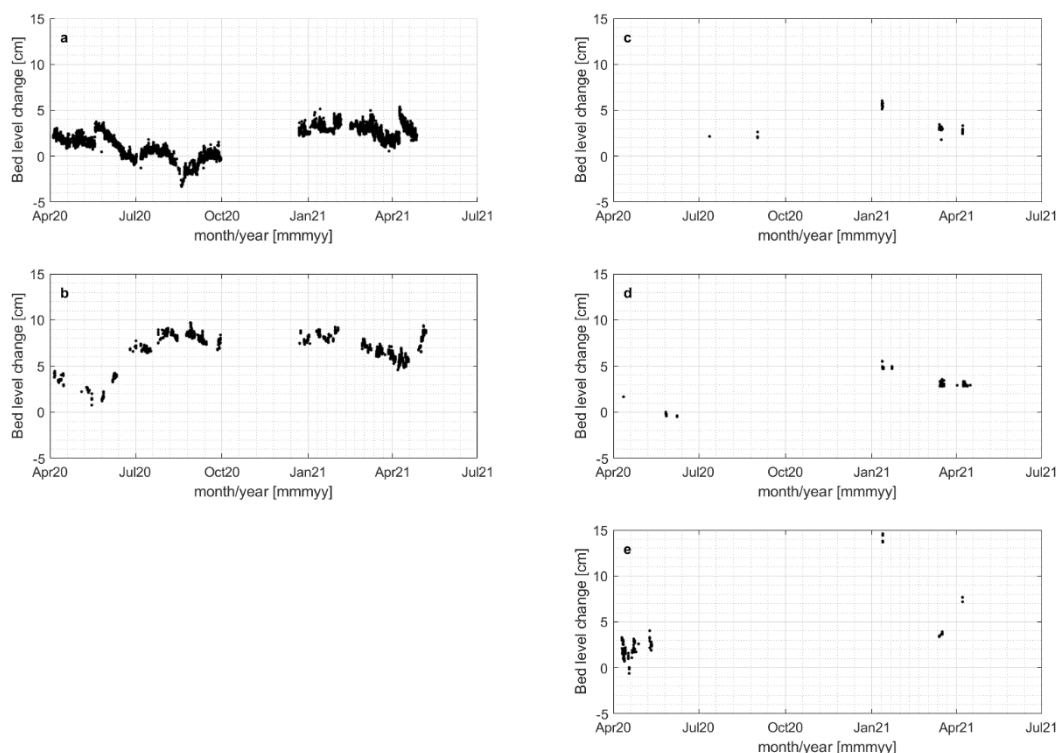


**Figure A.1:** The bed level changes compared to the start of the measurement period (April 2020) and measured by the ASEDs from April 2020 till April 2021 at five different locations; (a) at the front of the marsh, (b) at the entrance of area F and at the marsh on the seaside plots of area (c) E, (d) F and (e) G.

## Appendix B – Input parameters regression analysis

**Table A.1:** The parameters presenting the summer period, created for the correlation and regression analysis.

Parameter	Area E			Area G		
	Land	Mid	Sea	Land	Mid	Sea
Density [%]	15	25	20	10	3	0
Inundation frequency [d <sup>-1</sup> ]	1.28	1.30	0.74	0.33	0.46	1.52
Absolute bed level change [cm]	1	3	3	4	3	5
Maximum significant wave height [cm]	13.28	13.28	13.28	13.82	13.82	13.82

Table A.2: The parameters over the winter period created for the correlation and regression analysis.

Parameter	Period	Area E			Area G		
		Land	Mid	Sea	Land	Mid	Sea
Density decay [%]	24 November – 22 December	9.09	21.43	53.75	0	0	0
	22 December – 22 January	12.00	12.73	5.41	13.33	18.18	0
	22 January – 22 February	12.00	12.73	5.41	13.33	18.18	0
	22 February – 23 March	18.42	21.95	18.18	72.73	57.14	0
	23 March – 23 April	19.35	34.38	11.11	0	0	0
Inundation frequency [d <sup>-1</sup> ]	24 November – 22 December	0.64	1.07	0.79	0.07	0.04	1.89
	22 December – 22 January	0.79	1.18	0.98	0.11	0.10	1.77
	22 January – 22 February	0.79	1.18	0.98	0.11	0.10	1.77
	22 February – 23 March	0.86	1.31	1.00	0.35	0.24	1.90
	23 March – 23 April	1.00	1.55	1.26	0.33	0.26	1.97
Absolute bed level change [cm]	24 November – 22 December	0.78	0.35	0.52	0.15	0.34	0.32
	22 December – 22 January	0.14	0.29	0.74	0.60	0.48	3.13
	22 January – 22 February	0.14	0.29	0.74	0.60	0.48	3.13
	22 February – 23 March	0.04	0.49	1.09	0.15	0.02	1.80
	23 March – 23 April	0.12	0.21	2.02	0.09	0.42	6.49
Maximum significant wave height [cm]	24 November – 22 December	7.76	7.76	7.76	9.45	9.45	9.45
	22 December – 22 January	7.76	7.76	7.76	9.45	9.45	9.45
	22 January – 22 February	7.76	7.76	7.76	9.45	9.45	9.45
	22 February – 23 March	15.50	15.50	15.50	28.16	28.16	28.16
	23 March – 23 April	21.00	21.00	21.00	8.27	8.27	8.27
Maximum flow velocity [m/s]	24 November – 22 December	0.46	0.46	0.46	0.50	0.50	0.50
	22 December – 22 January	0.49	0.49	0.49	0.49	0.49	0.49
	22 January – 22 February	0.49	0.49	0.49	0.49	0.49	0.49
	22 February – 23 March	0.45	0.45	0.45	0.49	0.49	0.49
	23 March – 23 April	0.46	0.46	0.46	0.50	0.50	0.50

Table A.3: The vegetation characteristics during the winter period created for the correlation and regression analysis.

Parameter	Period	Area E			Area G		
		Land	Mid	Sea	Land	Mid	Sea
Density [%]	24 November	18.33	23.33	26.67	5.00	3.67	0.00
	22 December	16.67	18.33	12.33	5.00	3.67	0.00
	22 January	12.67	13.67	11.00	3.67	2.33	0.00
	22 February	12.67	13.67	11.00	3.67	2.33	0.00
	23 March	10.33	10.67	9.00	1.00	1.00	0.00
	23 April	8.33	7.00	8.00	1.00	1.00	0.00
Aboveground length [cm]	24 November	14.48	15.40	16.57	15.23	16.37	-
	22 December	16.63	17.50	17.68	13.41	14.17	-
	22 January	14.60	15.13	14.07	12.80	15.20	-
	22 February	14.60	15.13	14.07	12.80	15.20	-
	23 March	15.27	17.20	14.93	12.13	12.00	-
	23 April	14.13	13.17	13.57	10.67	13.07	-
Root length [cm]	24 November	7.80	8.80	12.80	15.13	15.60	-
	22 December	8.13	8.03	12.51	15.08	14.75	-
	22 January	7.40	8.33	11.80	10.37	11.00	-
	22 February	7.40	8.33	11.80	10.37	11.00	-
	23 March	8.07	8.67	11.67	7.33	9.67	-
	23 April	9.17	9.33	11.75	9.03	9.67	-
Number of side roots [-]	24 November	0.00	0.00	0.00	0.00	0.00	-
	22 December	0	3.73	10.93	9.80	13.07	-
	22 January	6.67	6.33	9.00	9.73	15.33	-
	22 February	6.67	6.33	9.00	9.73	15.33	-
	23 March	6.13	6.20	12.87	4.67	14.67	-
	23 April	8.40	5.87	7.47	2.93	5.33	-
Length side roots [cm]	24 November	0.00	0.00	0.00	0.00	0.00	-
	22 December	0.00	2.47	8.33	8.73	13.14	-
	22 January	4.40	4.67	10.27	8.07	12.67	-
	22 February	4.40	4.67	10.27	8.07	12.67	-
	23 March	5.00	4.80	8.73	8.27	7.00	-
	23 April	5.30	3.75	6.97	5.25	5.33	-
Strength [N]	24 November	22.20	28.47	16.57	26.27	40.03	-
	22 December	26.27	15.87	29.93	23.00	34.07	-
	22 January	20.73	16.27	22.60	20.40	29.87	-
	22 February	20.73	16.27	22.60	20.40	29.87	-
	23 March	14.73	18.13	30.07	16.93	22.93	-
	23 April	18.33	16.20	25.90	14.50	23.87	-
Number of available seeds [-]	22 February	26.00	21.00	27.33	7.67	6.67	0.00
	23 March	34.00	13.67	7.67	0.67	2.33	0.00
	23 April	34.67	35.67	7.67	1.00	6.33	0.00